**REPUBLIQUE ALGERIENNE DEMOCRATIQUE ET POPULAIRE**
**الجمهورية الجزائرية الديمقراطية الشعبية**

**MINISTERE DE L'ENSEIGNEMENT SUPERIEUR ET DE LA RECHERCHE SCIENTIFIQUE**

**ECOLE SUPERIEURE EN SCIENCES APPLIQUEES**
**--T L E M C E N--**

المدرسة العليا في العلوم التطبيقية
École Supérieure en Sciences Appliquées

**وزارة التعليم العالي والبحث العلمي**

**المدرسة العليا في العلوم التطبيقية**
**-تلمسان-**

Mémoire de fin d'étude

**Pour l'obtention du diplôme d'ingénieur**

Filière : Électrotechnique
Spécialité : Energie et environnement

Présenté par : **Mohammed Yacin MARKMAL**

Thème

# Simulation Numérique du Comportement Dynamique et Thermique d'un capteur solaire plan à eau

Soutenu publiquement, le 11 / 07/ 2021, devant le jury composé de :

| | | | |
|---|---|---|---|
| Dr. BOUDGHENE STAMBOULI Naouel Ep BENDIMERAD | MAA | ESSA-Tlemcen | Présidente |
| Dr. KORTI Mohamed Choukri | MCB | URER-MS ADRAR | Directeur de mémoire |
| Dr. KHERBOUCHE Djamila Ep FARADJI | MCA | ESSA-Tlemcen | Co-directeur de mémoire |
| Dr.BENNEKROUF Mohammed | MCB | ESSA-Tlemcen | Examinateur |
| Dr.BOUKLI HACENE Souhila | MCB | Univ de Tlemcen | Examinateur |

Année universitaire : 2020 / 2021

# Acknowledgements

I want to thank the Almighty God for the strength, the will and capacity to carry out and persist and accomplish this job successfully.

I would like to thank my supervisors, **Mr Mohammed Choukri KORTI** and **Mrs Djamila KHERBOUCHE**, for their guidance, their assistance ,the precious time they gave me and their precious advices and useful critiques. Their skills and experience in the field have been of great help to me and i was really lucky to work with them during this period.

I am grateful to all the members of the jury for agreeing to read this manuscript and to provide the necessary critiques for the final form of this work.

# Dedication

I dedicate this work..

To my family, the ones who made me the man I am.

To my heaven and the light of my eyes, my mother, who believed in me the most and taught me the meaning of life.

To my father, the hero who gave me the strength and encouraged me through the entire journey.

To Ali, The example that I always tried to follow his steps.

To all my brothers and sisters, who always surrounded me with their unconditional support through all their priceless advices.

To all my friends we s7ab, all my beloved ones and for everyone who helped me either directly or indirectly during my studies.

Mohammed Yacin Markmal

# ملخص

الهدف من هذا العمل هو المحاكاة العددية للسلوك الحراري لسخان المياه الشمسي (التسخين المسبق). يقودنا التبادل الحراري المنخفض بين مائع نقل الحرارة والممتص إلى استكشاف طرق أخرى لتحسين كفاءة اللاقط الشمسي، لذلك كان من المفيد جدًا دراسة الشكل الهندسي والأبعاد ومعدل التدفق داخل الأنابيب. تم استخدام نموذج رقمي ثلاثي الأبعاد للتسخين الشمسي المستوي، بطول 94 سم وارتفاع 4.5 سم ، مع تكوين أنبوب متوازي لتقييم ظاهرة انتقال الحرارة الهيدروديناميكية. يعتبر السائل صفائحيًا بخصائص ثابتة. المعادلات الحاكمة هي معادلاتNavier-Stokes ، مقترنة بمعادلة الحفاظ على الطاقة التي تم حلها باستخدام الكود التجاري .(ANSYS FLUENT) تبحث الدراسة في تأثير معدل تدفق درجة الحرارة المحيطة على ملامح درجة حرارة الماء لتحديد أفضل أداء ممكن للنموذج المقترح.

# Abstract

The objective of this work is the numerical simulation of the thermal behaviour of a solar water heater (preheater). The low heat exchange between the heat transfer fluid and the absorber leads us to investigate other ways to improve the efficiency of the collector, for this it was very useful to study the geometrical shape, the dimensioning and the flow rate inside the tubes. A 3D numerical model of a planar solar preheater, 94 cm long and 4.5 cm high, with a parallel tube configuration was used to evaluate the hydrodynamic heat transfer phenomena. The fluid is considered to be laminar with constant properties. The governing equations are the Navier-Stokes equations, coupled with the energy conservation equation solved using the commercial code (ANSYS FLUENT). The study examines the influence of the ambient temperature flow rate on the water temperature profiles to select the best possible performance for the suggested model.

# Résumé

L'objectif de ce travail porte sur la simulation numérique du comportement thermique d'un chauffe-eau solaire (préchauffeur). Les faibles échanges thermiques entre le fluide caloporteur et l'absorbeur nous ramènent à investiguer d'autres moyens pour améliorer le rendement du capteur, pour cela, il été très utile d'étudier la forme géométrique, le dimensionnement et le débit qui circule à l'intérieur des tubes. Un modèle numérique en 3D d'un préchauffeur solaire plan, de longueur 94 cm et de hauteur 4,5 cm, avec une configuration en tube parallèle a été utilisé pour évaluer les phénomènes de transfert de chaleur hydrodynamique. Le fluide est considéré comme laminaire avec des propriétés constantes. Les équations qui gouvernent l'écoulement sont celles de Navier-Stokes, couplées à l'équation de conservation d'énergie résolue à l'aide du code commercial (ANSYS FLUENT). L'étude examine l'influence du débit de la température ambiante sur les profils de la température d'eau pour choisir le meillieur rendement possible au modèle proposé.

# Contents

**1 Literature Review** **3**

1.1 The Sun . . . 3

1.1.1 Structure of the Sun . . . 4

1.2 Earth Characteristics . . . 5

1.2.1 The terrestrial atmosphere . . . 5

1.3 Earth's Movement . . . 5

1.3.1 Earth's Movement Around the Sun . . . 5

1.3.2 The Apparent Motion Of The Sun . . . 6

1.3.3 The Celestial Sphere . . . 7

1.4 Solar Energy . . . 7

1.4.1 Specific Caracteristics Of Solar Energy . . . 8

1.5 The Position Parameters . . . 9

1.5.1 The geographical coordinates of a site . . . 9

1.5.2 The coordinates of the sun relative to an observer . . . 9

1.6 Solar times . . . 14

1.6.1 True solar time (Tsol) . . . 14

1.6.2 Mean Solar Time (MST) . . . 14

1.6.3 Universal Time (UT) . . . 15

1.6.4 Legal time (LT) . . . 15

1.6.5 Sunrise and sunset . . . 15

1.6.6 The length of the day . . . 16

1.7 Solar radiation . . . . . 16
1.7.1 The spectrum of solar radiation . . . . . 17
1.7.2 Solar radiation . . . . . 17
1.7.3 Attenuation of solar radiation (role of the atmosphere) . . . . . 18
1.7.4 Sunshine rate . . . . . 19
1.7.5 The solar potential in Algeria . . . . . 19
1.8 Modes of Heat Transfer . . . . . 20
1.8.1 Conduction . . . . . 21
1.8.2 Convection . . . . . 21
1.8.3 Radiation . . . . . 21
1.9 Solar water heaters . . . . . 22
1.9.1 Types of solar water heaters . . . . . 22
1.9.2 The main components of a solar water heater . . . . . 23
1.9.3 Other components . . . . . 25
1.10 SOLAR COLLECTORS . . . . . 29
1.10.1 Definition and working principle of a flat plate solar collector . . 30
1.10.2 The different types of solar collectors . . . . . 30
1.10.3 The main components of a glazed flat plate collector . . . . . 34
1.10.4 How does a flat plate collector work . . . . . 37
1.10.5 Parameters characterising the operation of a flat plate collector . 38

**2 mathematical modeling 40**

2.1 Introduction . . . . . 40
2.2 Setting up the problem into equations : . . . . . 41
2.2.1 Continuity equation : . . . . . 41
2.2.2 Momentum equation : . . . . . 42
2.2.3 Energy equation : . . . . . 42
2.2.4 Flow regimes : Laminar and turbulent . . . . . 43
2.3 Principle of the finite volume method: . . . . . 44
2.3.1 Description of a control volume . . . . . 45

2.4 Subdivision of the study domain (mesh) . . . 46
2.4.1 STRUCTURED MESHES . . . 47
2.4.2 UNSTRUCTURED MESHES . . . 51
2.4.3 MIXED MESHES . . . 51
2.4.4 General mesh generation techniques . . . 52
2.4.5 Mesh quality . . . 52
2.5 Discretisation by the finite volume method . . . 53
2.5.1 Discrete equations . . . 53
2.6 Conclusion . . . 55

**3 Problem's position 56**
3.1 Introduction . . . 56
3.2 Physical model . . . 58
3.3 Mathematical formulation . . . 61
3.3.1 Steps involved in creating the sensor geometry : . . . 62
3.4 Mesh . . . 62
3.5 Boundary conditions . . . 68
3.5.1 Initial conditions . . . 68
3.5.2 Definition of the main enclosure : . . . 69
3.5.3 Definition of boundary conditions . . . 69
3.5.4 Mesh exportation : . . . 70
3.5.5 Calculation Preparation Steps in FLUENT: . . . 71
3.6 Gambit and Fluent simulation tools . . . 78
3.6.1 Gambit . . . 78
3.6.2 Fluent code . . . 81
3.7 conclusion . . . 84

**4 Results and discussion 85**
4.1 Introduction . . . 85
4.2 Results and discussion . . . 86

4.2.1 Evolution of water temperature profiles for different flow rates . 86
4.2.2 Evolution of water temperature profiles during the day . . . . . 92
4.3 Conclusion . . . . . 100

# List of Figures


1.1 sectional view of the sun. [1] . . . . . 4
1.2 Earth's orbit around the sun. [2] . . . . . 6
1.3 apparent motion of the sun [3] . . . . . 6
1.4 The Celestial Sphere [4] . . . . . 7
1.5 Illustration of geographic latitude and longitude of the earth [5] . . . . . 9
1.6 Variation of the declination angle $\delta$ throughout the year [6] . . . . . 10
1.7 Horizontal frame of reference [6] . . . . . 11
1.8 Solar altitude angle [7] . . . . . 12
1.9 sun's azimuth [6] . . . . . 13
1.10 Orientation of a solar collector [6] . . . . . 13
1.11 Modeling of sunset and sunerise time in algeria [8] . . . . . 16
1.12 Solar spectrum outside the atmosphere [9] . . . . . 17
1.13 Solar radiation types [6] . . . . . 17
1.14 Attenuation of solar radiation as it passes through the atmosphere [6] . 19
1.15 Solar radiation potential in algeria [10] . . . . . 20
1.16 Thermosyphon SWH and its schematic [11] . . . . . 23
1.17 Forced circulation ISWH [12] . . . . . 24
1.18 SWH components [13] . . . . . 24
1.19 Storage tank [14] . . . . . 25
1.20 Energy balance of a solar collector [12] . . . . . 26
1.21 circuit piping [14] . . . . . 26
1.22 A pump [14] . . . . . 26

1.23 A non return valve [14] . . . 27
1.24 Expansion tank [14] . . . 27
1.25 A safety valve [14] . . . 27
1.26 Drain taps [14] . . . 28
1.27 A bleeder valve[14] . . . 28
1.28 The controller [14] . . . 29
1.29 Classification of solar collectors [12] . . . 29
1.30 A flate plate solar collector [14] . . . 30
1.31 A Flat plate collectors without glazing [14] . . . 31
1.32 Water collector [15] . . . 32
1.33 air collector [12] . . . 32
1.34 Evacuated-tube collectors [14] . . . 33
1.35 Line focus concentrator [14] . . . 33
1.36 Point focus concentrator [14] . . . 34
1.37 Cross section of a flate plate [16] . . . 35
1.38 Flate plate collector [17] . . . 37

2.1 the transition from the laminair to the turbulent regime: the reynlods experience [18] . . . 43
2.2 visualisation of a turbulent flow [19] . . . 44
2.3 structured mesh . . . 45
2.4 schematic representing a two-dimensional control volume . . . 46
2.5 Examples of the structured (left) and untructured mesh (right) . . . 46
2.6 regular cartesian grid . . . 47
2.7 irregular cartesian grid . . . 48
2.8 Transformation from physical domain to computational domain . . . 49
2.9 BLOCK STRUCTURED GRID . . . 49
2.10 refined mesh (left) and different mesh (right) . . . 50
2.11 chimera grid . . . 50
2.12 unstructured triangle mesh . . . 51

2.13 mixed mesh with non-conforming interface . . . . . 52
2.14 the principle of staggered meshing . . . . . 53
2.15 staggring meshing figure's symboles definition . . . . . 53
2.16 control volume around the node p ( one-dimensional case) . . . . . 55

3.1 cross section of the collector with dimensions . . . . . 59
3.2 overall view of the collector with dimension . . . . . 59
3.3 A view of the collector suggested design in Gambit . . . . . 63
3.4 A zoomed-in view of the tubes intersections inside the collector in gambit 63
3.5 A zoomed-in view of tubes design inside the collector in gambit . . . . . 64
3.6 mesh command button . . . . . 64
3.7 volume command button . . . . . 65
3.8 mesh volume button . . . . . 65
3.9 mesh volume définition . . . . . 65
3.10 a veiw of the collector's mesh . . . . . 66
3.11 a zoomed-in veiw of the mesh inside the collector . . . . . 66
3.12 a zoomed-in view of the mesh inside a main tube . . . . . 66
3.13 a zoomed-in view of the mesh on the intersection region between main and secondary tubes . . . . . 67
3.14 a view of different types of mesh in the collector . . . . . 67
3.15 collector's components definition scheme . . . . . 68
3.16 definition of the box in gambit . . . . . 69
3.17 definition of the galss in gambit . . . . . 69
3.18 definition of tubes in gambit . . . . . 70
3.19 definition of the absorber in gambit . . . . . 70
3.20 definition of the inlet in gambit . . . . . 71
3.21 definition of the outlet in gambit . . . . . 71
3.22 the circulation region of the water in gambit . . . . . 72
3.23 the circulation region of the air in gambit . . . . . 72
3.24 mesh exportation . . . . . 72

3.25 Scale verification . . . 73
3.26 definition of model parameters . . . 73
3.27 establishing the energy equations . . . 73
3.28 chosing « laminar » as a flow regime . . . 74
3.29 defining the radiation parameters of the model . . . 74
3.30 definition of a new material . . . 75
3.31 Setting boundary conditions . . . 76
3.32 Setting the mass flow inlet value . . . 76
3.33 Setting the inlet temperature . . . 76
3.34 Solution initialization . . . 77
3.35 Starting calculations . . . 77
3.36 Gambit's interface . . . 78
3.37 operation tool window . . . 79
3.38 geometrie construction window . . . 79
3.39 geometrie generation window . . . 80
3.40 boundary conditions definition buttons . . . 80
3.41 tools buttons . . . 80
3.42 global control window . . . 81
3.43 Fluent launcher window . . . 82
3.44 Fleunt interface . . . 83

4.1 A 3D model of the collector using Tecplot software . . . 86
4.2 A zoomed-in view of the 3D tube design . . . 87
4.3 Evolution of the (X, Z)-temperature profiles of the water for a mass flow rate of 0.001 kg/s . . . 88
4.4 Evolution of the (X, Z)-temperature profiles of the water for a mass flow rate of 0.0008 kg/s . . . 89
4.5 Evolution of the (X, Z)-temperature profiles of the water for a mass flow rate of 0.0004 kg/s . . . 90

4.6 Evolution of the (X, Z)-temperature profiles of the water for a mass flow rate of 0.0001 kg/s . . . . . 91
4.7 Evolution of the (X, Z)-temperature profiles of the water for a flow rate of 0.0001 kg/s at 08:00 am (Tamb = 274,75 K , Di = 189 W/m², DH = 7 W/m²) . . . . . 92
4.8 Evolution of the (X, Z)-temperature profiles of the water for a flow rate of 0.0001 kg/s at 10:00 am (Tamb = 278,95 K, Di = 922 W/m², DH = 49 W/m²) . . . . . 93
4.9 Evolution of the (X, Z)-temperature profiles of the water for a flow rate of 0.0001 kg/s at 12:00 (Tamb = 285, 95, Di = 1025 W/m², DH = 60 W/m²) 94
4.10 Evolution of the (X, Z)-temperature profiles of the water for a flow rate of 0.0001 kg/s at 13:30 (Tamb = 289, 95, Di = 1044 W/m², DH = 60 W/m²) 95
4.11 Evolution of the (X, Z)-temperature profiles of the water for a flow rate of 0.0001 kg/s at 14:00 (Tamb = 291, 05, Di = 1037 W/m², DH = 60 W/m²) 96
4.12 Evolution of the (X, Z)-temperature profiles of the water for a flow rate of 0.0001 kg/s at 16:15 (Tamb = 293,15 K , Di = 903 W/m², DH = 55 W/m²) 97
4.13 Evolution of the (X, Z)-temperature profiles of the water for a flow rate of 0.0001 kg/s at 20:00 (Tamb = 286,75 K, Di = 0 W/m², DH = 0 W/m²) . 98
4.14 3D distribution of the temperature evolution on the main regions of collector at 13:00 (GLASS, TUBES, INLET, OUTLET) . . . . . 99

# List of Tables

3.1 symbols and units for collector dimensions . . . . . 60
3.2 collector's dimensions . . . . . 60
3.3 Physical properties of materials used in the simulation . . . . . 60
3.4 suggested mass flows . . . . . 68
3.5 different parameters of the 5th of january 2020 obtained from the URER-MS daily archive. . . . . 68

# Nomenclature

| | | |
|---|---|---|
| A | Area of the wing | $m^2$ |
| L | Length of the box | cm |
| H | Box height | cm |
| W | Width of the box | cm |
| D | Diameter of the main tubes | $cm$ |
| $T_{amb}$ | Ambiante temperature | $K$ |
| $D_i$ | Direct solar irradiation | $W/m^2$ |
| $D_H$ | Diffuse solar irradiation | $W/m^2$ |
| d | Diameter of the two secondary tubes | $cm$ |
| w | Distance between two secandary tubes | $cm$ |

# General Introduction

Since the dawn of creation, people have tried to put solar radiation to use. he advancement of knowledge of radiation and in the design of technical devices for its collection and conversion has marked the scientific and industrial development of societies.
The various solar technologies are now at different stages of development, from research to industrial implementation and market penetration.

Today, the technologies developed concern the collection of solar gains through bioclimatic architecture, the production of low temperature heat for the housing and tertiary sectors, etc.

These techniques can provide a certain number of energy services in place of conventional energy: hot water supply, space heating. They can also provide an energy service where other energies do not: isolated sites, rural areas in developing countries.

Among the renewable energies, solar energy is the most dominant and also the most easily exploitable. Because of the diversity of its use and the interest it has aroused throughout the world, this form of energy has experienced a great expansion in recent years. However, the high price of this energy compared to non-renewable energies is a handicap to the expansion of its use.

The optimisation of solar devices is among the recommended solutions to reverse the current trend and see the use of solar energy spread further around the world, which is why this study was aimed at studying the thermal behaviour of a solar water

collector designed for solar distillation, which will give us useful information if we want to focus on the optimisation of this device.

The work has been structured in the following way:

-A general introduction presenting the aim of the work and showing the interest of the numerical study.

- The second chapter presents the generalities on solar thermal storage as well as the bibliographical research carried out on the various analytical, numerical and experimental works on solar energy storage systems in relation to the treated subject.

-The third chapter is based on the mathematical modelling of the theoretical problem and a brief description of the finite volume method.

- The fourth chapter is devoted to the problem position with descriptions of the software Fluent and Gambit as well as the numerical simulation steps using the calculation code FLUENT. -The fifth chapter presents the different results obtained and their interpretations.

-At the end, a conclusion summarises the critical analysis of the results obtained.

# Chapter 1

# Literature Review

## 1.1 The Sun

The sun is a small star in the universe that is nearest to the earth and is located at the middle of a solar system. The sun has a pseudo-spherical form, similar to a massive ball of extremely hot gas made up of 80% hydrogen and 19% helium, with the remaining 1% made up of a combination of over 100 elements, nearly all known chemical elements [20, 21].

The sun is the origin of all energy sources on earth. This is true as well for non-renewable energies of fossil origin, such as hydrocarbons which are the result of photosynthesis; as for renewable energies, such as solar energy, geothermal energy, biomass...etc. [20, 21].

Comparable to a huge ball of very hot gas, the sun is a dwarf star with a pseudo-spherical shape that consists mainly of 80 % hydrogen and 19% helium, the remaining 1% being a mixture of over 100 chemical elements, Although the sun is a medium-sized star, it alone accounts for 99.9% of the mass of the solar system, which is dominated by the gravitational effects of the sun's large mass.

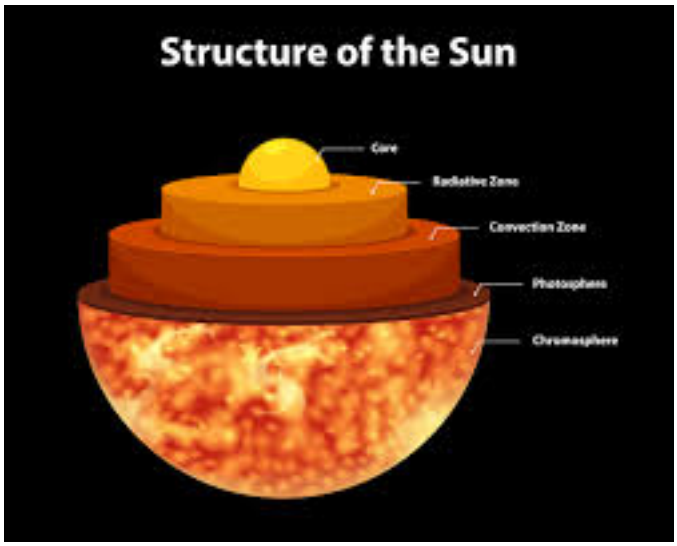


Figure 1.1: sectional view of the sun. [1]

### 1.1.1 Structure of the Sun

The sun is not a homogeneous sphere, it consists of 5 main areas: the interior, the photosphere, the chromosphere and the solar corona, the solar protuberances.

**The interior** : The interior contains the core, the radiation zone and the convection zone, it represents the energy source of the sun, it is composed of 2/3 of hydrogen and 1/3 of helium. The temperature reaches 16MK.

**The photosphere** : It is the gaseous layer that envelops the sun, it is responsible for almost all the radiation that the earth receives.

**Chromosphere** : It surmounts the photosphere, it is a gaseous layer that is assimilated to the solar atmosphere, its thickness does not exceed 800 (km) and its temperature is $43x10^3K$.

**The corona** : It is an irregular white halo without defined limits, its thickness is about $3x10^6km$ [22].

**The solar protuberances** : One of the most spectacular phenomena in the corona is the formation of protuberances. These are gigantic columns of gas, less hot but

denser than that of the corona, which are created near the surface and can extend over hundreds of thousands of kilometers.

## 1.2 Earth Characteristics

The main characteristics are given in table :

### 1.2.1 The terrestrial atmosphere

**The atmosphere** is made up of several layers, among which are: The troposphere is the region between the earth's surface and 15 kilometers above sea level.

**The stratosphere** is located between 15 and 80 kilometers above sea level.

**The ionospheric zone** , located between 80 and 200 kilometers above sea level.

## 1.3 Earth's Movement

### 1.3.1 Earth's Movement Around the Sun

The Earth's orbit around the Sun is an ellipse, with the Sun as one of the foci. The plan of this ellipse is known as the ellipsis. This ellipse has a low eccentricity.
The complete revolution takes place in a period of 365.25 days. The earth also turns on itself around an axis called the axis of the poles. This rotation takes place in one day. The axis of the poles and the ellipsis make an angle between them called declination, it is equal to 23°27'.
It is at the winter solstice (December 21) that the earth is closest to the sun: 147 million km.
On June 21, the distance between the earth and the sun is 152 million km, this is the day when the earth is the farthest away, it is the summer solstice.

March 21 and September 21 are called respectively spring and autumnal equinoxes. At the equinoxes the day and the night are equal.

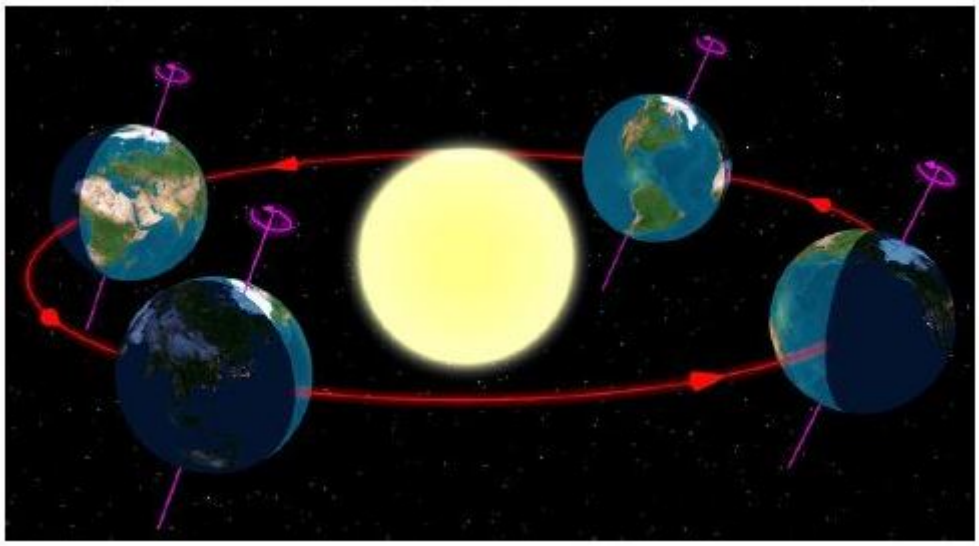

Figure 1.2: Earth's orbit around the sun. [2]

### 1.3.2 The Apparent Motion Of The Sun

The movement that the Sun appears to make in a day seen by an observer located on Earth is called on Earth is called "The apparent motion of the Sun". Outside of the polar regions, the the Equator and the tropics. [3]

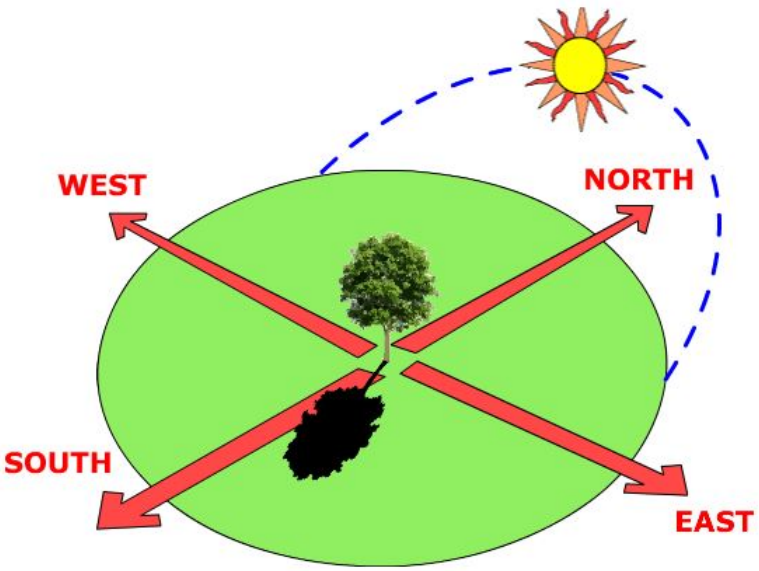


Figure 1.3: apparent motion of the sun [3]

-In the morning; the Sun is in the East, low on the horizon, it is the "Sunrise".

-At noon; the Sun is positioned in the South or in the North, and it is at the highest of its path apparent.

-In the evening; the Sun appears in the West, low on the horizon, it is the "sunset".

The apparent movement of the Sun observed by a fixed man at a point of latitude L north of the Equator is shown in figure 1.3.

### 1.3.3 The Celestial Sphere

The celestial sphere is a fictitious sphere with a huge diameter, which has as its center the earth, and as its radius the distance (earth-sun). It is assumed that all visible objects in the sky are located on the surface of the celestial sphere. The direction of the objects can be precisely evaluated with the help of a celestial coordinate system,We can summarize the different characteristics on the sphere itself as shown in figure 1.4.

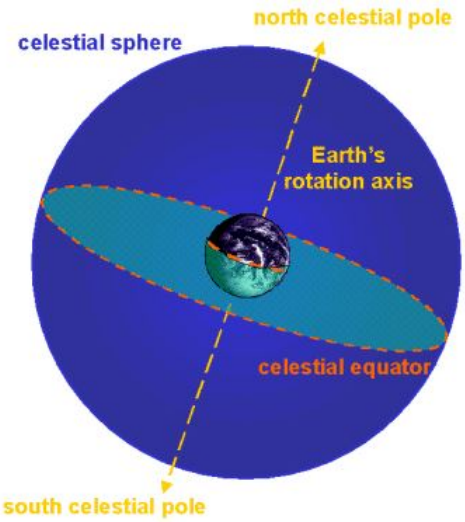


Figure 1.4: The Celestial Sphere [4]

## 1.4 Solar Energy

Solar energy is the energy emitted by the sun through its radiation on the earth can be converted into other forms of energy useful for human activity, such as heat, electricity, or biomass, by a variety of processes. Furthermore, the term "solar energy"

is sometimes used to refer to the electricity or thermal energy produced as a result of this [23].

**Solar Photovoltaic Energy** Photovoltaic solar energy refers to the electricity produced by transforming part of the sun's radiation with a photovoltaic cell.

**Solar thermal energy** Solar thermal energy consists of using solar radiation by transforming it into thermal energy. It is presented in different ways: thermodynamic solar power plants, solar water heaters and heating, solar cooling, solar stoves and dryers.

### 1.4.1 Specific Caracteristics Of Solar Energy

Some particularities of solar energy must be taken into account to optimize its use, the main characteristics are dilution and intermittence.

**Dilution** : The dilution requires the use of a large surface of capture to obtain high powers or to provide a concentration of solar rays to obtain high temperatures.

**Intermittency** : The intermittency of solar radiation and the other Specific characteristics of solar energy, In temperate climate regions, the problem of intermittency is difficult to solve. A solution often used is to consider storage of very variable importance depending on the applications considered.
For example, it is necessary to plan a daily storage and to use it during the night, as well as to plan the nebulous storage which corresponds to accidental cloudy passages.

## 1.5 The Position Parameters

### 1.5.1 The geographical coordinates of a site

Every point on the earth's sphere can be located by two coordinates, called earth coordinates, namely latitude and longitude, figure 1.5:

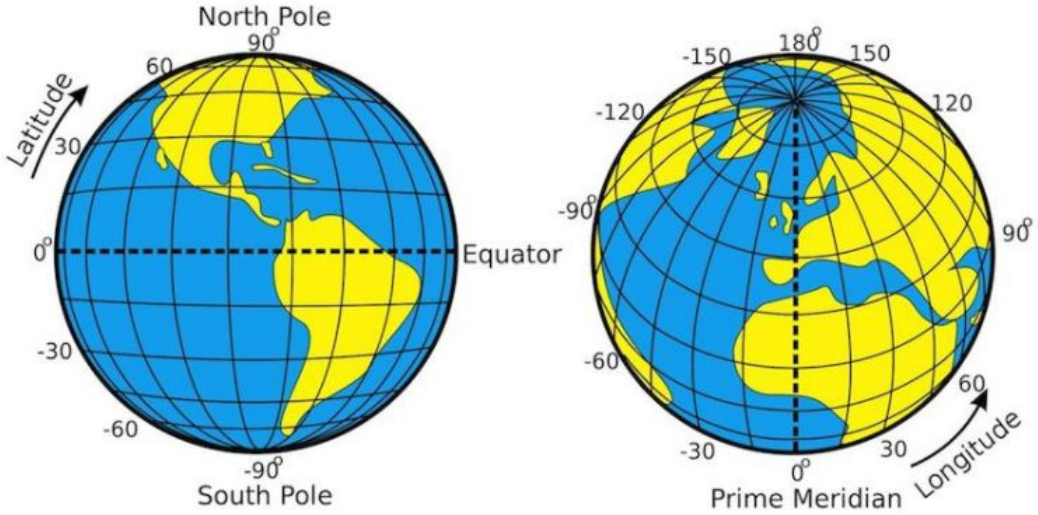


Figure 1.5: Illustration of geographic latitude and longitude of the earth [5]

**The latitude of the location $\phi$ :** This is the angle that the ray joining the center of the earth at this location and the equatorial plane. It varies from -90° at the South Pole to +90° at the North Pole:

$\phi < 0$ *The Southern Hemisphere.*

$\Phi > 0$ *The Northern Hemisphere.*

$\phi = 0$ *On the plane of the equator.*

**The longitude of the location Ł:** This is the angle between the meridian plane passing through this location and the original meridian plane (Greenwich 0°).

### 1.5.2 The coordinates of the sun relative to an observer

To determine the coordinates of the sun relative to an observer located on the surface of the earth surface of the earth we define two reference frames, the equatorial frame

and the horizontal frame.

**The equatorial reference frame**

The equatorial frame of reference is a frame of reference that takes as its origin the center of the earth and as reference plane the plane of the equator. In this frame, the position of the sun in the sky is determined by two sky is determined by two coordinates, the declination and the hour angle [20].

**The declination of the sun ($\delta$) :** Corresponds to the angle formed by the equatorial plane and the direction of the earth sun. It varies according to Cooper's equation, [20]:

$$\delta = 23.45.sin((284 + Nd).(360/365)) \quad (1)$$

With, Nd: the number of the day of the year (January 1=1).

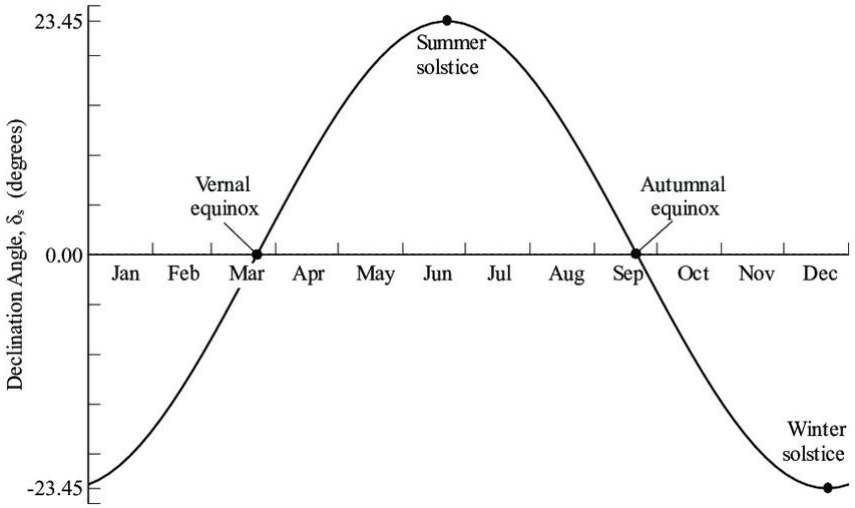


Figure 1.6: Variation of the declination angle $\delta$ throughout the year [6]

As we can see in figure 1.6 , it varies from -23, 45° at the winter solstice to +23,45° at the summer solstice, and it is zero at the equinoxes

**The hour angle ($\omega$) :** Corresponds to the angle between the projection of the sun on the equatorial plane and the meridian of the location under consideration passing through the south. It is given by the following relation:

$$\omega = 15.(Tsol - 12) \tag{2}$$

where, Tsol , is the true solar time.

**The horizontal reference frame**.

The horizontal frame of reference is a reference frame that takes the observer's location as its origin and the plane of the astronomical horizon as its reference plane. In this frame of reference. The position of a star in space can be identified by its horizontal coordinates defined on the celestial sphere in figure 1.7, namely the height of the sun **h** and its azimuth **a**.

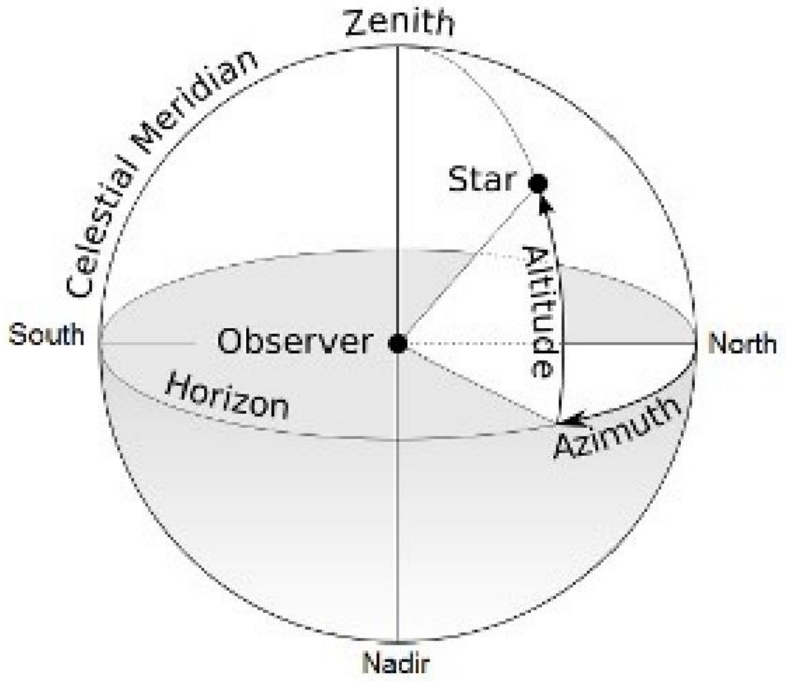


Figure 1.7: Horizontal frame of reference [6]

**The height of the sun (h)** It corresponds to the angle formed by the directional vector of the sun and its projection on the horizontal plane, figure 1.8, it is 0° at sunrise and sunset and takes its maximum value (90°) at solar midday . It is evaluated by the following relation [20] :

$$sinh = cos\delta.cos\phi.cos\omega + sin\delta.sin\phi \tag{3}$$

The maximum height of the sun corresponds to $\omega = 0$ , obtained at midday in true solar time, and is evaluated by the following relation:

$$hmax = 90 - (\phi - \delta) \tag{4}$$

It varies with the latitude of a location and the declination of the sun (the day of the year). Figure (1-8) shows the evolution of the latter for different locations.

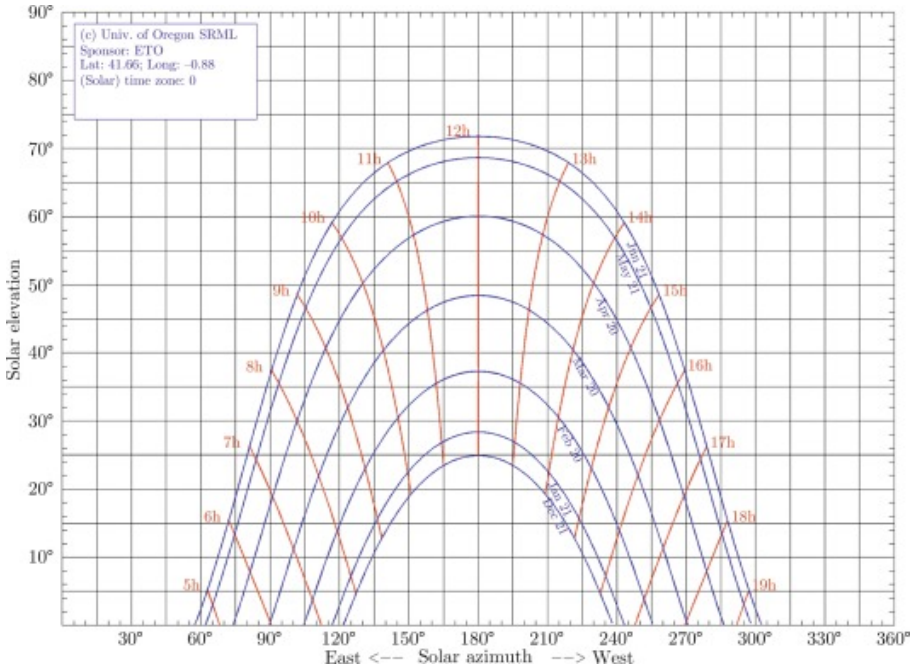


Figure 1.8: Solar altitude angle [7]

**Sun's azimuth (a)** This is the angle formed by the projection of the direction of the sun on the horizontal plane and the meridian of the location. It is counted positively towards the east and negatively towards the west. It is given by the following relation [20] :

$$sina = (cos\delta \ .sin\omega)/cosh \tag{5}$$

**Orientation of a plane**

In solar applications, the positioning of the surface of solar devices (e.g. flat plate collector) is essential. the following figure shows the orientation of a sensor with the main angles, the collector tilt (beta, $\beta$) and azimuth (gamma, $\gamma$) are positioned to reflect a site somewhere in the Northern Hemisphere. The Sun's position is described

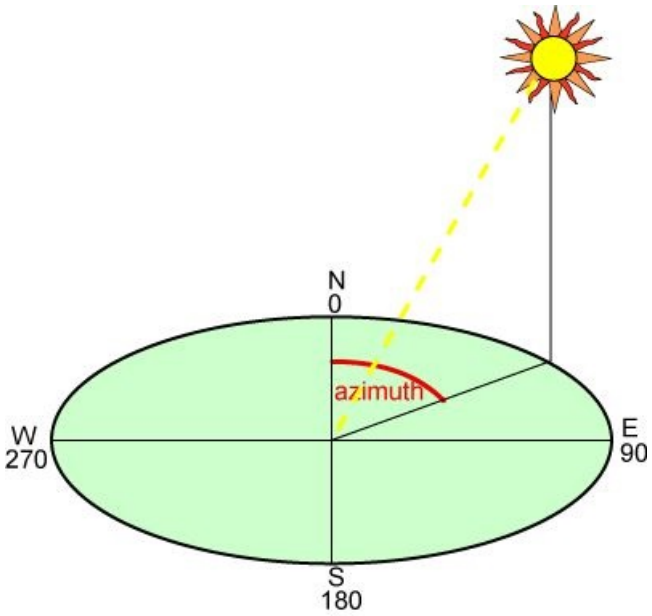


Figure 1.9: sun's azimuth [6]

fully using the solar altitude angle ($\alpha$s) and the solar azimuth angle ($\gamma s$).

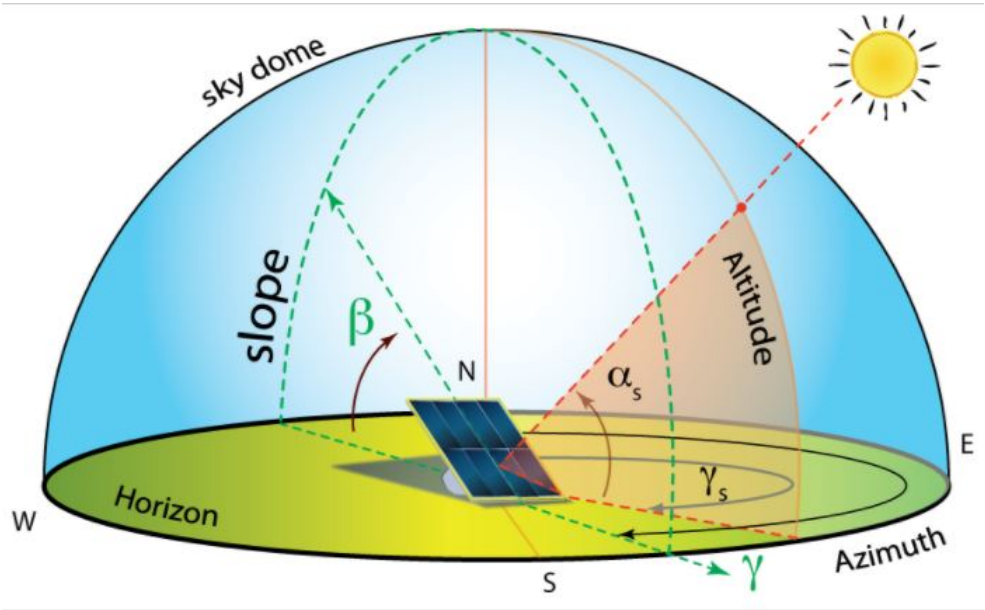


Figure 1.10: Orientation of a solar collector [6]

## 1.6 Solar times

### 1.6.1 True solar time (Tsol)

The sun rotates in the plane of the equator by 360° in 24 hours, i.e. 15° per hour, so there is a simple relationship between the true solar time TSV and the hour angle $\omega$ [24].

$$\omega = 15.(Tsol - 12) \tag{6}$$

### 1.6.2 Mean Solar Time (MST)

The path of the earth around the sun is elliptical (Kepler's first law). During this motion, the Sun-Earth vector ray sweeps equal areas in equal times (Kepler's second law). All this, added to the fact that the Earth's axis of rotation is inclined to the ecliptic plane, means that the length of the true solar day varies according to the time of year[20].
We then introduce the notion of mean solar time (MST) which varies by ±16mn with respect to true solar time (Tsol) which corresponds to the equation of time. MST is given by the following relation [24] :

$$MST = Tsol - ET \tag{7}$$

Where ET is the corrective term called the time's equation The sun rotates in the plane of the equator by 360° in 24 hours, i.e. 15° per hour, so there is a simple relationship between the true solar time TSV and the hour angle $\omega$[24].

$$\omega = 15(Tsol - 12) \tag{8}$$

$$ET = -0.0002 + 0.4197cos(0.984j) - 7.3509sin(0.984j) - 3.2265cos(20.984j) - 9.3912sin(20.984j) - 0.0903cos(30.984j) - 0.3361sin(30.984j) \quad (9)$$

### 1.6.3 Universal Time (UT)

Universal time is equal to the mean solar time of the prime meridian (Greenwich meridian). It is expressed as follows [1]:

$$UT = MST + \frac{L}{15} \quad (10)$$

with L: the longitude given in degrees and the times in hours.

### 1.6.4 Legal time (LT)

Legal time is the time we read on clocks and is given by the following relationship [1]:

$$LT = UT + C1 + C2 \quad (11)$$

With : C1 is the time difference from Greenwich Mean Time

C2 is summer and winter time, if applicable.

### 1.6.5 Sunrise and sunset

The hour angle at sunrise and sunset corresponds to = 0, by replacing in formula (1.3), we find:

$$\omega r = arc(-tan\delta.tan\phi) \quad (12)$$

According to the relation (1.7) the solar time at sunrise has therefore the expression:

$$(Tsol)s = 12 - \frac{\omega r}{15} \quad (13)$$

The hour angle $\omega$ c at sunset is the opposite of the hour angle at sunrise, Therefore, $\omega s = -\omega r, the\ solar\ time\ at\ sunset\ has\ the\ value$ :

$$(Tsol)s = 12 - \frac{\omega s}{15} = \frac{\omega r}{15} \tag{14}$$

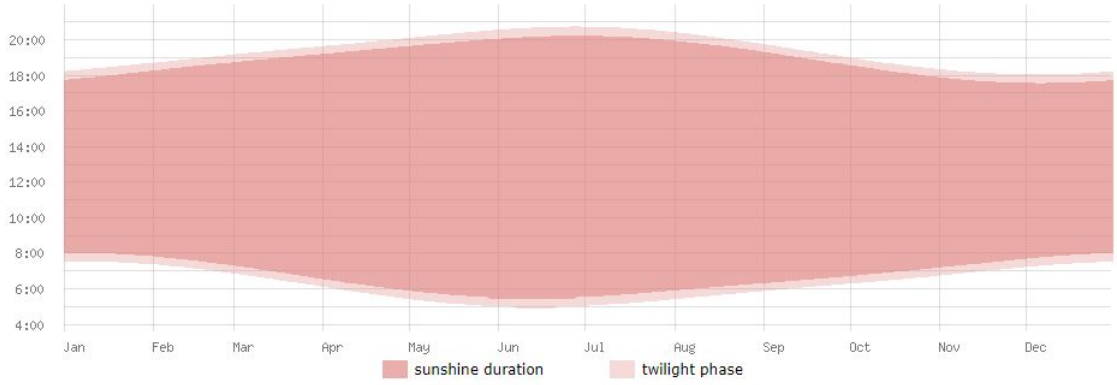


Figure 1.11: Modeling of sunset and sunerise time in algeria [8]

### 1.6.6 The length of the day

The duration of the day is given by the following formula [24]:

$$d = (Tsol)s - (Tsol)r = 2x\frac{\omega l}{15} \tag{15}$$

## 1.7 Solar radiation

The radiation emitted by the sun is the external manifestation of the nuclear interactions nuclear interactions that take place in the core of the sun and the set of secondary interactions that they generate in its envelope. This radiation constitutes almost all of the energy expelled by the sun [25] .

The thermonuclear reactions produced in the core of the sun generate particle and electromagnetic radiation and electromagnetic radiation propagating in all directions in the vacuum with a speed of $3x10^8$ m/s and covering all wavelengths from X-rays

and gamma rays to the far infrared. However 99.9% of the energy is between 0.2 and 0.8 $\mu m$.

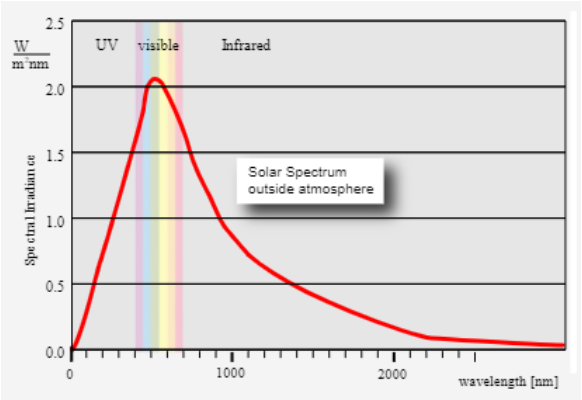


Figure 1.12: Solar spectrum outside the atmosphere [9]

### 1.7.1 The spectrum of solar radiation

The spectrum of solar radiation can be approximately divided into ultraviolet (UV), visible light, infrared (IR) and long wavelength (heat).

### 1.7.2 Solar radiation

solar radiation is the energy received over a certain period of time. It depends on several parameters such as: season, latitude and orientation of the receiving surface.

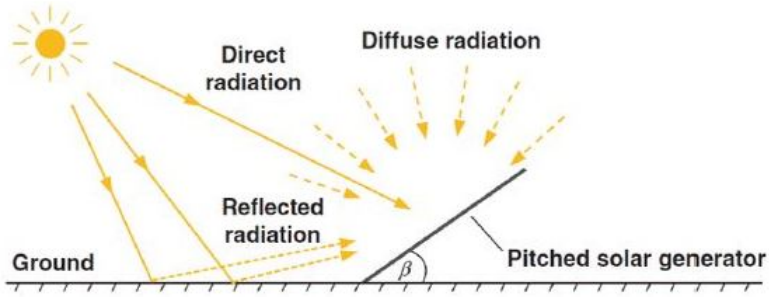


Figure 1.13: Solar radiation types [6]

Such radiation consists mainly of :

**Direct radiation**

is the radiation that passes through the atmosphere without undergoing it is received directly from the sun, without diffusion through the atmosphere, its rays are parallel to each other. are parallel to each other.

**diffused radiation**

is the part of the solar radiation scattered by solid or liquid particles suspended in the atmosphere. solid or liquid particles suspended in the atmosphere (air, clouds, aerosols, etc.). It does not have a preferred direction.

**Global radiation** is the sum of direct and diffused radiation.

**The albedo**

A part of the incident solar radiation is reflected by the atmosphere (mainly by clouds) and by the ground. This is the albedo flux [25].
It is the ratio of the solar energy reflected by a surface to the incident solar energy.

### 1.7.3 Attenuation of solar radiation (role of the atmosphere)

Solar energy is attenuated by various atmospheric components such as air molecules, aerosols, gases air molecules, aerosols, gases, cloudy water droplets or ice crystals suspended in the atmosphere ice crystals suspended in the atmosphere...
In fact , it undergoes transformations as it passes through the atmosphere by absorption and diffusion.
The absorption is selective and depends mainly on 4 elements, which are :
- Ozone which forms a screen and stops UV (<0.28m) harmful to life. Oxygen which absorbs narrow bands of the visible spectrum (around 0.69 and 0.76m).
- Carbon dioxide which absorbs part of the far IR (>2m). Water vapour which causes multiple absorption bands especially in the IR, it is found almost only at ground level (Z<5km).
- Dust and clouds are also important in the scattering of solar radiation.

**The influence of atmospheric components on the spectral distribution**

The influence of atmospheric components on the spectral distribution of direct and diffuse solar radiation can be seen in the following figure 1.14:

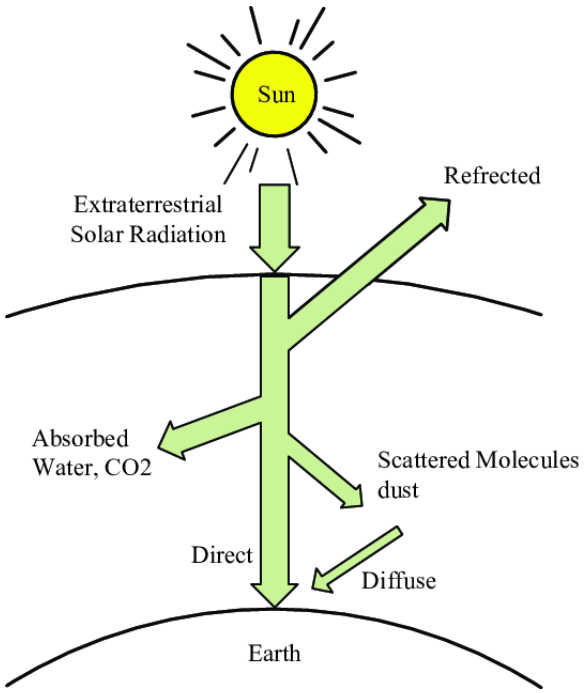


Figure 1.14: Attenuation of solar radiation as it passes through the atmosphere [6]

### 1.7.4 Sunshine rate

Under clear, cloudless skies, the ground receives direct solar radiation for the entire duration of the day, or more precisely for the maximum sunshine duration. The sunshine rate is defined as the ratio between the actual and the maximum sunshine duration.

### 1.7.5 The solar potential in Algeria

The solar potential is a set of data describing the evolution of available solar radiation over a given period. It is used to simulate the operation of a solar energy system and to of a solar energy system and to make a dimensioning as exact as possible taking into account the demand to be met. Due to its geographically solar deposit as shown in Figure 1.15 :

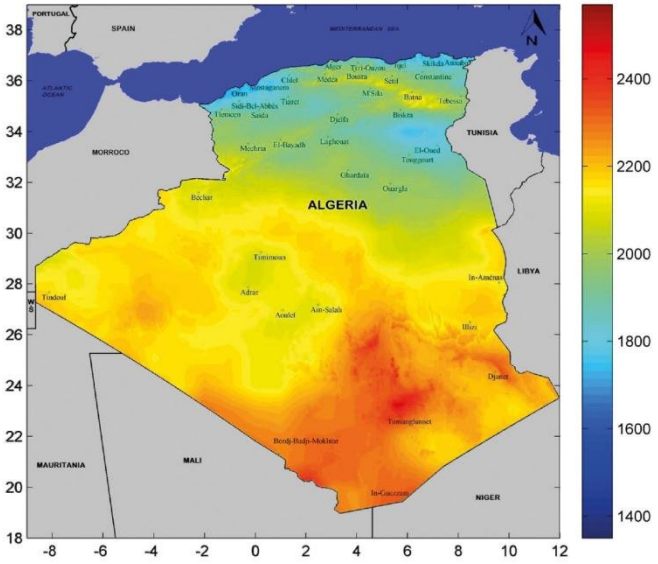


Figure 1.15: Solar radiation potential in algeria [10]

Following a satellite evaluation, the German Space Agency (ASA) has concluded that Algeria has the largest solar potential in the Mediterranean region, i.e. 169,000 TWh/year for solar thermal, 13.9 TWh/year for solar photovoltaic. Algeria's solar potential is the equivalent of 10 large natural gas deposits that would have been discovered in Hassi R'mel [26]

The duration of insolation in the Algerian Sahara is of the order of 3500 h/year and is the highest in the world; it is always higher than 8 hours per day and can reach 12 hours per day during the summer, with the exception of the extreme south where it drops to 6 hours per day during the summer. The Adrar region is particularly sunny and has the greatest potential of all Algeria.

## 1.8 Modes of Heat Transfer

There is a total of 3 Modes of Heat transfer which is: 1. Conduction

2. Convection

3. Radiation

### 1.8.1 Conduction

In conduction, heat or energy is transmitted by physical interaction, such as when you touch a hot object with your palm. When we heat the iron on one side, the molecules contained in it migrate to the other side and heat the field as well. As a result, we can assume that Conduction is equivalent to Direct touch. It is known as the transfer of heat by molecular agitation within a material without the material as a whole moving [27].

**Heat Conduction Rate Equations (Fourier's Law) :**

Heat Flux :

$$q = -k.\frac{dT}{dx} \tag{16}$$

k : thermal conductivity W/m.K

### 1.8.2 Convection

Heat or energy is transmitted by mass motion of a substance, such as air or water, as warm fluid is induced to travel away from the source of heat-carrying energy [27].

**Heat Convection Rate Equations (Newton's Law of Cooling) :**

Heat Flux :

$$q = h(T_f - T_s) \tag{17}$$

h : Convection Heat Transfer Coefficient $W/m^2.K$

### 1.8.3 Radiation

The Radiation is defined as Everybody emits radiation in the form of an electromagnetic wave or rays or particles. In this process does not require a medium to transfer the Thermal (Heat) energy [27].

**Heat Radiation power :**

$$E_b = e\sigma T^4 \tag{18}$$

e : emissivity $(0 \leq e \leq 1)$

$\sigma$ : $Stefan - Boltzmann's\ constant\ W/m^2.K^4$

## 1.9 Solar water heaters

A solar water heater is a solar energy collection device designed to provide to supply domestic hot water (DHW) partially or totally. This type of heating generally complements other types of water heating using other energy sources (electricity, fossil fuels, biomass, etc.). In favourable conditions it can replace them completely. An individual solar water heater (ISWH) makes it possible to capture solar energy to provide hot water to provide hot water for various uses: sanitary, washing machine, swimming pool, etc. It consists mainly of thermal solar collectors and a hot water storage tank. and a hot water storage tank. Types of solar water heaters.

### 1.9.1 Types of solar water heaters

The energy intercepted by the solar collector and converted into heat is transmitted to the and transferred to a storage tank. Thus, depending on the nature The energy intercepted by the solar collector and converted into heat is transmitted to the heat transfer fluid and transferred to a storage tank.

**Thermosiphon ISWH**

Under the effect of solar radiation, the water contained in the collector heats up and its density decreases, according to the gravitational principle. density decreases, according to the principle of gravitation it rises in the circuit and is replaced by replaced by colder (and therefore heavier) water from the tank. This is the the thermosiphon effect. In order for the fluid to circulate in the circuit, the storage tank

must be placed storage tank must be placed higher than the collectors according to a predefined height. predefined height.

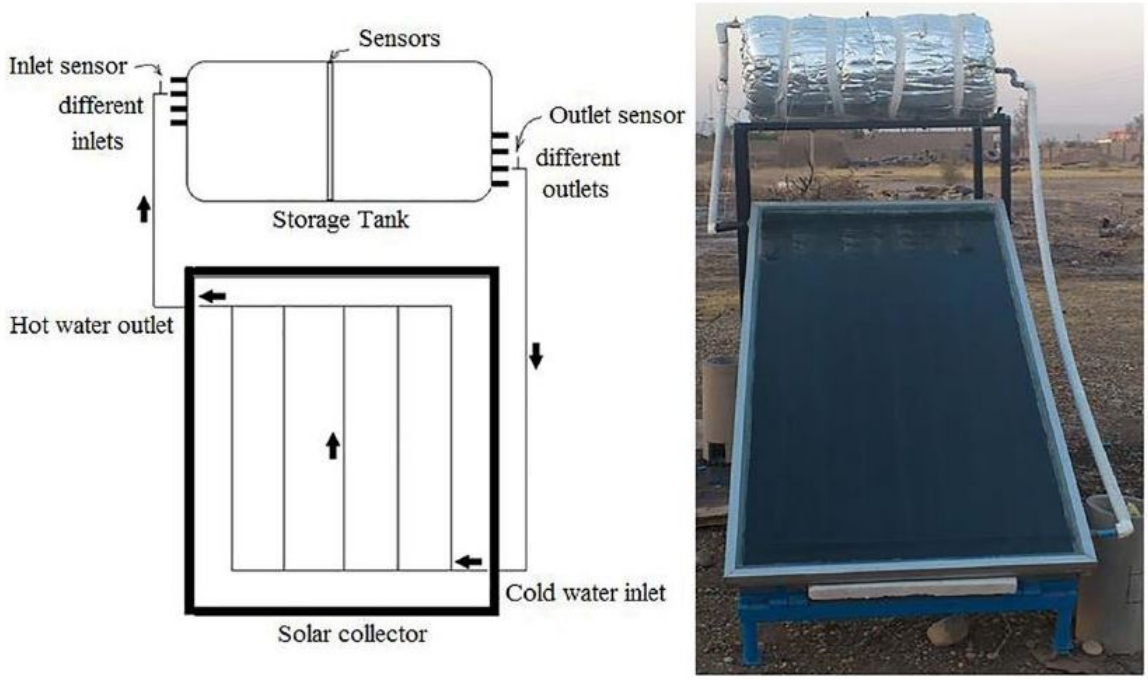


Figure 1.16: Thermosyphon SWH and its schematic [11]

The advantages of a thermosiphon SWH are:

-It does not require pumps or regulation, and does not need to be connected to an electrical It does not require connection to an electrical network.

-The risks of breakdowns and malfunctions are therefore very low.

**Forced circulation ISWH**

This category includes solar water heaters that use a circulator to transfer the water heated in the collector from the solar collector to the storage tank. Unlike thermosyphon water heaters, the relative arrangement of the storage tank and collector is completely free. This is one of the advantages of a forced circulation solar water heating system. [28]

### 1.9.2 The main components of a solar water heater

A solar water heater is composed mainly of two elements :

-The storage tank,

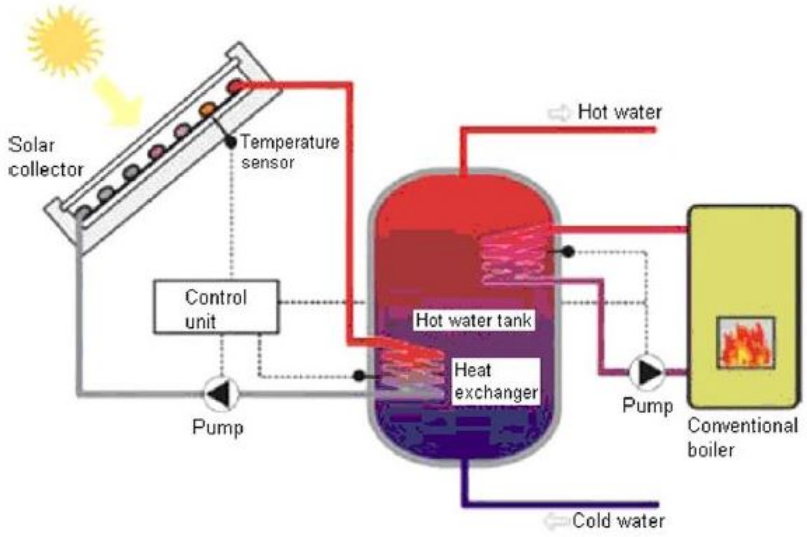


Figure 1.17: Forced circulation ISWH [12]

-The solar collector.

To which are added other components, namely: the circuit pipes, a pump, an isolating valve, an expansion tank, a safety valve, drain valves and a controller.

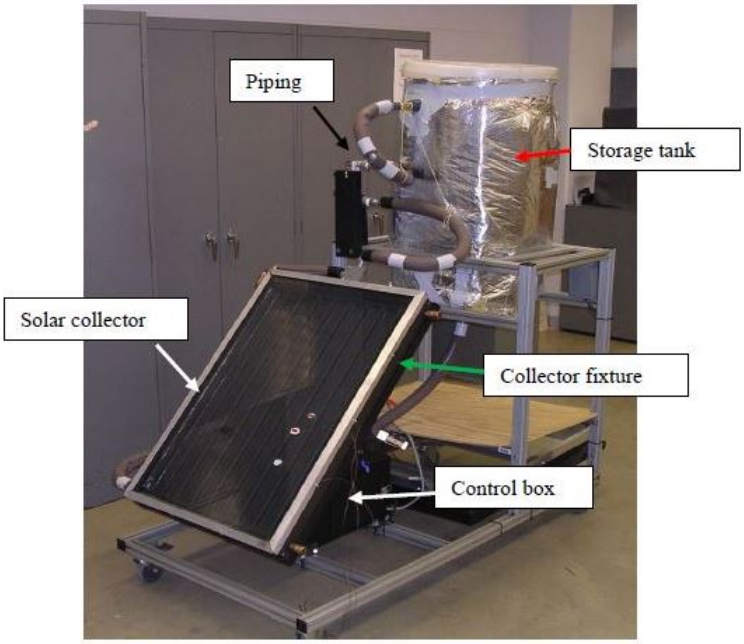


Figure 1.18: SWH components [13]

**The storage tank**

Except in specific cases (when collector area less than 20-30 $m^2$), storage tanks are " buffer" type tanks without built-in heat exchangers. In In fact, for reasons of cost and

performance, plate heat exchangers are recommended to to transfer the energy to the domestic hot water. For some applications, or more specifically some storage tank locations with low temperatures, it is storage tanks with low temperatures, tanks with internal heat exchangers are used to avoid the risk of freezing in the pipes and in the plate exchanger. In this case, the cold and hot water pipes must be well insulated. Particular attention is paid to the temperature resistance of the hot water tanks. hot water tanks.

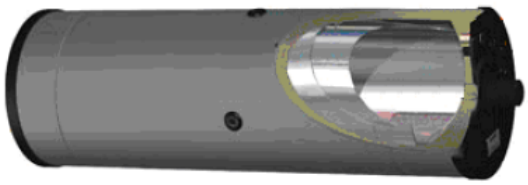

Figure 1.19: Storage tank [14]

Some products are only guaranteed if the storage temperature is 60°C or less. 60°C or lower. A minimum temperature resistance of 80°C is required for solar storage tanks. for solar storage tanks.

**The Solar collector**

Thermal solar collectors are the most important element in installations for the thermal conversion of solar energy. Solar radiation is absorbed by a black surface, through which a heat transfer fluid flows, extracting the thermal energy and transferring it to its place of installation or storage.

### 1.9.3 Other components

**Circuit piping**

Usually, the materials used for the piping are copper tubes or single steel tubes. Complete systems including the flow and return pipes as well as the cable for the sensor temperature probe and insulation. This piping system saves installation time. The primary circuit pipes should be insulated to limit heat loss between the collectors and the storage tank. The insulation of these systems can never be carried out with

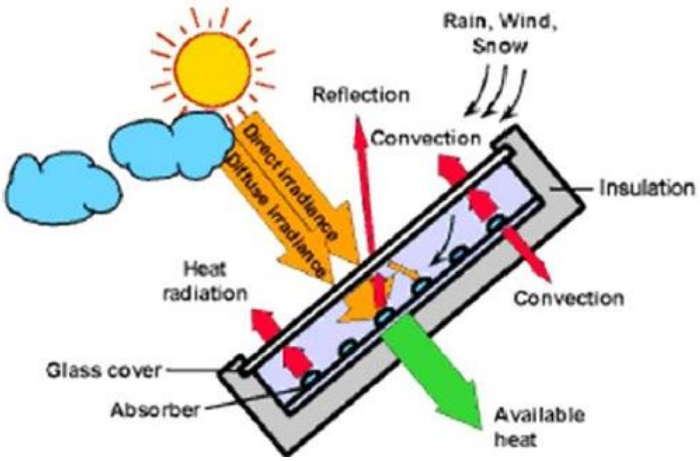


Figure 1.20: Energy balance of a solar collector [12]

the usual sanitary pipe insulation, as it is essential to take into account the temperatures at which these will be explored, the insulation usually used can withstand a continuous temperature of 150 to 180 °C.

Figure 1.21: circuit piping [14]

**A pump (circulator)**

The role of the circulator is to ensure the circulation of the heat transfer fluid in the solar loop, circulators used in central heating systems with radiator The circulators used in central heating systems with radiators (resistant to temperatures of up to 120 °C) are normally also suitable for solar water heating systems.

Figure 1.22: A pump [14]

**Non-return valve**

The non-return valve is designed to prevent a thermosyphon effect in non-drainage systems from reversing the primary circuit when the pump is stopped.

Figure 1.23: A non return valve [14]

**Expansion tank**

The expansion tank must allow the expansion of the heat transfer fluid and allow the volume of the heat transfer fluid expelled from the solar collector to be absorbed when boiling occurs, without excessive pressure rise.

Figure 1.24: Expansion tank [14]

**Safety valve**

The safety valve is used to limit the maximum pressure in the primary circuit, safety valves consist of a brass housing and can be associated with a pressure gauge, usually safety valves have opening pressures of 4 to 6 bars.

Figure 1.25: A safety valve [14]

**Drain taps**

Drain and fill taps should be placed at the lowest point of the solar circuit and on the cold water inlet in order to be able to drain the system completely.

Figure 1.26: Drain taps [14]

**Bleeders**

bleeder valves allow air to escape from the pipes, which occurs during filling and, if necessary, later during operation of the system. This occurs during filling and, if necessary, during operation of the system. The traps must be installed at the highest points of the system and are only intended for systems without draining.

Figure 1.27: A bleeder valve[14]

**The controller**

In a solar thermal system, a minimum regulation is required (except for thermosiphon systems) to control the heat exchange process between the collector and the storage tank. Therefore, in all cases, differential control is used. The basic principle of the regulation of a solar hot water system is simple. Two sensors are required: one sensor in the solar collectors, another on the return line to the collectors at the outlet of the domestic hot water storage tank, this regulation is based on the principle of an integrated comparator circuit.

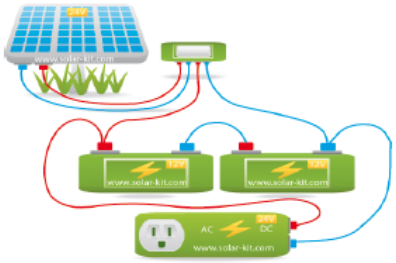

Figure 1.28: The controller [14]

## 1.10 SOLAR COLLECTORS

Solar collectors are devices whose operating principle is based on the transformation of solar energy into heat. In what's next we will see the concept, the components and the types of a solar collector.

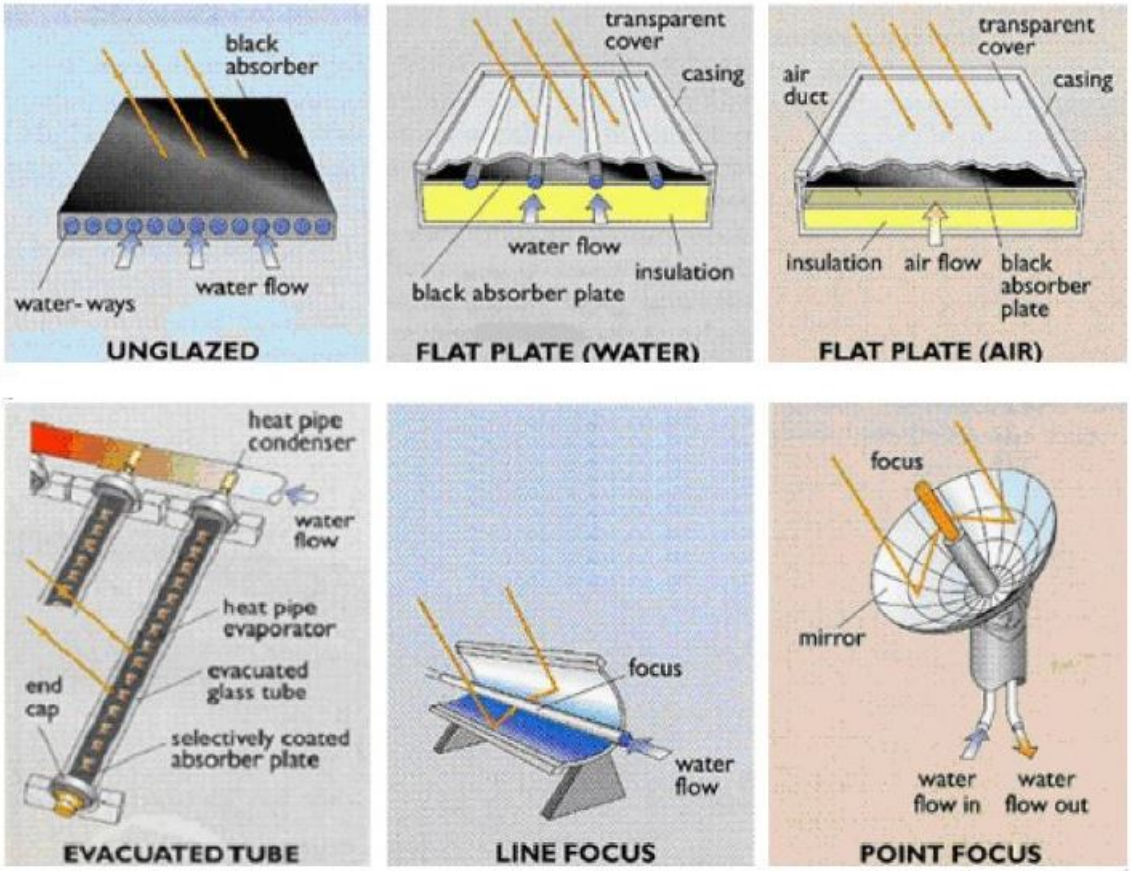


Figure 1.29: Classification of solar collectors [12]

### 1.10.1 Definition and working principle of a flat plate solar collector

A flat plate solar collector refers to all systems that are exposed to solar radiation in order to capture it and transform it into thermal energy. This collection system is based on the greenhouse effect where radiation is collected in the visible and near infrared range (wavelengths between 0.3 and 3 $\mu$m). This radiation passes through the glass of the sensor, where it is trapped inside, and then captured by the absorber surface. The absorber in turn emits thermal radiation in the far infrared range (between 4 and 30 $\mu$m). This radiation is completely stopped by the glass wall, which by the glass wall, which heats up and radiates half towards the absorber surface and half towards the outside. half towards the outside. The fluid that circulates under this wall (heat transfer fluid) recovers part of this absorbed energy by convection and undergoes a rise in temperature as it passes through [29].

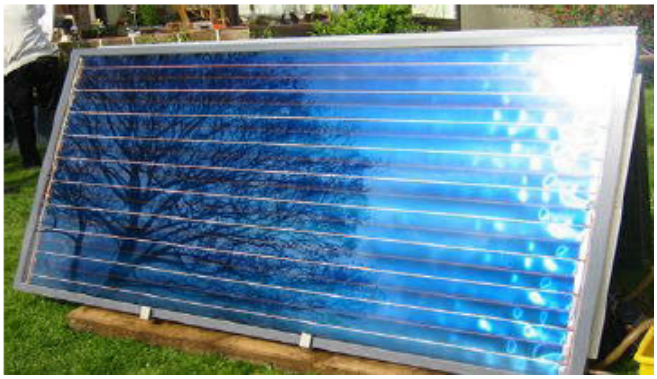

Figure 1.30: A flate plate solar collector [14]

### 1.10.2 The different types of solar collectors

In order to intercept the energy from solar radiation, there are several types of solar collectors. The following is a brief description of the five most common types of flat plate solar collectors.

**Flat plate collectors without glazing**

This is the simplest, most economical but least efficient model. It is usually made up of a simple metal or plastic plate (absorber) on which several tubes carrying the

heat transfer fluid are glued. Flat plate collectors unglazed flat plate collectors are not insulated on the front side, which is why they are better suited to applications at low temperatures (below 30°C). This type of collector is mainly used for heating outdoor swimming pools. Because they have no glazing, these collectors absorb a large proportion of the sun's energy. However, because they are not insulated on the front, much of the heat absorbed is lost when it is windy and the outside temperature is not high enough. The collectors are stirred by warm air and absorb the heat exchanged, especially during the night when the temperature is high and there is wind outside. The typical architectural integration of this type of product allows the implementation of a larger to compensate for the difference in efficiency with flat-plate glazed collectors, especially during the winter.

Figure 1.31: A Flat plate collectors without glazing [14]

**flat-plate glazed collectors (water)**

Flat-plate glazed solar collectors are very common. They are available as water collectors and air collectors. These collectors are best suited to moderate temperature applications where the desired temperatures are between 30°C and 70°C. Circulating water collectors are most commonly used for domestic hot water production on an individual or collective scale, for industrial use, and for indoor swimming pools.

**Flat plate glazed collectors (air)**

As their name indicates, they produce hot air. These collectors are used in some ventilation, soft ventilation and space heating systems. In the case of air heating, the air to be heated can be passed directly through the collector. through the collector. A

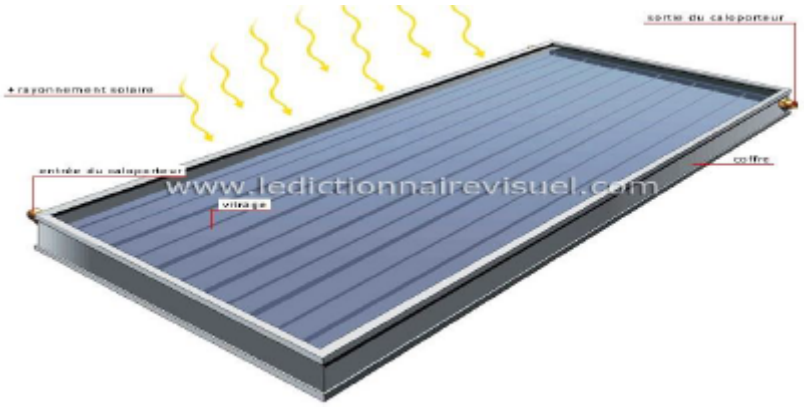


Figure 1.32: Water collector [15]

particular application of these collectors is the drying of certain agricultural products: hay, figs, apricots, etc. Note that these solar systems are light and have no cooling or boiling problems, which is an advantage over liquid collectors. Air collectors are used for drying, space heating and ventilation air. ventilation air.

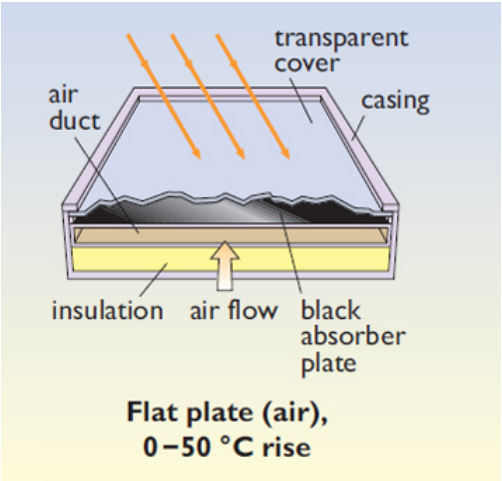


Figure 1.33: air collector [12]

**Evacuated-tube collectors**

Evacuated-tube solar collectors consist of a series of transparent glass tubes. In each tube there is an absorber plate to collect the solar radiation and an exchanger to help transfer the heat energy. The tubes are evacuated to prevent convective heat loss from the absorber plate and the absorber plate is selectively treated to prevent the radiation from dissipating in the form of long wave radiation. Thus, efficient solar collectors can be realized without solar collectors can be realised without the need for

additional thermal insulation or a protective casing.

Figure 1.34: Evacuated-tube collectors [14]

**Line focus concentrators**

This type of solar concentrators use parabolic or parabolic-cylindrical reflecting surfaces (mirrors) (figure III.9) to concentrate the sun's rays in the point or linear focus of these surfaces respectively. In the point focus or along the linear focus are the receivers (absorbers) that capture the concentrated solar heat. Naturally, these concentrators must follow the movement of the sun.

Figure 1.35: Line focus concentrator [14]

**Point focus concentrators**

These collectors use parabolic reflective surfaces to concentrate the sun's rays in the focalpoint where the absorber is located to capture the concentrated solar heat . The idea of using a parabolic surface comes from the fact that it is stigmatic (gives at the exit of the parabola a beam converging in a point) for the points at infinity located

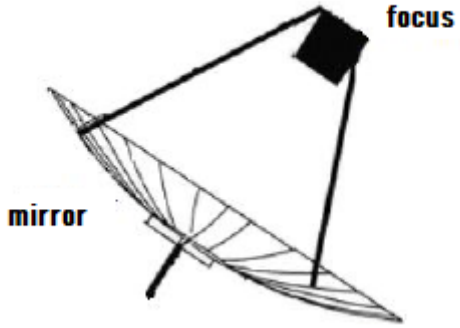


Figure 1.36: Point focus concentrator [14]

on its axis. According to the laws of reflection, any light ray parallel to the axis of the parabola is reflected by the parabola along a straight line passing through the focus. Thus the parabola focuses all reflected rays at a point called the "focus". This implies that these concentrators must follow the movement of the sun. Parabolic reflector systems can reach higher temperatures (up to 1500°) on the absorber. [30].

### 1.10.3 The main components of a glazed flat plate collector

A glazed flat plate collector consists mainly of a transparent cover (glazing) , an absorber and thermal insulation, as shown in the next figure :

**The transparent glass cover**

Because of its resistance to mechanical aggression (impact, hail, snow, etc.) and thermal aggression thermal aggression (sudden cooling, etc.), safety glass is especially used as a transparent used as a transparent cover. In order to be as transparent as possible and transmitting solar radiation, it is preferable that the glazing is low in iron oxide. For roof-integrated collectors, synthetic materials are sometimes used. They are lighter, cheaper and easier to install, but have a shorter life span than ordinary glass. than that of ordinary glass. More often, the glazing is slightly structured, so that it spreads the reflected fraction of the incident solar radiation, to reduce possible glare. The main characteristics of a glazing are :

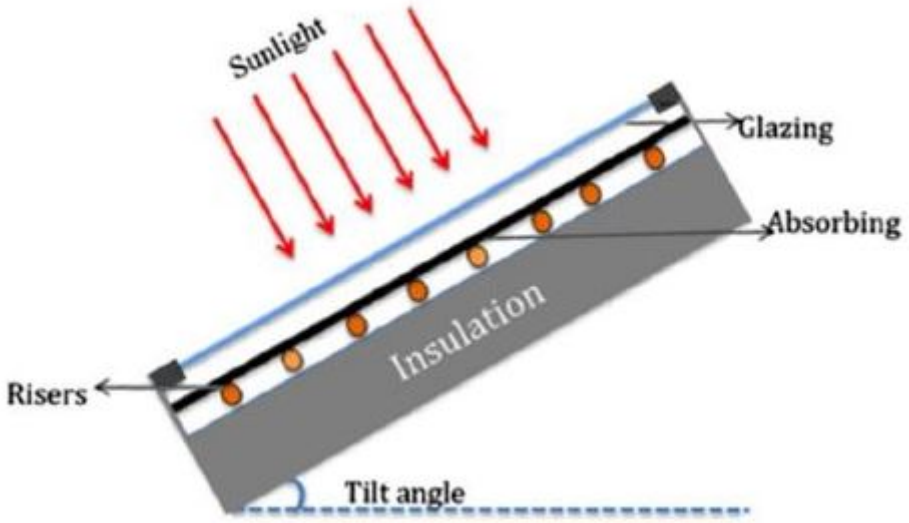


Figure 1.37: Cross section of a flate plate [16]

-Its transmission coefficient

-Its emission coefficient

The special feature of good glass is that it absorbs little solar radiation and therefore transmits the maximum amount of energy to the absorber. Currently, the most common glass used for flat collectors is prismatic glass. Its specificity is its low reflection of radiation (1.5%). It can transmit up to 96% of the radiation.

**The absorber**

The main role of an absorber is to capture solar radiation and convert it into heat energy. It is usually painted black to absorb all radiation in the visible, ultraviolet and a small amount of infrared radiation. infrared spectrum.

The absorber is chosen according to the following characteristics:

- A good absorption coefficient.
- A Good thermal conductivity.
- A Good corrosion resistance.

The choice of material and the construction process have a great influence on the quality of a sensor. Due to their high conductivity, copper, steel and aluminium are the most commonly used materials. are the most commonly used materials. In order

to reduce radiation losses, absorbers are usually coated with a selective layer. Nickel and chromium are the main metals used for selective for selective coatings for most collectors.

**The heat transfer fluid**

To remove the heat stored by the absorber plate, either air or water is generally used as the heat transfer fluid. Compared to water, air has the following advantages:
- It does not have problems with freezing in winter or boiling in summer.
- Dry air has no corrosion problems.
- Ther is no air leakage problem.
- There is no need to use a heat exchanger in the case of space heating.
- The system to be implemented is simpler and more reliable.

The use of air instead of water has the following disadvantages:
- Air can only be used for space heating.
- The pipes must have a large cross-section to allow sufficient flow.
- Heat transfer is less good than with water.

In the case of pipes welded to the back of the absorber plate, care must be taken with the welds to reduce the risk of care must be taken with the welds to reduce the thermal contact resistance as much as possible resistance [20].

**Insulation**

A collector must be well insulated with suitable materials. These materials should have a low thermal conductivity to minimise heat loss by conduction through the conduction through the faces of the collector. Typically, the thickness of The thickness of the insulation is usually in the order of 5 to 10 cm. Mineral wools, synthetic materials (glass wool, expanded foams, etc.) are used. glass wool, polyurethane foam or polystyrene) are generally the insulating materials used. insulating materials used. They must be able to withstand the high temperatures that can be reached inside a collector. For an optimal choice of an insulating material, the following parameters should be considered:

- Density
- Maximum operating temperature
- Resistance to fire, rodents and rot
- Sensitivity to moisture
- Its cost

**Frame**

The enclosure, commonly made of aluminium or wood, encloses the absorber and the thermal insulation of the collector, protecting them from moisture and mechanical damage.

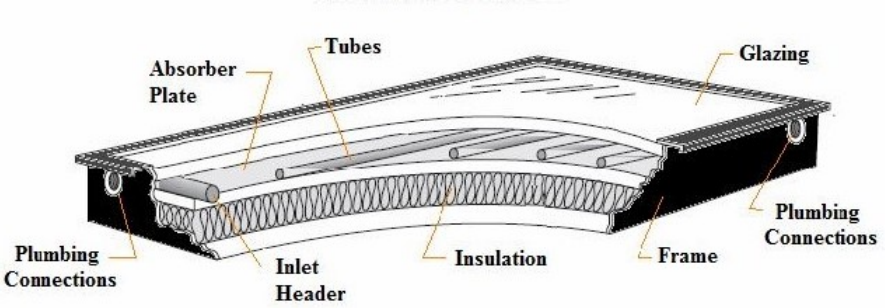


Figure 1.38: Flate plate collector [17]

### 1.10.4 How does a flat plate collector work

Part of the solar radiation that reaches the glass pane passes through it to reach the absorber plate. This plate heats up and transfers the heat to the heat transfer fluid which circulates in the tubes. Like any body that heats up, the absorber emits radiation (mainly in the infrared range) which is reflected by the glass, this is the This is the principle of the "greenhouse effect". The function of the insulator is to minimise heat loss to the outside. with the outside. Indeed, most of the energy absorbed must be transmitted to the fluid. to the fluid, so losses to the surrounding environment must be minimised.

**ADVANTAGES:**

-Economical price

-Reliability

-Long service life

-Energy efficiency

-Integration into roofs

**Disadvantages:**

-Not suitable for high temperatures

-The internal temperature can rise very high when there is no liquid circulation.

### 1.10.5 Parameters characterising the operation of a flat plate collector

These parameters can be classified into two categories: external and internal parameters.

**External parameters**

The main external parameters that can directly influence the performance of a flat plate collector are:

-solar radiation, position of the sun, duration of insolation, ...etc

-Ambient temperature

-Wind speed

**Internal parameters**

**Geometric parameters:**

-Positional parameters: tilt angle, orientation of the collector.

-The surface of the collector

-Dimensions of different elements: thickness, length and width

**Working parameters:**

-The inlet temperature of the heat transfer fluid.

-The mass flow rate of the heat transfer fluid.

-The temperatures of the different elements of the collector

These parameters are very important. They allow, taking into account the cost, to have a high fluid outlet temperature (high power output). In other words, a better efficiency of the collector.

# Chapter 2

# mathematical modeling

## 2.1 Introduction

To solve a fluid mechanics or heat transfer problem, it is possible to solve it either mathematically (analytical solution) or numerically (numerical solution). The analytical solutions, based on the local form of the problem (Partial Differential Equations: "PDE" associated with initial and boundary conditions), cannot be determined in the case. The problem under study (the flow and heat exchange inside a flat plate solar collector) is modeled by the partial differential equations of conservation of mass, momentum and energy. These equations are known as the Navier-Stokes equations. These equations are strongly coupled to each other and they are not linear. In general, these equations do not admit analytical solutions except in very simplified cases [31]. The general analytical solution of these equations fits into in the seven millennium problems. The objective of this chapter is therefore to present the mathematical model governing the problem studied. First, the geometry of the sensor studied will be presented. Then, the mathematical formulation of the Navier-Stokes equations will be presented for the two flow regimes: laminar and turbulent.

## 2.2 Setting up the problem into equations :

The advantage of writing the differential equations describing the turbulent flow in general form is to construct a general numerical procedure that applies for the different equations considering the specific boundary conditions. It is known that for some cases of simple flows an exact analytical solution is possible. For the general case of turbulent flows, the system of Navier-Stockes equations cannot be solved directly due to the non-linearity of the equations and the appearance of the Reynolds constraints of the turbulence as new unknowns in the transport equations. The system of equations is closed using turbulence models. In fluid mechanics, the fluid is assumed to be a continuous, which allows the use of the classic conservation laws, which are [18][19]: 1. Conservation of mass. 2. Conservation of momentum. 3. Conservation of energy.

The mathematical formulation of conservation laws governing physical phenomena, such as fluid flows, is usually written in the form of partial differential equations as follows:

### 2.2.1 Continuity equation :

The differential equation describing the principle of conservation of mass and is expressed mathematically, for the case of a stationary flow, as :

$$\frac{\partial}{\partial t}\rho + \frac{\partial}{\partial x}(\rho.u) + \frac{\partial}{\partial y}(\rho.v) + \frac{\partial}{\partial z}(\rho.\omega) = 0 \tag{1}$$

Where t is time, u v and w are the components of the fluid velocity in the x, y and z directions respectively.

or in a more compact notation, we have :

$$\frac{\partial}{\partial t}\rho + div(\rho u) = 0 \tag{2}$$

for an incompressible fluid we have : $\frac{\partial u}{\partial x + \frac{\partial v}{\partial y} + \frac{\partial w}{\partial z} = 0}$

Physically, it represents the change in properties with time following a given element of mass as it moves through the fluid.

### 2.2.2 Momentum equation :

The principle of conservation of momentum establishes the relationships between the characteristics of the fluid as it moves and the causes that produce it. It states that the rate of change of momentum contained in the control volume is equal to the sum of all external forces applied to it. The momentum equations (or Navier-Stokes equations) for incompressible Newtonian fluids in the laminar regime are given by the following expressions : following x :

$$u\frac{\partial u}{\partial x} + v\frac{\partial u}{\partial y} + w\frac{\partial u}{\partial z} = -\frac{1}{\rho}\frac{\partial P}{\partial x} + \mu\left(\frac{\partial^2 u}{\partial x^2} + \frac{\partial^2 u}{\partial y^2} + \frac{\partial^2 u}{\partial z^2}\right) \tag{3}$$

following y :

$$u\frac{\partial v}{\partial x} + v\frac{\partial v}{\partial y} + w\frac{\partial v}{\partial z} = -\frac{1}{\rho}\frac{\partial P}{\partial x} + \mu\left(\frac{\partial^2 v}{\partial x^2} + \frac{\partial^2 v}{\partial y^2} + \frac{\partial^2 v}{\partial z^2}\right) \tag{4}$$

following z :

$$u\frac{\partial w}{\partial x} + v\frac{\partial w}{\partial y} + w\frac{\partial w}{\partial z} = -\frac{1}{\rho}\frac{\partial P}{\partial x} + \mu\left(\frac{\partial^2 w}{\partial x^2} + \frac{\partial^2 w}{\partial y^2} + \frac{\partial^2 w}{\partial z^2}\right) \tag{5}$$

### 2.2.3 Energy equation :

It is derived from the law of conservation of energy. It is written as follows:

$$\left(\frac{\partial\left(\rho u T\right)}{\partial x} + \frac{\partial\left(\rho v T\right)}{\partial y} + \frac{\partial\left(\rho w T\right)}{\partial z}\right) = \frac{\partial}{\partial x}\left[\left(\frac{\mu}{Pr}\right)\frac{\partial T}{\partial x}\right] + \frac{\partial}{\partial y}\left[\left(\frac{\mu}{Pr}\right)\frac{\partial T}{\partial y}\right] + \frac{\partial}{\partial z}\left[\left(\frac{\mu}{Pr}\right)\frac{\partial T}{\partial z}\right] \tag{6}$$

Where: u, v and w represent the velocities of the flow in the x, y and z directions respectively. P is the pressure. T, is the temperature. , is the dynamic viscosity of the fluid. Pr= .Cp / $\lambda$ , represents the Prandtl number.

The set of all equations (1 to 6) forms the Navier-Stokes equations for a Newtonian, stationary, three-dimensional, viscous (non-perfect) fluid.

### 2.2.4 Flow regimes : Laminar and turbulent

A flow is laminar when the movement of the fluid particles is regular and orderly. Flow is turbulent when the motion is irregular and random fluctuations in velocity are superposed on the mean motion of the fluid. One of the first analyses of the transition from a laminar regime to turbulence, based on observations of flows in a cylindrical duct, was performed by Reynolds in 1883 [32]. Reynolds showed that the transition from the laminar to the turbulent regime does not depend separately on each parameter but on a single quantity grouping them all together. For a viscous fluid of density $\rho$ and dynamic viscosity , passing through a pipe of diameter D with an average velocity U, the Reynolds number (Re) is defined as: Re = $\rho$UD/ $\mu$ [18] [33].

The Reynolds number is a dimensionless quantity representing the ratio of inertial forces to viscosity forces, and characterises the occurrence of turbulence [33]. Experience shows that for internal flows (flows in pipes), the critical Reynolds number (Re cr) for switching from laminar to turbulent is approximately equal to Re cr= 2300.

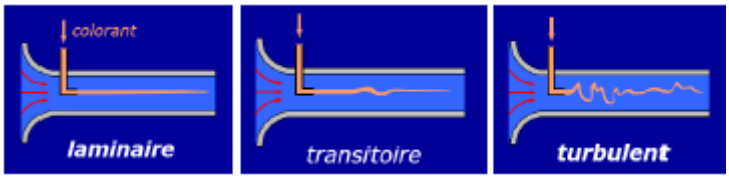


Figure 2.1: the transition from the laminair to the turbulent regime: the reynlods experience [18]

**Description of turbulence :**

Most flows found in the real world are turbulent, the term actually denoting a motion in which an irregular fluctuation is superimposed on the main flow. the main flow. Turbulence is governed by the Navier-Stokes equations, as it is characterised by spatial and temporal scales of very different sizes. According to Reynolds [32] turbulence is defined by the irregular and random motion in space and time, which appears significantly in flows with high Reynolds numbers.

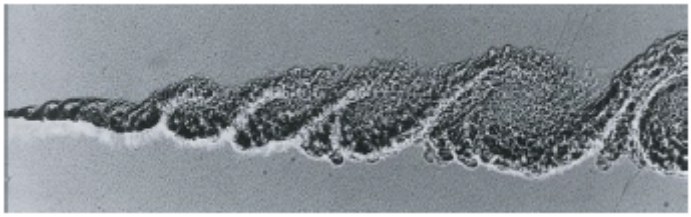

Figure 2.2: visualisation of a turbulent flow [19]

## 2.3 Principle of the finite volume method:

The finite volume method was first described in 1971 by Patankar and Spalding and published in 1980 by Patankar (Numerical Heat Transfer and Fluid Flow). It is a discretization technique that converts conservation partial differential equations into algebraic equations that can be solved numerically. In this method the domain is divided into a finite number of control volumes that cover the computational domain. The control volume technique consists of the integration of the partial differential equations over each control volume to obtain discretised equations that preserve all physical quantities over a control volume. On each control volume or cell the conservation laws are applied to determine the different variables associated with the problem at points (or nodes) that do not necessarily correspond with the points of the mesh or grid. The mesh associated with the calculation can be structured or unstructured as for example in finite elements, which gives a great flexibility to the method.

**advantages:** - Preservation of the conservative character of the equations on each control volume (continuity of the flows at the interfaces), valid for any fineness of the mesh - Relatively easy to implement; - Applicable to complex geometries; - Reasonable computation time and memory storage (tape type matrix).

**Disadvantages:** - Less accurate than spectral methods.

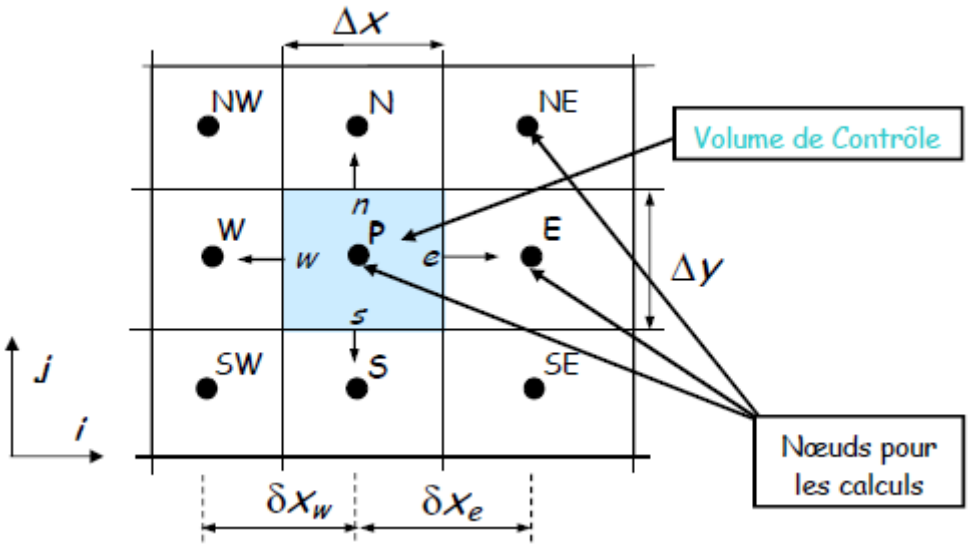


Figure 2.3: structured mesh

### 2.3.1 Description of a control volume

In finite volume simulation, the computational domain is divided into a finite number of elementary subdomains, called control volumes. The finite volume method consists of integrating the partial differential equations over each control volume. Each of these (control volume) contains a node called the node. An example of a control volume is shown in (fig 2.4). For a main node (P'), the points E and W (E: East, W: West) are neighbours in the X direction, while N and S (N: North, S: South) are neighbours in the Y direction. The surrounding control volume (P') is shown by the dashed lines. The faces of the control volume are located at points (e) and (w) in the X direction, (n) and (s) in the Y direction [34].

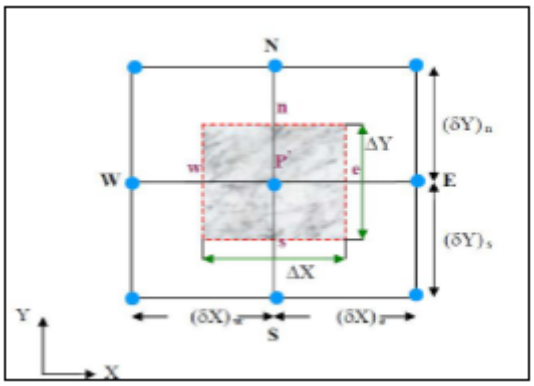


Figure 2.4: schematic representing a two-dimensional control volume

## 2.4 Subdivision of the study domain (mesh)

The location of the variables of the problem to be computed is defined by the mesh (or grid) which corresponds to a discrete representation of the physical domain to be represented. The computational domain is then divided into a finite number of elements and control volumes that do not necessarily coincide (as we will see later). The distinction we make here between elements and control volumes is essential. We call here an element a surface or a 3D volume created from points and which is only used in the construction of the mesh and allows the spatial discretisation of the medium. The control volume corresponds to a surface or a volume in which the balance equations are calculated. The discretization of the domain is obtained by a mesh consisting of a network of points (nodes).

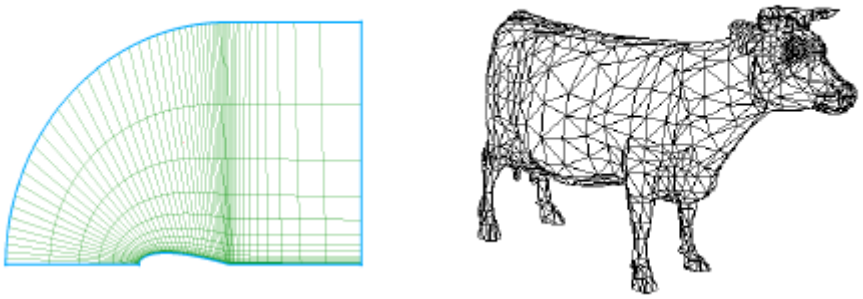

Figure 2.5: Examples of the structured (left) and untructured mesh (right)

The possibilities offered by the finite volume method are very varied and We present here only an overview of the most commonly used meshing techniques:

### 2.4.1 STRUCTURED MESHES

In this category the possibilities are numerous, the calculation grid can be regular, or structured by blocks, with or without overlapping subdomains. The calculation grid can be regular, or structured by blocks, with or without overlapping subdomains. In general, the implementation of the finite volume method is easier in this category, it often leads to simpler numerical schemes and in particular to " band " structures of the matrix systems to be solved when using an implicit scheme for example. The associated data structure is simplified compared to a non-structural finite element mesh and the method is more efficient in terms of computation time. However, complex domains are difficult to represent.

#### CARTESIAN STRUCTURAL GRIDS

In this category we find the purely cartesian grids, i.e. the dimensions of the elements are parallel to the axes of a cartesian reference frame and which and can therefore be created very easily. It can be regular (Figure 2.6), i.e. that two neighbouring points are always at the same distance, or irregular if this is not the case. or irregular if this is not the case.

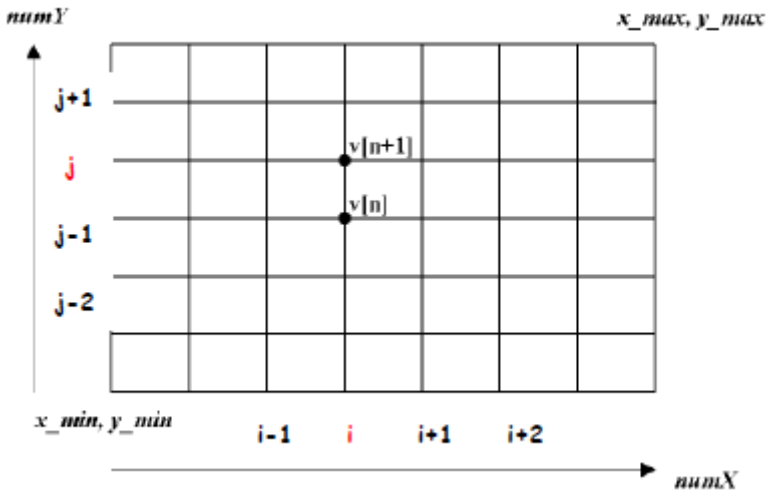


Figure 2.6: regular cartesian grid

The positions of the grid points are then simply marked by a set of two or three

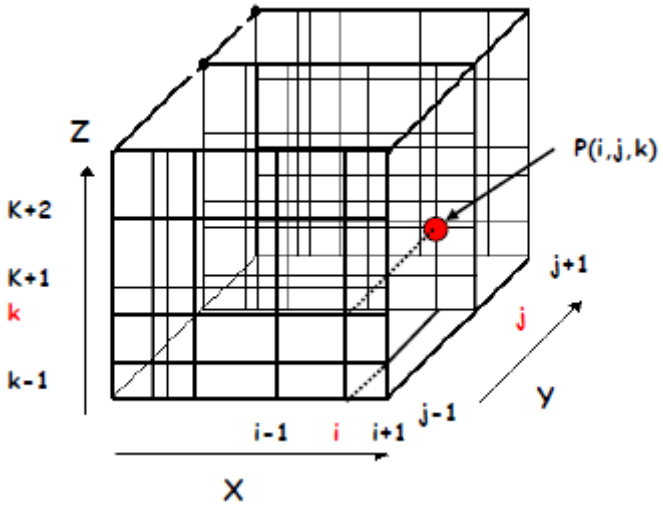


Figure 2.7: irregular cartesian grid

indices i,j,k. Each grid point thus has 4 "close" neighbours in 2D and 6 for a three-dimensional mesh. This makes it very easy to identify the neighbours of a grid node, which greatly simplifies the programming of the method and allows us to obtain matrices whose regular structure can be exploited for an efficient resolution with an implicit scheme.

**CURVILINEAR STRUCTURAL GRIDS (BODY FITTING)**

This technique allows better representation of boundary conditions for more complex geometries. It requires a transformation from the physical to the computational domain. The equations to be solved are then more complex, which makes the calculations more complex and requires precautions if we want to keep the conservative character of the numerical schemes used and keep a good accuracy. In general, this method is rarely used with finite volumes, but is used to construct the mesh, the equations being solved directly on the physical domain.

**BLOCK STRUCTURED GRIDS**

When using a structural mesh it is very difficult to represent complex geometries, especially in 3D. To represent more "industrial" geometries and for example to refine some parts of the mesh, a block structure mesh can be used. Cartesian or

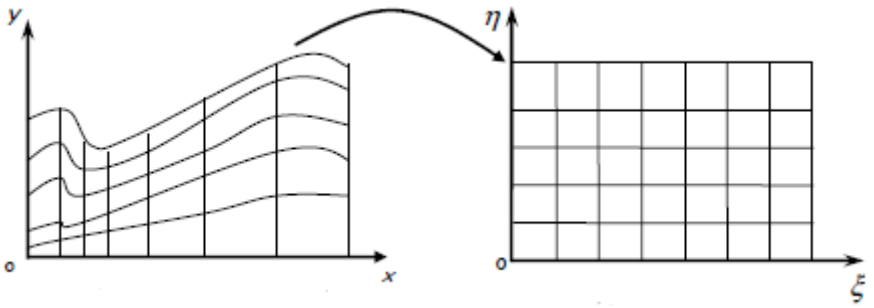


Figure 2.8: Transformation from physical domain to computational domain

non-orthogonal grids can be used. In the case where there is perfect coincidence between the different blocks, the method is then particularly efficient on parallel machines or in the calculations, each block can be attributed to a processor.

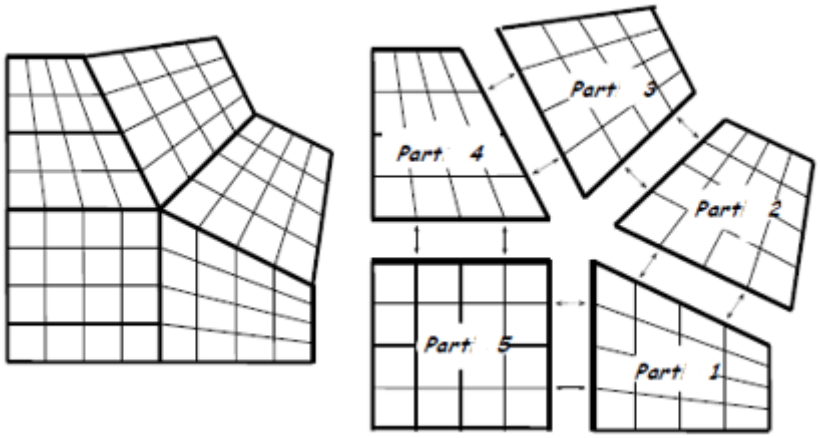


Figure 2.9: BLOCK STRUCTURED GRID

It is not necessary, however, that there be a perfect match at the interface of each block. the interface of each block. This is referred to as non-conforming grids or grids with non-conforming interfaces. In this case we add some complexity to the solver because a particular treatment of the interfaces is necessary to calculate the flows. On the other hand, it is possible to build the different domains separately and use finer meshes in certain regions (or blocks) or to "glue" two different meshes. Again this method offers interesting possibilities for implementation on parallel machines using the sub-domain method.

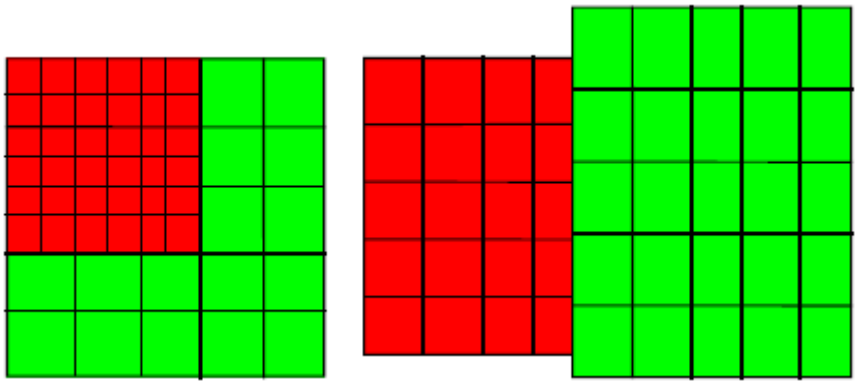

Figure 2.10: refined mesh (left) and different mesh (right)

**Composite mesh (Chimera grid)**

In this method, several blocks are used to represent the domain, for which there is an overlap of grids. In regions where there is overlap of several grids, the boundary conditions between the domains are obtained by interpolating the solutions of the different domains. This method makes it easier to deal with very complex geometries while using a structural mesh. This method is used, among other things, to track the motion of solid bodies. In this case a block is attached to the moving body and moves with it while a fixed grid covers the rest of the domain.

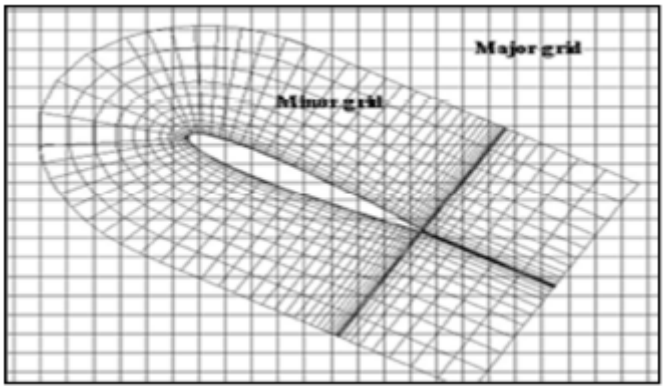


Figure 2.11: chimera grid

The advantage of this method is the possibility of creating meshes that are completely independent of each other, without any coincidence between the interfaces of the different domains. The major difficulty that arises is related to the flow conservation properties that are difficult to obtain and implement at the

interfaces of the different domains.

### 2.4.2 UNSTRUCTURED MESHES

This category of meshes offers the greatest flexibility in the construction of complex geometries. Indeed it is always possible to create meshes (or grids) automatically with 2D triangles (and 3D tetrahedrons), regardless of the complexity of Whatever the complexity of the domain envelope. In practice we prefer to use quadrangles and hexaedra which allow to obtain a better precision in calculations.

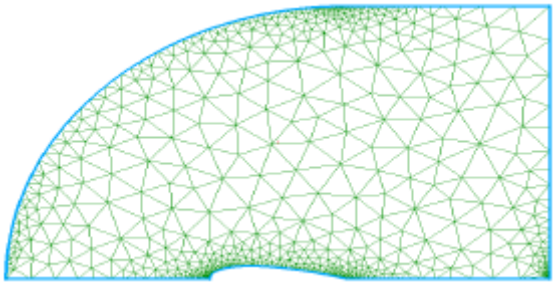

Figure 2.12: unstructured triangle mesh

The construction of unstructured meshes is in general much simpler and faster to implement in an industrial calculation context. It is also easier to refine locally some part of the domain.

Another advantage of unstructured meshes is that the nodes and connectivity do not have a global structure like structural meshes. Thus it is possible to add or remove nodes and/or elements during the calculation if needed.

### 2.4.3 MIXED MESHES

As the name implies, mixed meshes are composed of structural meshes in certain regions and non-structural meshes when the geometry is more complex. The meshes are usually connected "node to node" but can also have non-conforming interfaces.

This method improves the performance of the calculations compared to a unstructured mesh.

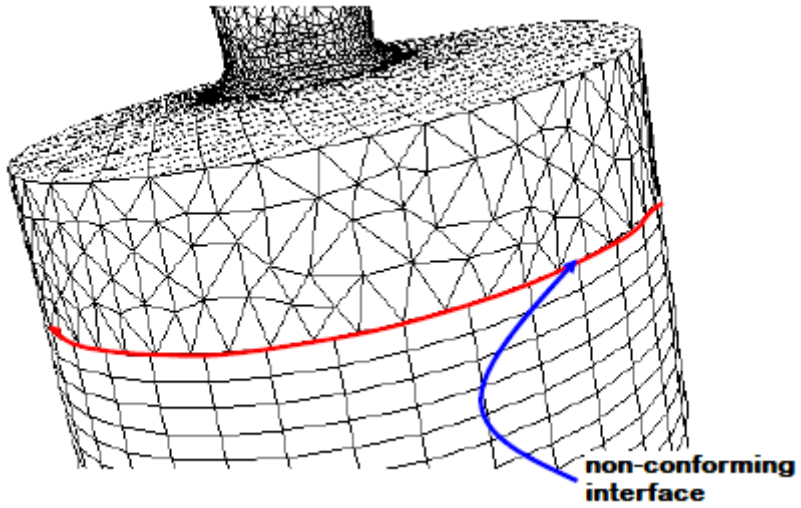


Figure 2.13: mixed mesh with non-conforming interface

### 2.4.4 General mesh generation techniques

In practice, there is no precise rule for creating a valid mesh, but there are different approaches to obtaining an acceptable grid. We can summarise these rules as follows: - Maintain good feature quality. - Ensure good resolution in high gradient regions. - Ensure good smoothness in the transition areas between the fine and coarse mesh parts. Ensure good smoothness in the transition areas between fine and coarse mesh parts. - Minimise the total number of elements (reasonable calculation time).

### 2.4.5 Mesh quality

The generation of a very good mesh quality is essential for an accurate, robust and meaningful calculation result. Good mesh quality is based on the following elements - Minimisation of skewness elements; - Good resolution in regions with a strong gradient (boundary layers, shock waves, etc.) Finally, the quality of the mesh has a serious impact on the convergence, the accuracy of the solution and, above all, the computation time. solution and especially the computation time.

## 2.5 Discretisation by the finite volume method

The discretization of the domain is obtained by a mesh consisting of a network of points (nodes). Thus a volume element (control volume) is defined around each node. After selecting the differential equations to be solved, it is necessary to transform these differential equations into algebraic equations where the continuous variations of the flow variables are represented by values at discrete points in time and space. The discrete locations in space are represented by nodal points (or nodes) chosen in a numerical grid that subdivides the flow domain according to the nature and geometry of the computational domain.

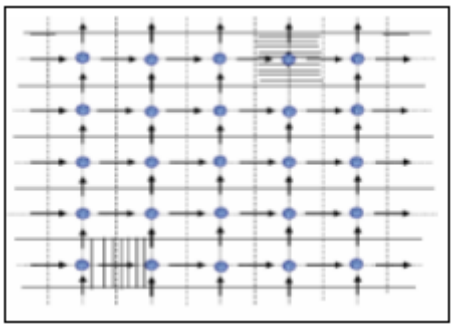

Figure 2.14: the principle of staggered meshing

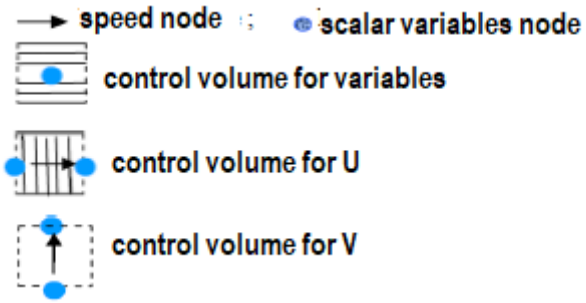


Figure 2.15: staggring meshing figure's symboles definition

### 2.5.1 Discrete equations

The mathematical equations outlined above governing flow express the transport of mass, momentum and energy quantities. The transport differential equations can be converted into a system of algebraic equations the into one equation. This equation is

written in the stationary, two-dimensional case as follows [35, 36] :

$$\frac{\partial}{\partial x}(\rho U\phi) + \frac{\partial}{\partial y}(\rho V\phi) = \frac{\partial}{\partial x}\left(\Gamma\frac{\partial\phi}{\partial x}\right) + \frac{\partial}{\partial x}\left(\Gamma\frac{\partial\phi}{\partial y}\right) + S\phi \tag{7}$$

To understand this method, we consider the simplest case. Let us consider the one-dimensional steady flow in which only the convection and diffusion terms are present. The governing differential equation in this case is :

$$\frac{\mathrm{d}}{\mathrm{d}x}(\rho u\phi) = \frac{\mathrm{d}}{\mathrm{d}x}\left(\Gamma\frac{\mathrm{d}\phi}{\mathrm{d}x}\right) \tag{8}$$

The continuity equation is written :

$$\frac{\mathrm{d}}{\mathrm{d}x}(\rho u) = 0 \quad ; where \quad \rho u = constant \tag{9}$$

To obtain the discretized equation, the three-node system, shown in Figure III-3, is used. It is assumed that "e" is located in the middle between P and E, and w is between W and P.

the integration gives us :

$$(\rho u\phi)_e - (\rho u\phi)_w = \left(\Gamma\frac{\mathrm{d}\phi}{\mathrm{d}x}\right)_e - \left(\Gamma\frac{\mathrm{d}\phi}{\mathrm{d}x}\right)_w \tag{10}$$

$$(\rho u)_e - (\rho u)_w = 0 \tag{11}$$

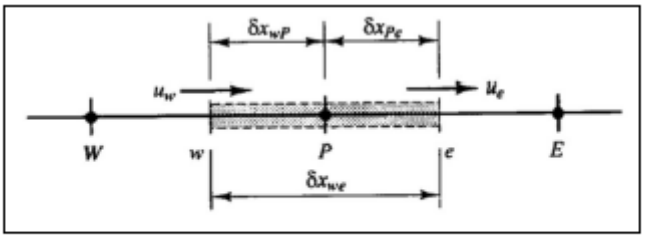


Figure III-3: Volume de contrôle autour du nœud P, cas monodimensionnel.

Figure 2.16: control volume around the node p ( one-dimensional case)

## 2.6 Conclusion

This chapter was reserved for the mathematical modelling of our study. The classic conservation equations and the finite volume method, a mathematical discretization technique to transform the differential writing of the governing equations into an algebraic writing, were briefly presented. - The visible non-linearities in the equations are mainly responsible for the difficulties in obtaining an analytical solution. Therefore, the use of numerical methods is essential to work on this simulation. The Gambit and Fluent software based on the finite volume method were used to solve the different equations (chapter 3). The methodology and the logic of the solution followed have been explained. The physical parameters, geometry, initial and boundary conditions applied were defined. The results of the numerical simulations are presented in the last chapter. As it is necessary to explain the way the numerical simulation is developed on the CFD software FLUENT, the following chapter is reserved for the presentation of this calculation code. This chapter ends with the discretized equations and a conclusion.

# Chapter 3

# Problem's position

## 3.1 Introduction

Numerical modelling and simulation is an important conception tool used to predict experimental implementation. In any solar energy application, it would be advisable to analyse theoretically any given system in as much detail as possible before moving on to the experimental stage.

Numerical simulation is almost always in the form of a computer program or tools known as simulation environments capable of transforming differential equations into algebraic equations in which continuous variations of flow variables are represented by values at discrete points in time and space.

Simulation does not replace, but rather enhances, experimentation. It allows the analysis of the problem to be performed under realistic conditions (reproducing experimental tests to better understand them and at a lower cost) or, on the opposite, under extreme/marginal test conditions (extreme climates, installation flaws). These latter cannot be done by experimentation (due to costs...), so simulation expands the field of tests for a system.

Through simulation, the system under study becomes more flexible. Parametric studies can easily be done. The use of simulation can also vary the time scale for a

study, which is otherwise impossible.

The appropriate mathematical formulation for our case is in the form of conservation equations, which govern the phenomenon of natural convection in a cylindric duct and thermal conduction in the studied domains. These equations are the following:
- Continuity equation.
- Equations of momentum.
- Energy equation.
In this study, the creation of the geometric model, the mesh, the definition of the boundaries were generated using ANSYS-Gambit 2.4.6 software, which is a computer aided design software. To determine the evolution of the (X, Y, Z)-temperature (K) profiles of the water inside a parallel tube configuration of a flat plate solar water heater and the absorbing wall, we chose the commercial code ANSYS-FLUENT 14.5 which allows the simulation of different types of flows with complex geometries. It can solve the equations governing laminar and turbulent, stationary and unsteady fluid motion. It can solve flow problems with structured and unstructured meshes, regardless of the complexity of the geometry, with relative ease. The meshes supported in 2D are triangular or quadrilateral, in 3D they are tetrahedral, hexahedral or pyramidal, or mixed (hybrid) meshes.

FLUENT facilitates the user's handling through the simplicity of its graphic interface. The code is not limited only by its own functions, but it offers the user the possibility to inject his own function and define any particularities of his problem.

## 3.2 Physical model

In this work, we will study a solar preheater intended for solar distillation, the used collector consists mainly of a box, absorbing plate, a glass and tubes for the circulation of the fluid (in our case it is water)

The geometry of the considered system is presented in the following figures (4.1 and 4.2). It is a flat plate solar water collector consisting of two main tubes for the inlet and outlet and seven tubes placed in parallel for the circulation of the water to be

heated in the collector. The water first circulates through the main inlet tube with an inlet flow rate and then branches off into the secondary tubes before it reaches the main outlet tube.

A small amount of the solar radiation incident on the collector is absorbed by the glass cover. The rest is reflected outwards and transmitted through the air to the absorber which absorbs the large amount due to its high absorption coefficient.


Figure 3.1: cross section of the collector with dimensions

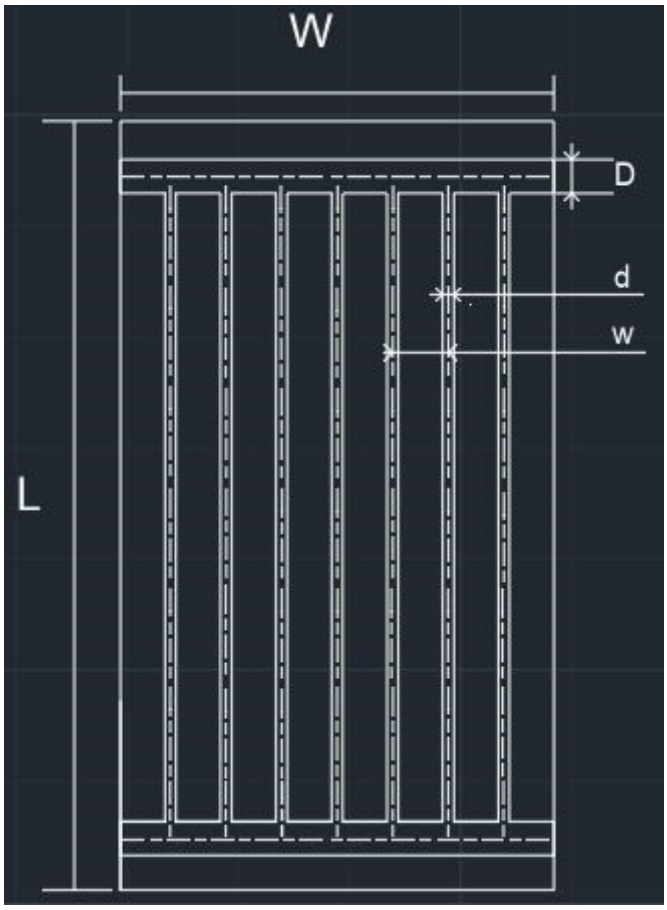


Figure 3.2: overall view of the collector with dimension

The studied model is a solar collector composed of a box of length **L** and width **w**,

this box contains (as the two previous figures show) two main tubes of length **W** and diameter **D** and seven secondary tubes of diameter **d** that connect between the two main tubes, with a distance of **W** between tubes.

**Tables of physical parameters**

| Size | Symbol | Unit |
|---|---|---|
| Length of the box | L | cm |
| Box height | H | cm |
| Width of the box | W | cm |
| Diameter of the main tubes | D | cm |
| Diameter of secondary tubes | d | cm |
| Distance between two secondary tubes | w | cm |

Table 3.1: symbols and units for collector dimensions

| Collector's dimension | value |
|---|---|
| L | 94 |
| H | 4.5 |
| W | 36 |
| D | 1.75 |
| d | 1 |
| w | 4.5 |

Table 3.2: collector's dimensions

The physical properties of the materials used in the simulation are shown in the following table :

| Materials | Thermal Conductivity (W/m K) | Density (Kg/m3) | Specific Heat « Cp » (J/kg K) |
|---|---|---|---|
| Copper | 387.6 | 8978 | 381 |
| Wood | 0.173 | 700 | 2310 |
| Glass | 1 | 250 | 720 |

Table 3.3: Physical properties of materials used in the simulation

## 3.3 Mathematical formulation

**Simplifying assumptions:**

In order to solve the equations governing the three-dimensional flow of water in the solar collector, the following simplifying assumptions are adapted: - The three-dimensional flow assumed to be stationary in the laminar regime. - The fluid is treated as an incompressible flow. - The three-dimensional flow of water presented as a Newtonian fluid, with constant properties. - The cover is opaque to IR radiation and does not absorb solar radiation.

The studied model is based on the mass and momentum conservation equations (Navier Stokes), coupled with the energy conservation equation, discretised by the finite volume method, governing the three-dimensional flow of an incompressible Newtonian fluid in laminar regime, these equations describe the flow phenomenon inside the water heater.

**Continuity equation :**

$$\frac{\partial u}{\partial x} + \frac{\partial v}{\partial y} + \frac{\partial w}{\partial z} = 0 \tag{1}$$

**Momentum equation :**

following x :

$$u\frac{\partial u}{\partial x} + v\frac{\partial u}{\partial y} + w\frac{\partial u}{\partial z} = -\frac{1}{\rho}\frac{\partial P}{\partial x} + \mu\left(\frac{\partial^2 u}{\partial x^2} + \frac{\partial^2 u}{\partial y^2} + \frac{\partial^2 u}{\partial z^2}\right) \tag{2}$$

following y :

$$u\frac{\partial v}{\partial x} + v\frac{\partial v}{\partial y} + w\frac{\partial v}{\partial z} = -\frac{1}{\rho}\frac{\partial P}{\partial x} + \mu\left(\frac{\partial^2 v}{\partial x^2} + \frac{\partial^2 v}{\partial y^2} + \frac{\partial^2 v}{\partial z^2}\right) \tag{3}$$

following z :

$$u\frac{\partial w}{\partial x}+v\frac{\partial w}{\partial y}+w\frac{\partial w}{\partial z}=-\frac{1}{\rho}\frac{\partial P}{\partial x}+\mu\left(\frac{\partial^2 w}{\partial x^2}+\frac{\partial^2 w}{\partial y^2}+\frac{\partial^2 w}{\partial z^2}\right) \tag{4}$$

**Energy equation :**

$$\left(\frac{\partial\left(\rho u T\right)}{\partial x}+\frac{\partial\left(\rho v T\right)}{\partial y}+\frac{\partial\left(\rho w T\right)}{\partial z}\right)=\frac{\partial}{\partial x}\left[\left(\frac{\mu}{Pr}\right)\frac{\partial T}{\partial x}\right]+\frac{\partial}{\partial y}\left[\left(\frac{\mu}{Pr}\right)\frac{\partial T}{\partial y}\right]+\frac{\partial}{\partial z}\left[\left(\frac{\mu}{Pr}\right)\frac{\partial T}{\partial z}\right] \tag{5}$$

The resolution by the numerical simulation software of flows ANSYS-FLUENT requires the presentation of GAMBIT software which is a software of Computer Aided Design and mesh generation. It allows the creation of 2D or 3D geometries and the generation of meshes. Widely used in industry (automotive, aeronautics, space, ...etc.) because of its simple and powerful graphical interface, GAMBIT also allows the creation of all types of complex geometries (fixed or mobile) associated with meshes. It also allows to define boundary conditions.

### 3.3.1 Steps involved in creating the sensor geometry :

**The solver's choice :**

The numerical calculation will be performed using FLUENT 14.5. For this purpose, the type of solver (FLUENT 5/6) was chosen in GAMBIT

**Creation of the geometry**

The geometry of the system has been created using the predefined geometries since our model is made in 3D.

## 3.4 Mesh

To build a mesh, the following steps must be followed: - define the geometry. - make the mesh. - define the parameters of the calculation zones.

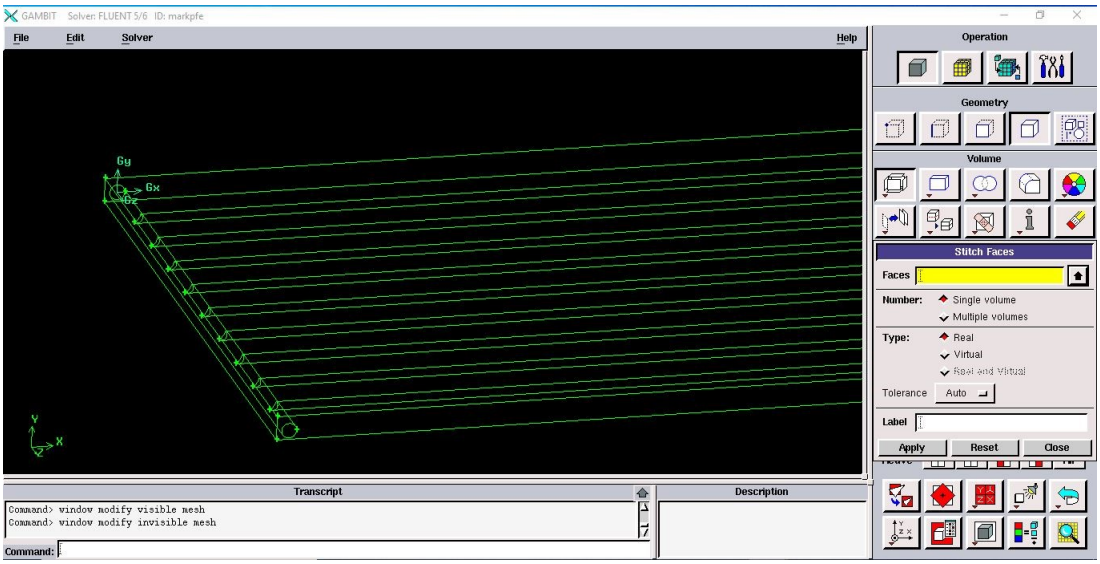


Figure 3.3: A view of the collector suggested design in Gambit

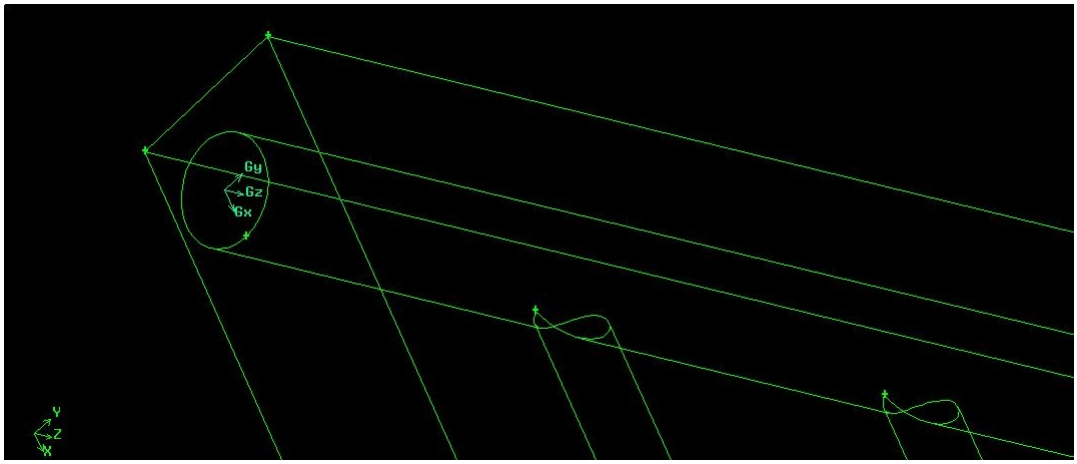


Figure 3.4: A zoomed-in view of the tubes intersections inside the collector in gambit

The numerous difficulties we have encountered in our attempts to use meshes have led us to adopt a hybrid mesh. The mesh size that seems to give the best ratio of accuracy to speed of convergence is 207502 nodes. To achieve this, we first mesh the surfaces and then the domain.

- We begin the mesh by choosing « MESH COMMAND BUTTON » (figure 3.6)

- Then we click on « VOLUME COMMANDE BUTTON » (figure 3.7)

- Then click on "MESH VOLUMES" and choose 0.8 for "Spacing" and "Tet/hybrid" as elements. (figures 3.8 and 3.9)

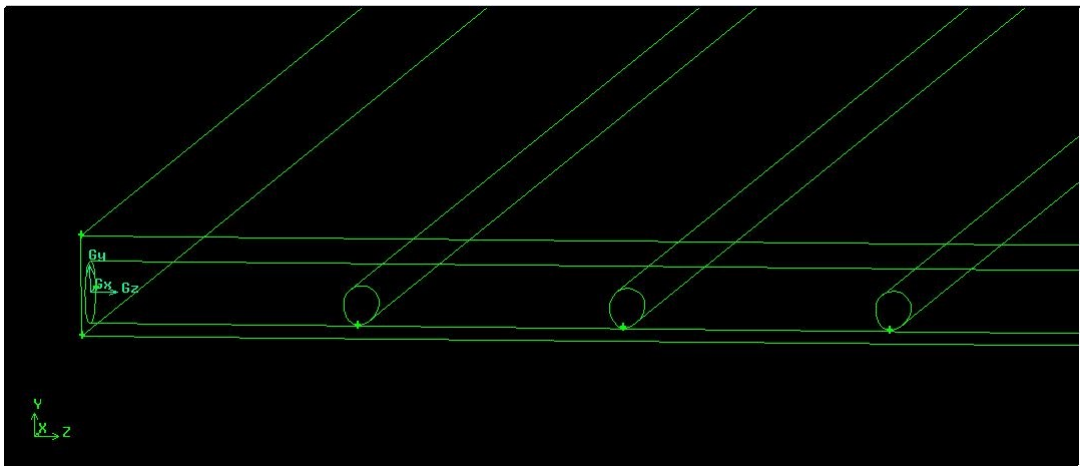


Figure 3.5: A zoomed-in view of tubes design inside the collector in gambit

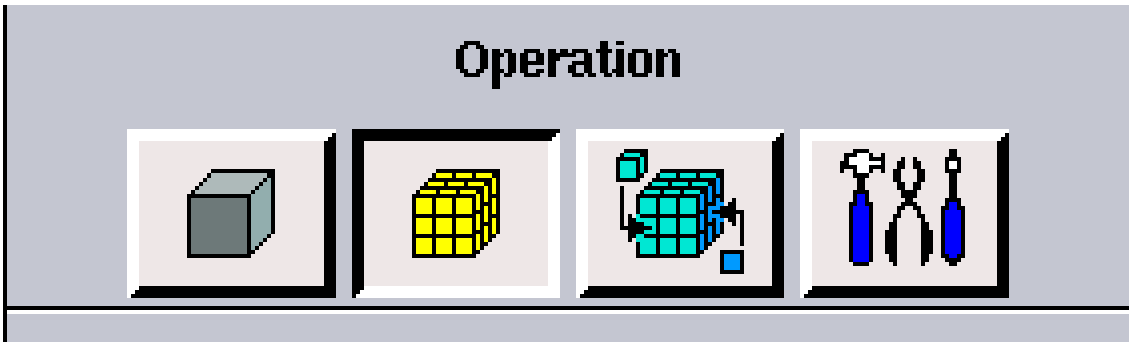


Figure 3.6: mesh command button

A structured mesh could be built for the drilling and the surrounding soil in either cylindrical or Cartesian reference frame by adopting a cylindrical and structured reference frame. But this highlights some errors induced in particular by the approximation of circular tube shapes. The solution to this is to construct a very fine mesh in this frame to reduce these errors, but this leads to a very large number of meshes. Furthermore, the use of a structured mesh is not efficient with small diameter tubes as in our study.

This is why we have chosen the hybrid mesh, because the latter means a mesh generated by mixing elements of different types: triangular or quadrilateral in two dimensions, tetrahedral, prismatic or pyramidal in three dimensions, and which has the advantage of combining the advantages of the structured mesh with those of the unstructured.

-The result of the meshing is shown in figures 3.10 to 3.14:

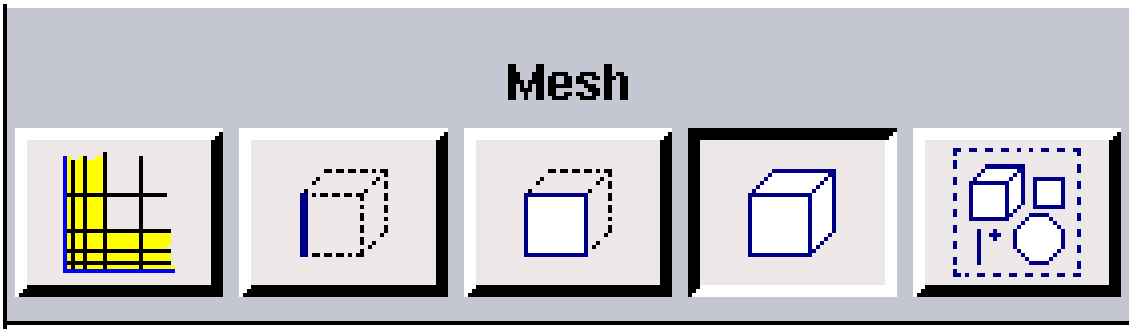


Figure 3.7: volume command button

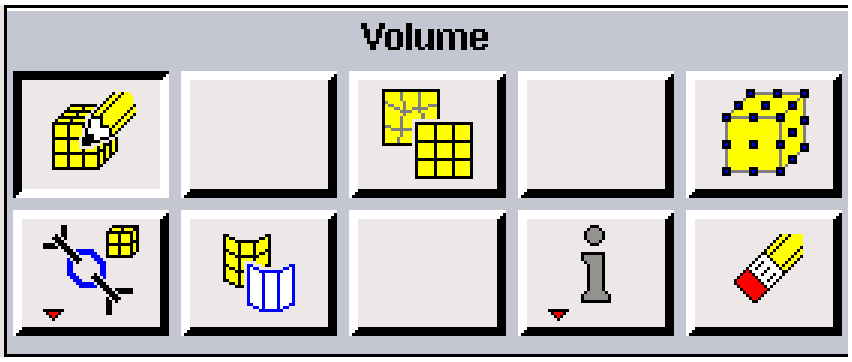


Figure 3.8: mesh volume button

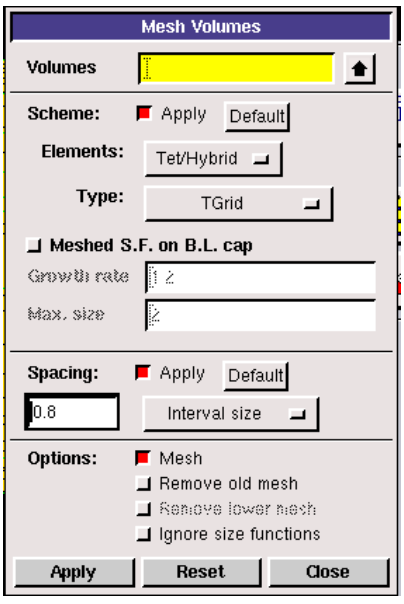


Figure 3.9: mesh volume définition

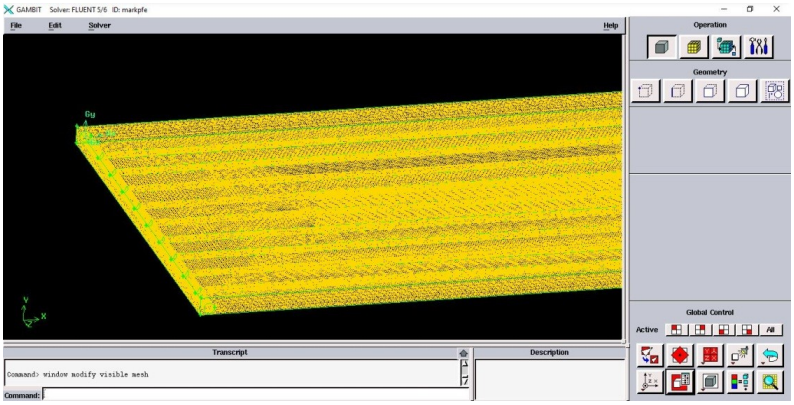


Figure 3.10: a veiw of the collector's mesh

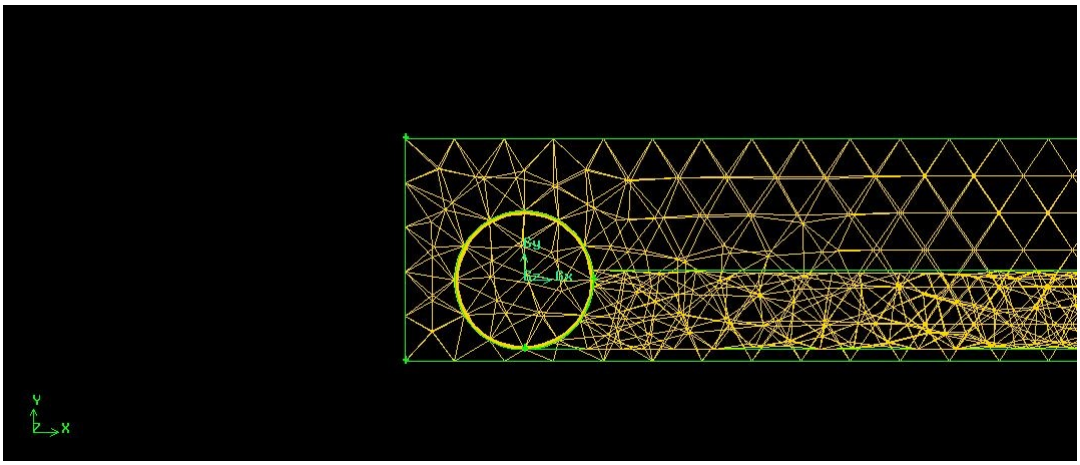

Figure 3.11: a zoomed-in veiw of the mesh inside the collector

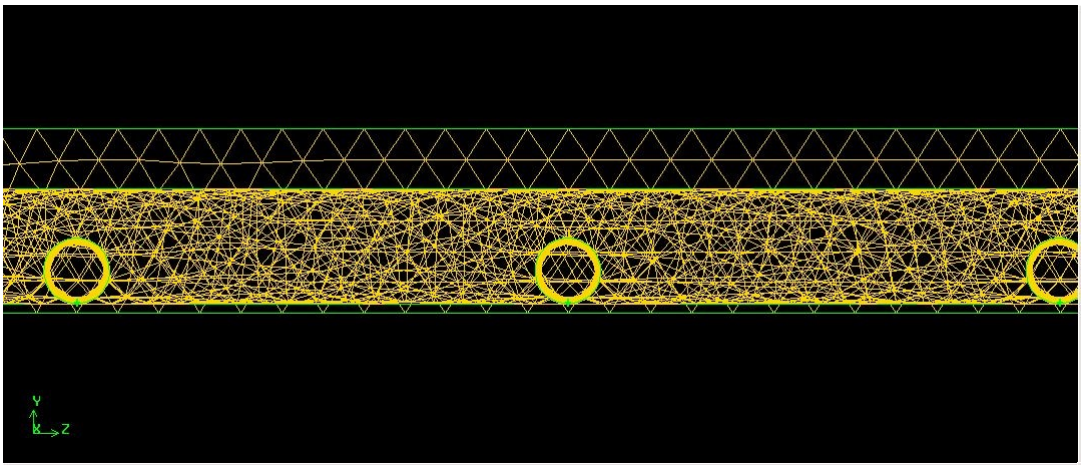

Figure 3.12: a zoomed-in view of the mesh inside a main tube

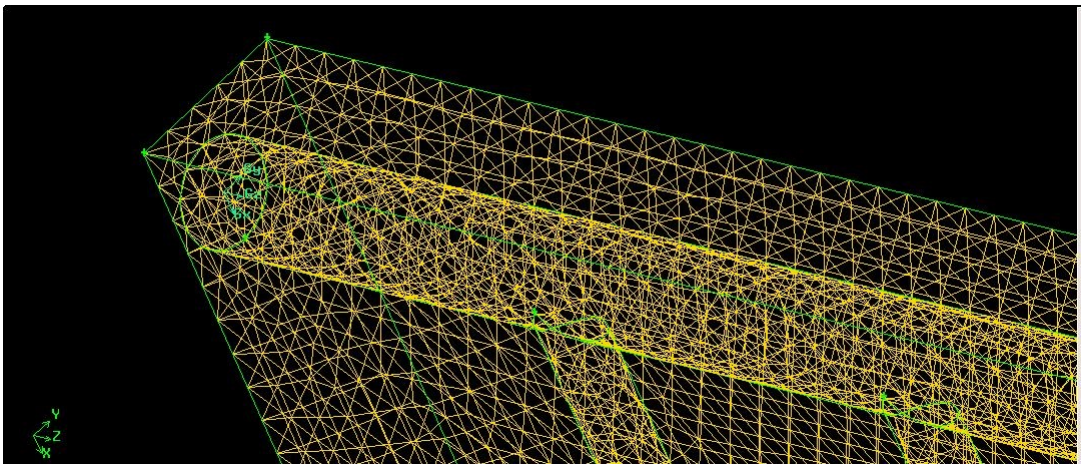

Figure 3.13: a zoomed-in view of the mesh on the intersection region between main and secondary tubes

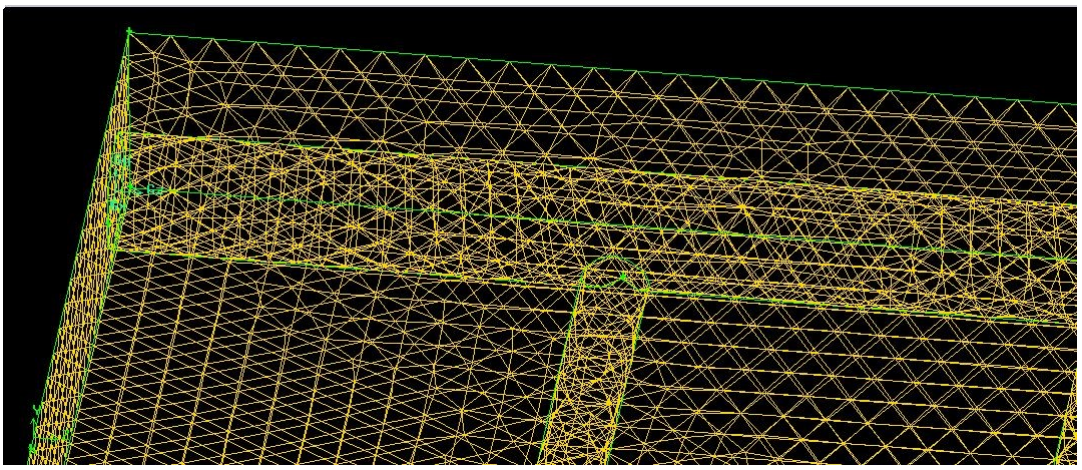

Figure 3.14: a view of different types of mesh in the collector

## 3.5 Boundary conditions

The solution of the momentum equation as well as the energy equation requires the definition of initial and boundary conditions on the boundaries of the calculation domain. The different conditions applied in our study are illustrated in

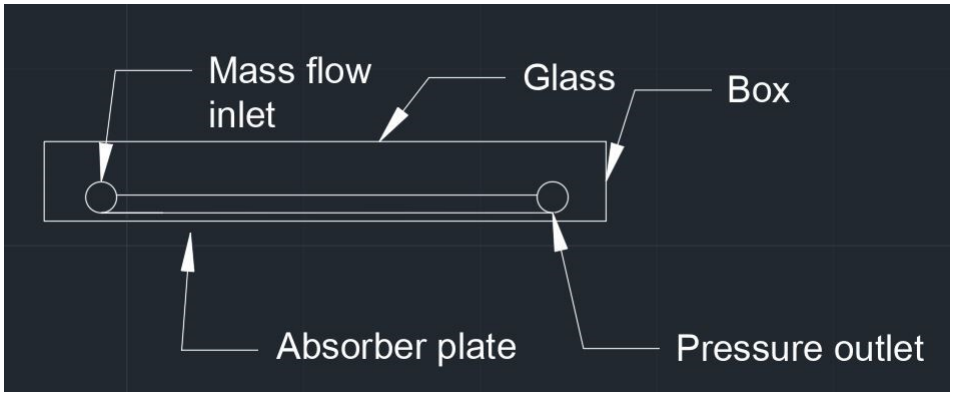


Figure 3.15: collector's components definition scheme

### 3.5.1 Initial conditions

-Mass flows and daytime temperatures :

| Mass flow 1 | Mass flow 2 | Mass flow 3 | Mass flow 4 |
|---|---|---|---|
| 0.001 kg/s | 0.0008 kg/s | 0.0004 kg/s | 0.001 kg/s |

Table 3.4: suggested mass flows

| Time of the day | Tempearture (K) | Direct solar irradiation (w /m² ) | Diffuse solar irradiation (w /m²) |
|---|---|---|---|
| 8:00 | 274.75 | 189 | 7 |
| 10:00 | 278.95 | 922 | 49 |
| 12:00 | 285.95 | 1025 | 60 |
| 13:30 | 289.95 | 1044 | 60 |
| 14:00 | 291.05 | 1037 | 60 |
| 16:15 | 293.15 | 903 | 55 |
| 20:00 | 286.75 | 0 | 0 |

Table 3.5: different parameters of the 5th of january 2020 obtained from the URER-MS daily archive.

The GAMBIT software allows you to declare the type of the different boundary conditions (the nature of each face is defined in the software)

### 3.5.2 Definition of the main enclosure :

Starting here with the outer box:

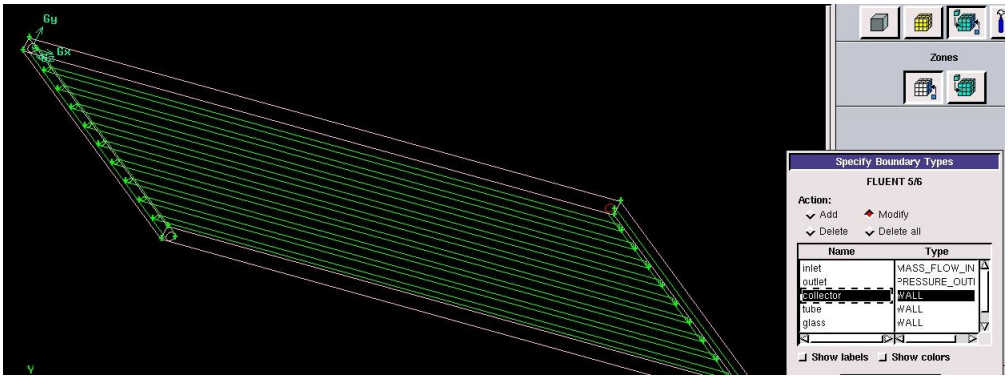


Figure 3.16: definition of the box in gambit

### 3.5.3 Definition of boundary conditions

-glass (declared as « wall ») :

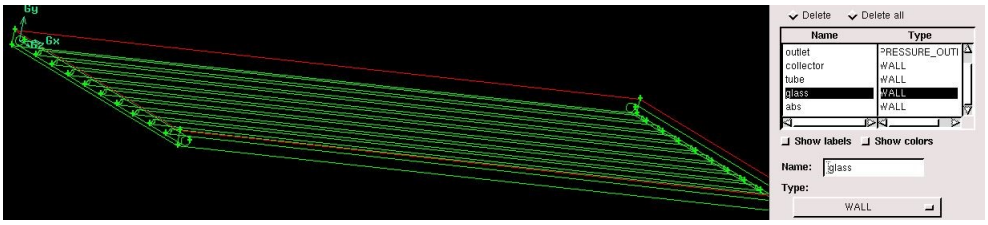


Figure 3.17: definition of the galss in gambit

- tubes (declared as « wall ») :

-the absorber (declared as « wall ») :

-inlet (declared as « mass flow inlet ») :

-outlet (declared as « pressure outlet ») :

The circulation regions of each fluid in the collector (water in the tubes and air in the remaining volume in the collector) are then defined as shown in the following two

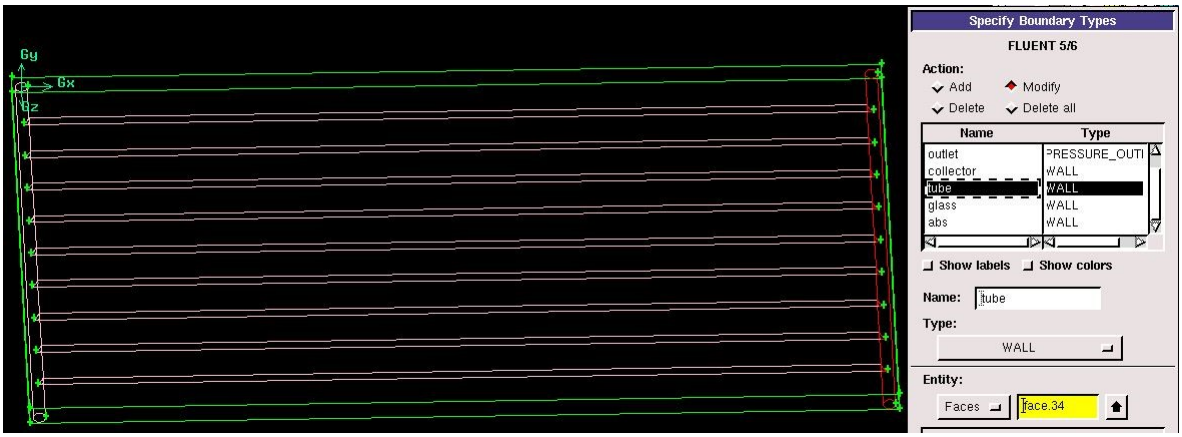


Figure 3.18: definition of tubes in gambit

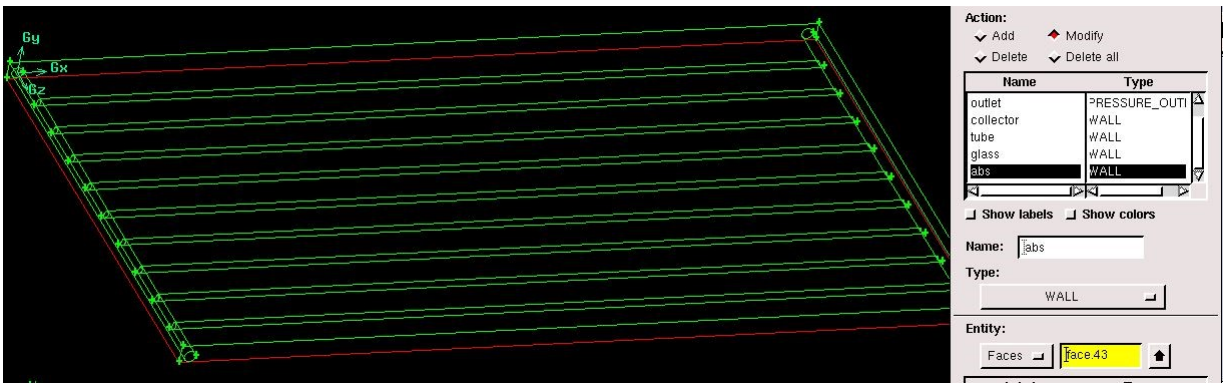


Figure 3.19: definition of the absorber in gambit

figures.

### 3.5.4 Mesh exportation :

Once the models have been created and the boundary conditions defined, they must be exported, in .mesh format, so that Fluent is able to read them and use them to simulate their thermal and dynamic behavior. We can then close Gambit by saving the session (if we wanted to open it later) and launch Fluent.

Here we come to the step of using the FLUENT software, after launching the software we open the recently exported **.mesh** file.

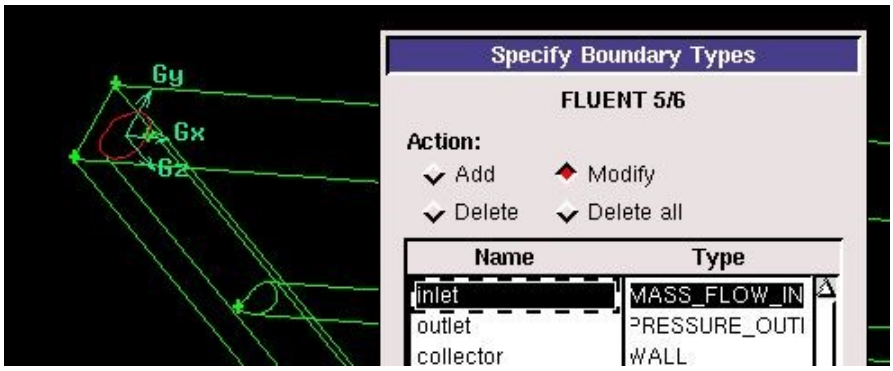


Figure 3.20: definition of the inlet in gambit

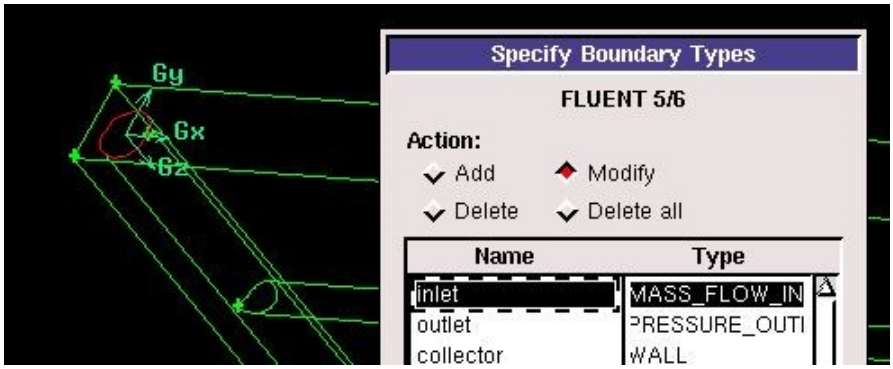


Figure 3.21: definition of the outlet in gambit

### 3.5.5 Calculation Preparation Steps in FLUENT:

**Step 1: Scale verification**

This step ensures that the model is in centimeters.

**Step 2 : model verification**

In this step, the main parameters of the model are defined, such as the flow regime and the irradiation parameters At the end of this step, the flow type is chosen.

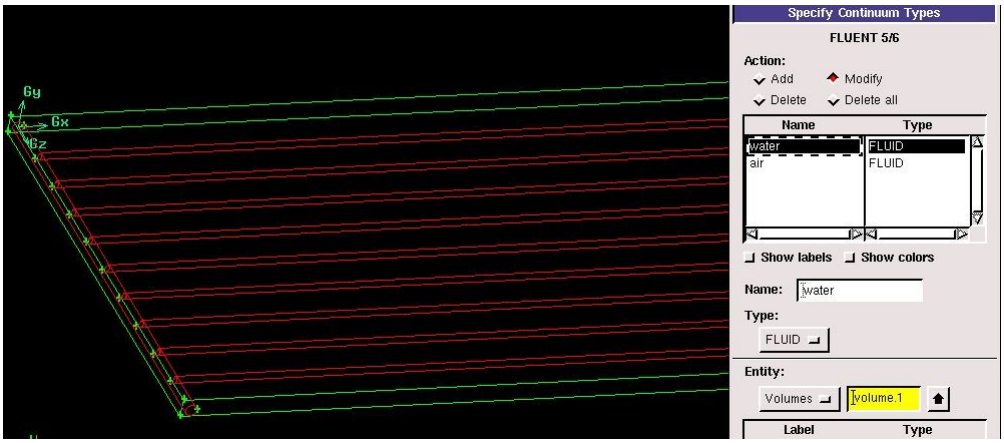


Figure 3.22: the circulation region of the water in gambit

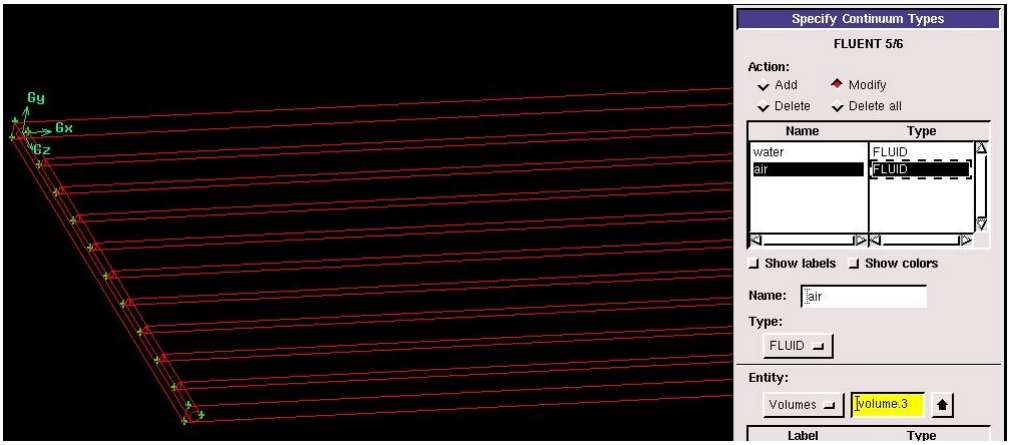


Figure 3.23: the circulation region of the air in gambit

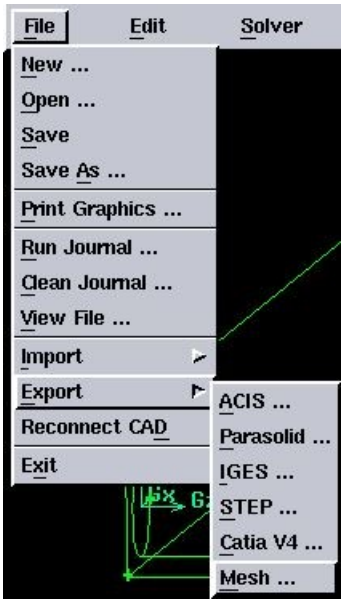


Figure 3.24: mesh exportation

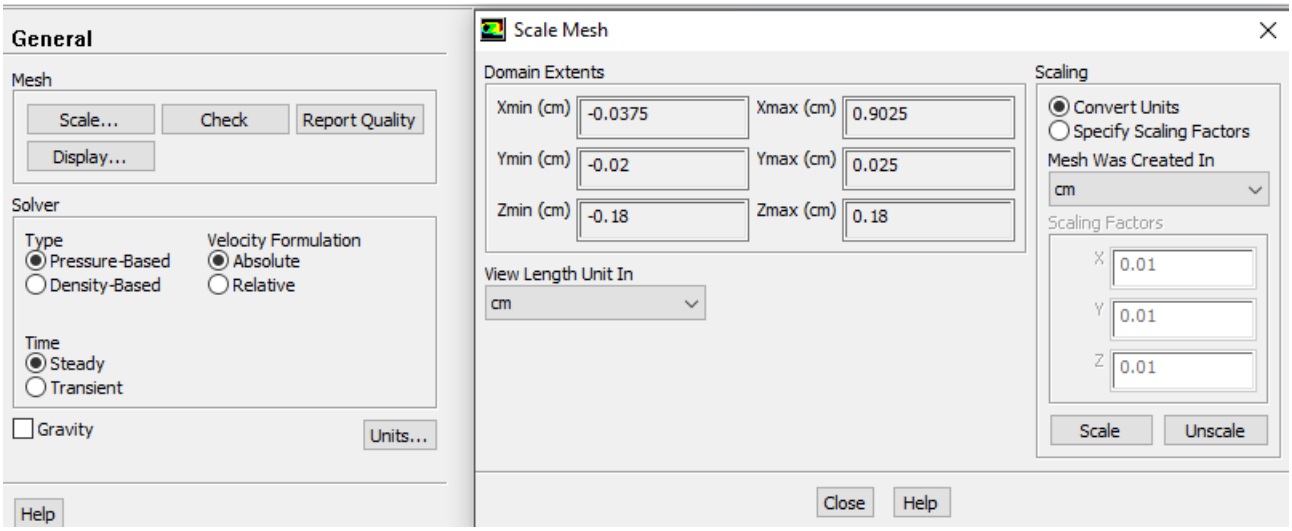


Figure 3.25: Scale verification

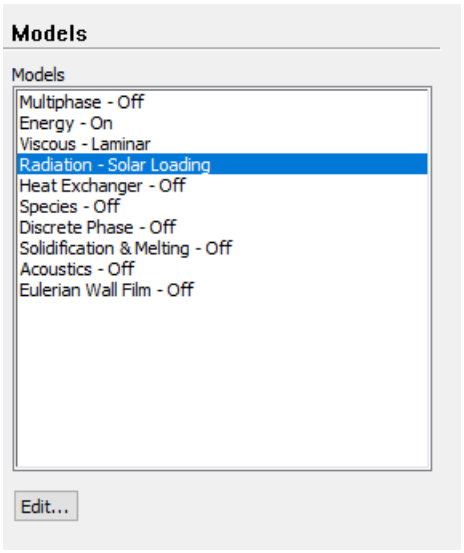


Figure 3.26: definition of model parameters

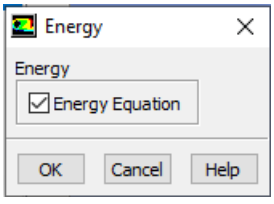


Figure 3.27: establishing the energy equations

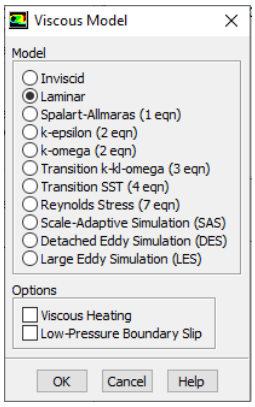


Figure 3.28: chosing « laminar » as a flow regime

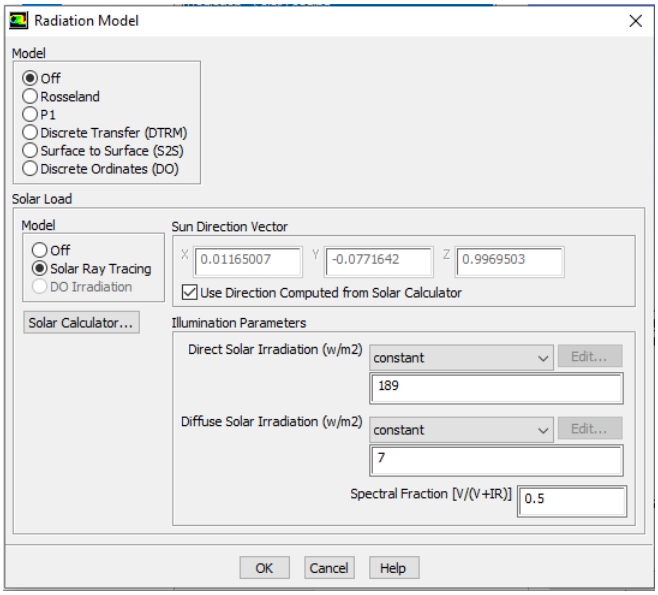


Figure 3.29: defining the radiation parameters of the model

Here, user can change the values of direct and diffuse solar irradiation based on the data he already have.

**step 3 : defining the properties of materials**

All thermo-physical data must be entered. The characteristics of the materials are loaded from the Fluent data library. Here we choose the materials used in our model from the existing lists, otherwise we have to introduce them according to our needs.

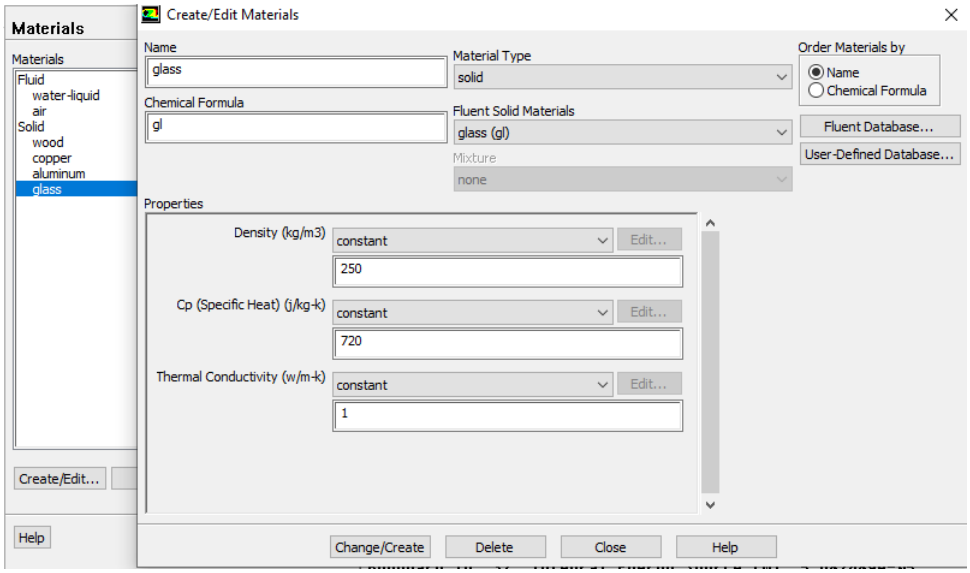


Figure 3.30: definition of a new material

The definition of a new material (glass) is given as an example:

1. The name of the solid "glass".

2. thermal density 250 kg.m-3 .

3. specific heat 720 J.Kg-1.K-1 .

3. thermal conductivity is defined through the data of the most used collectors in the market.

**Step 4 : defining boundary conditions**

One of the most important parameters in our study is the mass flow inlet and the inlet temperature, which can be defined through the following window:

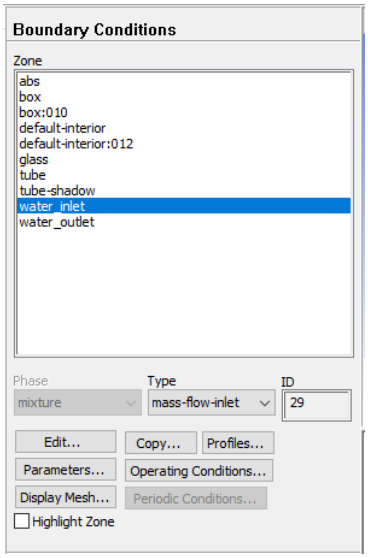


Figure 3.31: Setting boundary conditions

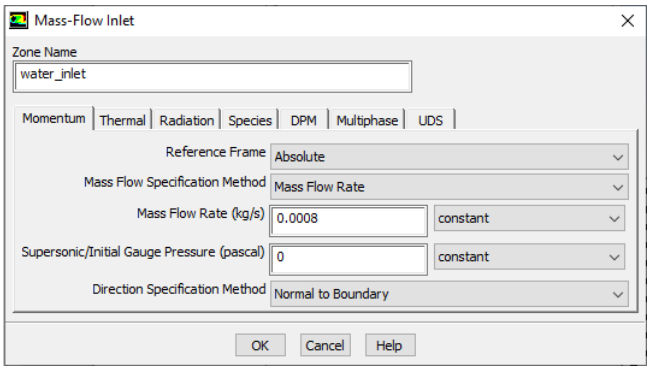


Figure 3.32: Setting the mass flow inlet value

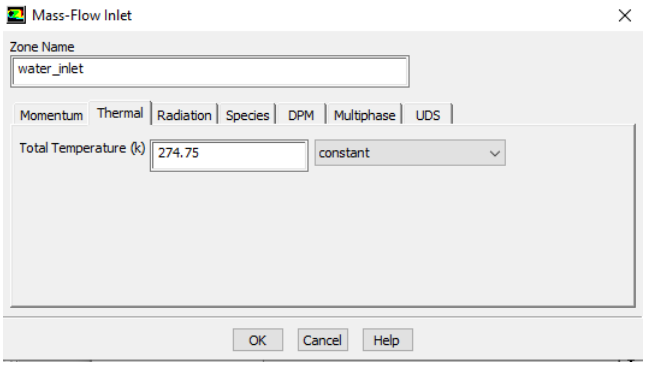


Figure 3.33: Setting the inlet temperature

### Solution initialization

it is required to initialize all variables before starting the calculations. Taking into account our imposed conditions, we start the calculations at the collector's inlet.

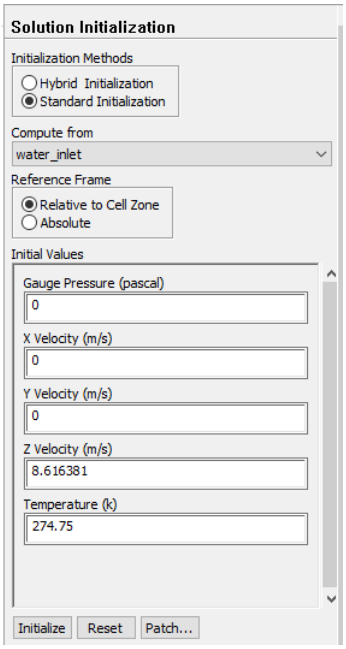


Figure 3.34: Solution initialization

### start of calculation

After deciding on the number of iterations, the calculations begin.

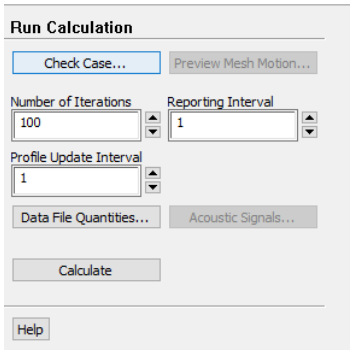


Figure 3.35: Starting calculations

## 3.6 Gambit and Fluent simulation tools

### 3.6.1 Gambit

**Gambit** is a software which allows to create meshes which can be used in particular under **FLUENT**.

The mesher is a preprocessing of the simulation software. It allows to generate a structured or unstructured mesh in Cartesian, polar cylindrical or axisymmetric coordinates. It can produce complex meshes in two or three dimensions It can produce complex two- or three-dimensional meshes with rectangular or triangular mesh shapes. It can be used to construct a geometry and generate a mesh for it, eventually, geometry from another CAD program can be imported into this preprocessor. preprocessor. Gambit's generation options offer flexibility of choice. It is possible to devide the geometry into several parts to generate a structured mesh. Otherwise, Gambit generates an unstructured maillage based on the type of geometry built. Defects are easily detected using the mesh verification tools.

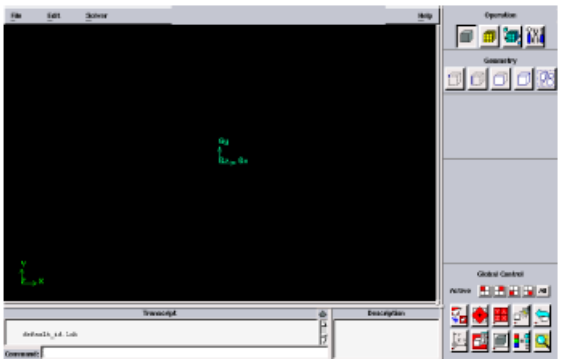

Figure 3.36: Gambit's interface

#### Construction of a mesh

To build a mesh, the following steps should be followed: The geometry includes the physical positions of characteristic points defining the area to be meshed: spatial coordinates of the four corners of a square, the start and end points of a line, the centre and angular opening of a circular arc. It is necessary to be able to represent the

area to be studied by a set of simple geometrical figures connected to each other.

### Gambit's user guide

This software is used to define and create the study model (surface or volume) and to mesh it according to the user's instructions. The different steps to use GAMBIT are defined in the following instructions.

### a. Operation tool window

Each button in this window corresponds to a well-defined function.


Figure 3.37: operation tool window

### b. Construction of geometry

Geometry is created from points, sides, areas, volumes or a group of all of these. It is possible to perform union, intersection, separation, deletion decomposition.

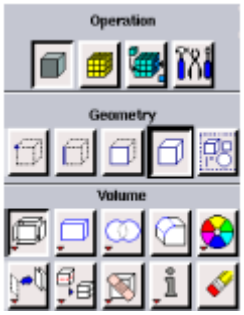


Figure 3.38: geometrie construction window

**c. Mesh generation**

This function allows the generation of all types of meshes, the manipulation of the generated mesh and even the creation of a boundary layer if required.


Figure 3.39: geometrie generation window

**d. Incorporation of boundary conditions**

Several types of boundary conditions are available depending on the problem being addressed. Note that that the mesh space is taken by default as being fluid.


Figure 3.40: boundary conditions definition buttons

**e. Tools buttons**

They allow to specify the coordinate system for example or other specific operations.


Figure 3.41: tools buttons

**f. Global control window**

It concerns orientation, display, light and mesh checking.


Figure 3.42: global control window

**Important :** Even before creating the geometry, it is necessary to choose the type of solver; in other words, the type of software (here Fluent) that will be used afterwards (choose the right version of the software), in our case it is to choose Fluent 5/6.

### 3.6.2 Fluent code

Fluent is a computer program designed for the simulation of fluid flow and heat transfer in complex geometries. It offers great flexibility of results and adaptation with any type of mesh. It allows the refinement of the mesh according to boundary conditions, dimensions and even results already obtained. This is very useful in the region of high gradients (boundary layers, free shear layers). Fluent is written in the C language and uses all the flexibility and power that this language offers. It uses the client-server architecture necessary for parallel computing on multiple machines. Fluent has a graphical tool for displaying and evaluating the results. Results can also be exported to other graphics software, and the user defined function option allows additional equations or additional user-defined source terms to be solved.

**Interface of the Fluent code:**

We can start 4 versions of Fluent 2D, 3D, 2DDP and 3DDP with the same interface.

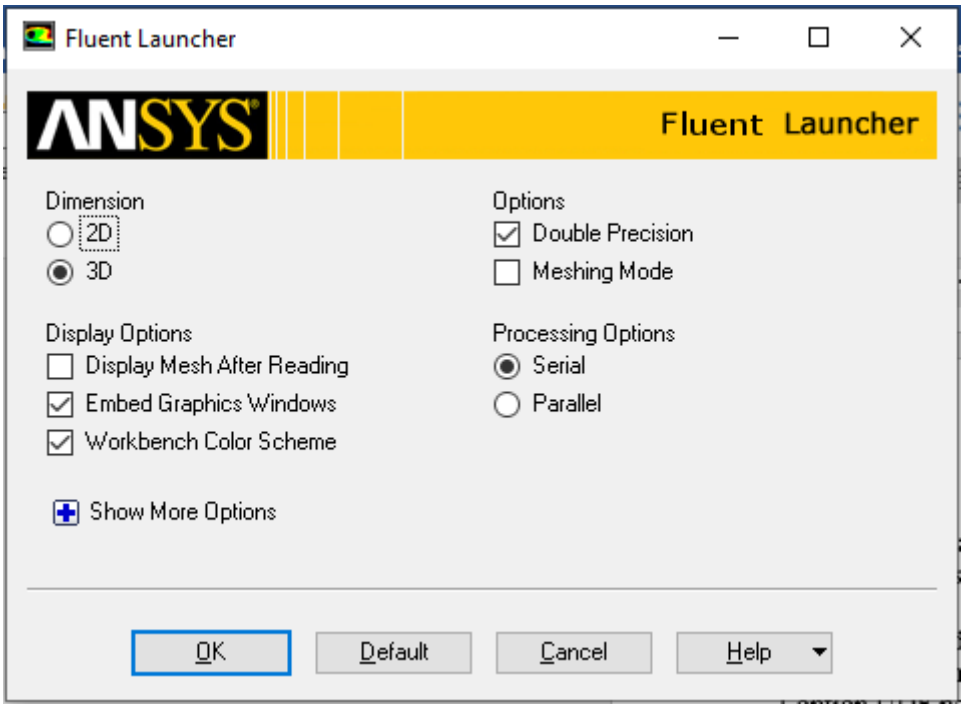


Figure 3.43: Fluent launcher window

The functions available for the digital procedure are :

**File:** for operations concerning files: reading, saving, importing, etc.

**Grid:** for checking and manipulating the mesh and geometry.

**Define:** for defining physical phenomena, materials and boundary conditions.

**Solve:** to choose the equations to be solved, the discretization schemes, the sub-relaxation factors, the convergence criteria and to initialize and proceed with the calculation.

**Adapt:** to adapt the mesh according to several parameters.

**Surface:** to create points, lines and planes necessary to display the results.

**Display and plot:** for the evaluation of the results. **Report:** for displaying reports containing details of the problem processed.

**Parallel:** for parallel calculation.

**Help:** for the exploitation of the code content.

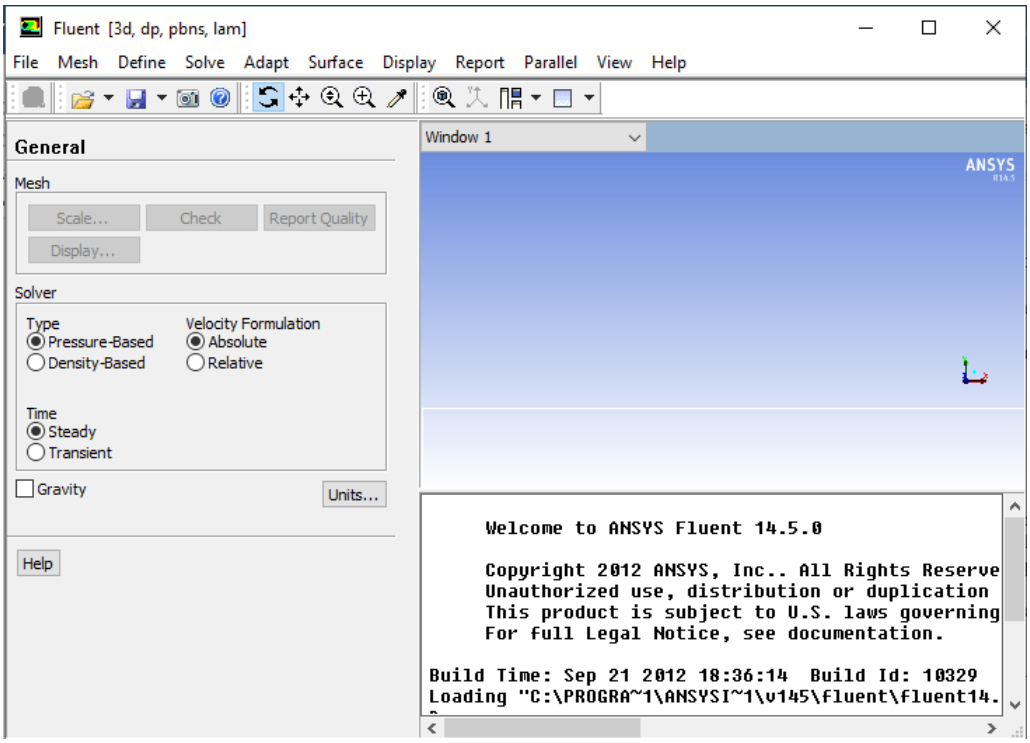


Figure 3.44: Fleunt interface

**Boundary condition used by the Fluent code :**

For the Fluent code the available types of boundary conditions are classified as follows:

**a) Flow inlet and outlet conditions:** pressure inlet, velocity inlet, mass flow inlet, intake, pressure outlet, outflow, pessure far-field, exhaust.

**b) Wall and pole condition:** wall, axis of symmetry, periodic conditions, plane of symmetry.

**c) Internal zone cells:** fluid or solid (of different types).

**d) Condition of the internal faces:** ventilation, radiation, internal wall.

But if we speak in a more general way we will have four types of boundary conditions or each of them needs a thorough study:

**-At the inlet:** the value of the variable is known.

**-At the outlet:** either the value of the given variable is known or it is assumed that the regime is established.

**-At the wall:** either the variable is known (e.g. velocity or temperature), or other physical quantities are known (velocity gradient, heat flow).

**-On the axis of symmetry:** where the gradient of the posed variable in the direction perpendicular to the axis of symmetry is zero.

**Numerical model used by the Fluent code:**

The Fluent code uses the finite volume method to discretise the transport equations. In this method, conservation equations are integrated and applied to each elementary control volume. From the known variables at the centres of the volumes, the flows at the surfaces of the volumes are evaluated by interpolation. The grid is a priori arbitrary, thus allowing to treat flows with complex geometry. This method gives very good results, because it guarantees the conservation of the mass and heat balances over the whole studied domain.

## 3.7 conclusion

This chapter has been dedicated to the description of the numerical modelling approach we have used for the problem to be solved. We started by presenting the geometry of the system. We then set out the set of governing equations and the associated simplifying assumptions and boundary conditions, in relation to the heat and mass transport within the sensor. This chapter ends with a brief description of the Gambit and Fluent software and the steps to follow to explain the simulation that was done to obtain the results that will be presented in the next chapter. In the following chapter, we will present the results obtained from the numerical simulation and their interpretations.

# Chapter 4

# Results and discussion

## 4.1 Introduction

This chapter is dedicated to the presentation of various numerical results obtained with ANSYS-FLUENT 14.5 software, using real data acquired during an internship at the Research Unit for Renewable Energies in the Saharan Environment (URER-MS) in Adrar.

The goal of this research is to provide a numerical simulation of the thermal behavior of water flowing through a solar panel. The low thermal exchanges between the caloporter fluid and the absorber compelled us to look into other ways to improve the capteur's performance; for this, it was quite useful to investigate the geometric shape, dimensioning, and debit that circulates inside the tubes. Our proposed model is commonly used in water preheating systems, such as solar distillation. The required parameters used in the numerical simulation are obtained using the URER-MS daily archive for January 5, 2020 in the Adrar region.

First, we will test several mass flow rates existing in the current literature and in the external market as being flow rates often used in the design of solar preheaters in order to see the influence of the flow rate on the heat transfer between the absorbing wall and the water circulating in the tubes. Next, we will check the evolution of the

water temperature profile during the day.

## 4.2 Results and discussion

In this work, we will focus on the heat transfer between the absorbing wall and the water flowing inside a parallel tube configuration of a planar solar preheater in steady state for the day of January 5, 2020 in the Adrar region.

### 4.2.1 Evolution of water temperature profiles for different flow rates

The different mass flow rates of water were applied to the 3D thermal model in order to determine the influence of the water flow rate and temperature on the ambient temperature.

Figure 4.1: A 3D model of the collector using Tecplot software

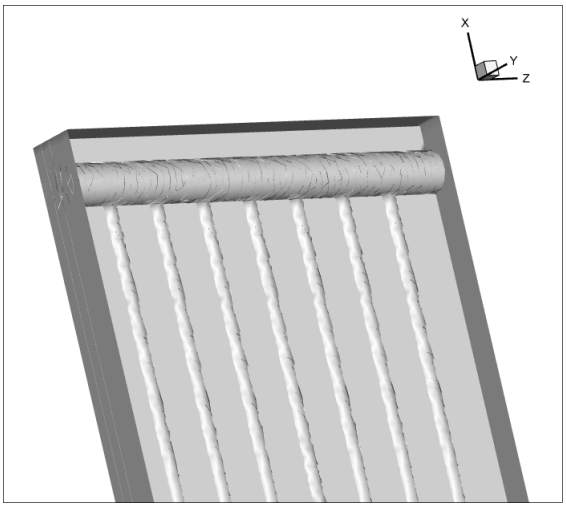


Figure 4.2: A zoomed-in view of the 3D tube design

Four mass flow rates were examined: 0.001 kg/s, 0.0008 kg/s, 0.0004 kg/s and 0.0001 kg/s with the maximum daytime temperature of 5 January 2020 in the Adrar region (Tamb = 293.15 K, Di = 903 W/m$^2$, DH = 55 W/m$^2$)

**a/ For a mass flow rate of 0.001 kg/s**

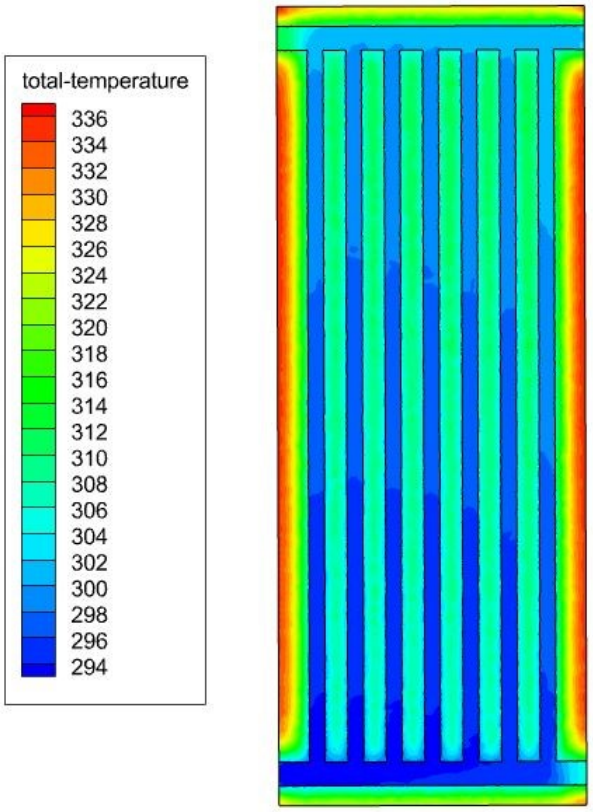


Figure 4.3: Evolution of the (X, Z)-temperature profiles of the water for a mass flow rate of 0.001 kg/s

Figure 4.3 shows the evolution of the water temperature profiles inside the seven tubes and the absorbing wall on an (X.Z) plane at the middle of the solar preheater, for a water flow rate of 0.001 kg/s and an inlet temperature of 294 K. The obtained result shows that the water temperature increases progressively all along the seven tubes in the (X, Z) direction. It can also be seen that the last tube receives more energy as the flow is divided over the seven tubes connected in parallel. The flow rate through the first tubes near the water inlet is greater than that of the last tube. The lower the flow rate, the more energy it receives. At the outlet of the solar collector the water reaches a temperature of 302 K. So the water leaves the collector with a gain of almost 8 degrees for a flow rate of 0.001 kg/s.

**b/ For a mass flow rate of 0.0008 kg/s**

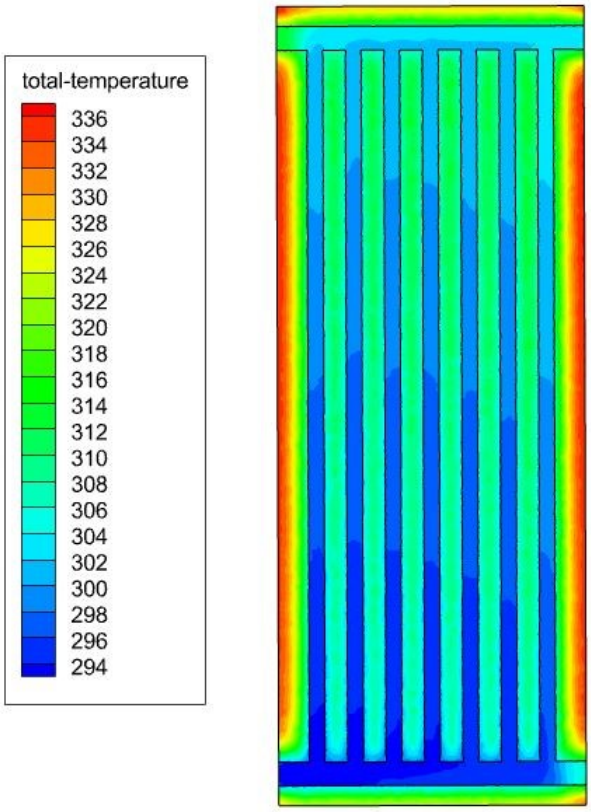


Figure 4.4: Evolution of the (X, Z)-temperature profiles of the water for a mass flow rate of 0.0008 kg/s

Figure 4.4 shows the evolution of the water temperature profiles inside the seven tubes and the absorbing wall on an (X.Z) plane in the middle of the solar preheater, for a water flow rate of 0.0008 kg/s and an inlet temperature of 294 K. At the outlet of the solar collector, we notice that the water reaches a temperature of 306 K. So the water received more energy compared to the flow rate of 0.001 kg/s. This means a gain of 4 degrees.

**c/ For a mass flow rate of 0.0004 kg/s**

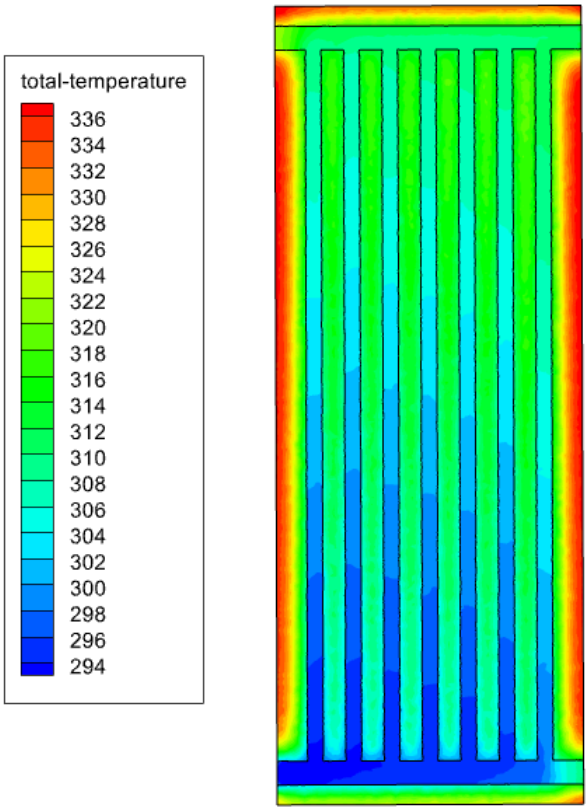


Figure 4.5: Evolution of the (X, Z)-temperature profiles of the water for a mass flow rate of 0.0004 kg/s

Figure 4.5 shows the evolution of the water temperature profiles inside the seven tubes and the absorbing wall on an (X.Z) plane in the middle of the solar preheater, for a water flow rate of 0.0004 kg/s and an inlet temperature of 294 K. At the outlet of the solar collector, we notice that the water reaches a temperature of 320 K. Therefore, the water leaves the solar collector with a gain of 18 degrees compared to the flow rate of 0.001 kg/s and a gain of 14 degrees compared to the flow rate of 0.0008 kg/s.

**d/ For a mass flow rate of 0.0001 kg/s**

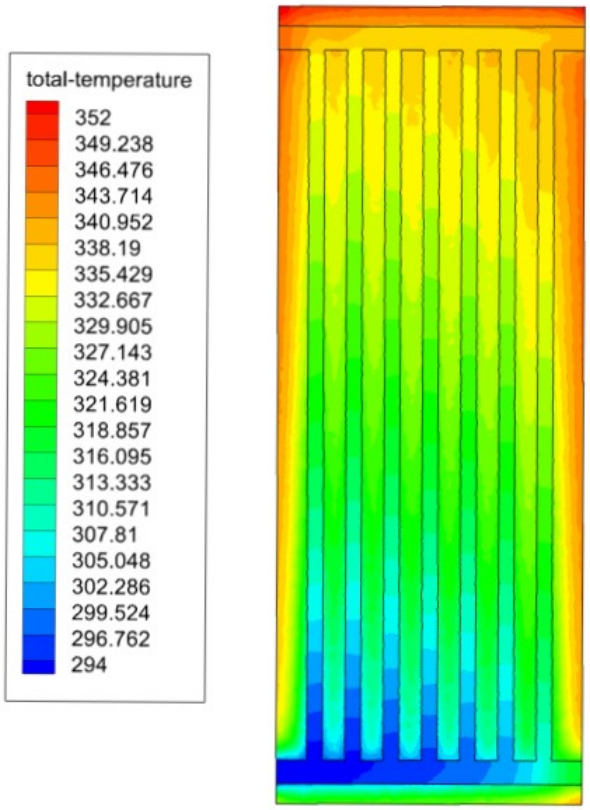


Figure 4.6: Evolution of the (X, Z)-temperature profiles of the water for a mass flow rate of 0.0001 kg/s

Figure 4.6 shows the evolution of the water temperature profiles inside the seven tubes and the absorbing wall on an (X.Z) plane in the middle of the solar preheater, for a water flow rate of 0.0001 kg/s and an inlet temperature of 294 K. At the outlet of the solar collector, we notice that the water reaches a temperature of 343 K. So the water leaves the solar collector with a gain of 41 degrees compared to the flow rate of 0.001 kg/s, a gain of 37 degrees compared to the flow rate of 0.0008 kg/s, and a gain of 23 degrees compared to the flow rate of 0.0004 kg/s.

The results obtained from the numerical simulation for the four proposed flow rates (0.001 kg/s, 0.0008 kg/s, 0.0004 kg/s and 0.0001 kg/s) highlight the influence of the flow rate on the water temperature, as the heat transfer between the absorbing wall and the tubes becomes increasingly important when the water flows slowly. In the present work, we will choose the flow rate of 0.0001 kg/s for the further calculations

of the evolution of the (X, Z)-temperature profiles of the water during the twenty-four hours. This is because it provides the best performance.

### 4.2.2 Evolution of water temperature profiles during the day

The evolution of the water temperature profiles during the day of 05 January 2020 in the Adrar region has been simulated for a flow rate of 0.0001 kg/s which represents the optimal flow rate previously calculated.

**a/ 08:00 (Tamb = 274,75 K, Di = 189 W/m², DH = 7 W/m²)**

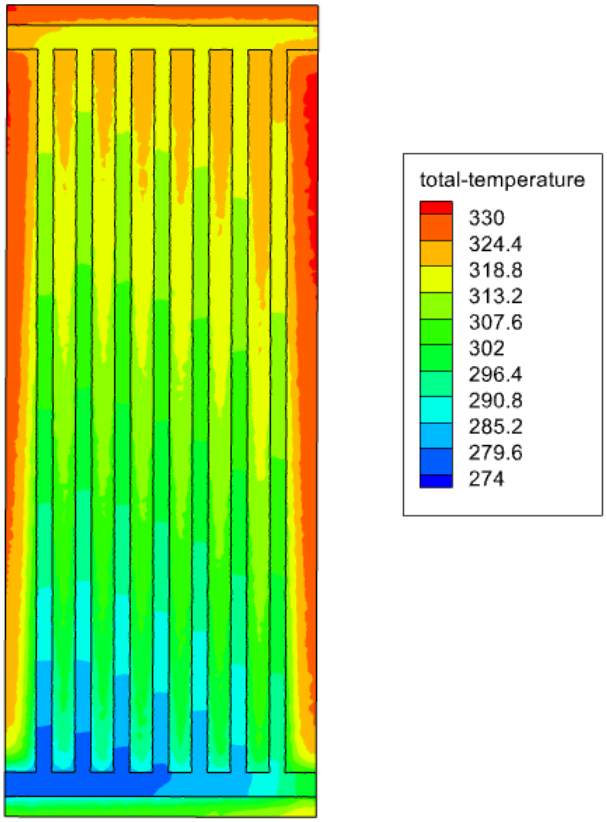


Figure 4.7: Evolution of the (X, Z)-temperature profiles of the water for a flow rate of 0.0001 kg/s at 08:00 am (Tamb = 274,75 K , Di = 189 W/m², DH = 7 W/m²)

Figure 4.7 shows the evolution of the water temperature profiles inside the seven tubes and the absorbing wall on an (X.Z) plane in the middle of the solar preheater, for a water flow rate of 0.0001 kg/s at 08:00 a.m, where the ambient temperature Tamb = 274.75 K, the direct normal irradiation Di = 189 W/m², and the diffuse

horizontal irradiation DH = 7 W/m².

It can be seen that the water enters the collector with a temperature of 274 K, the temperature of the water in the tubes increases slightly in the x- and z-direction until it arrives at the outlet with a temperature of 45°C (318 K), so the water leaves the collector with a gain of almost 44 degrees at this time because the solar radiation is not strong enough at the beginning of the day

**b/ 10:00 (Tamb = 278,95 K , Di = 922 W/m², DH = 49 W/m²)**

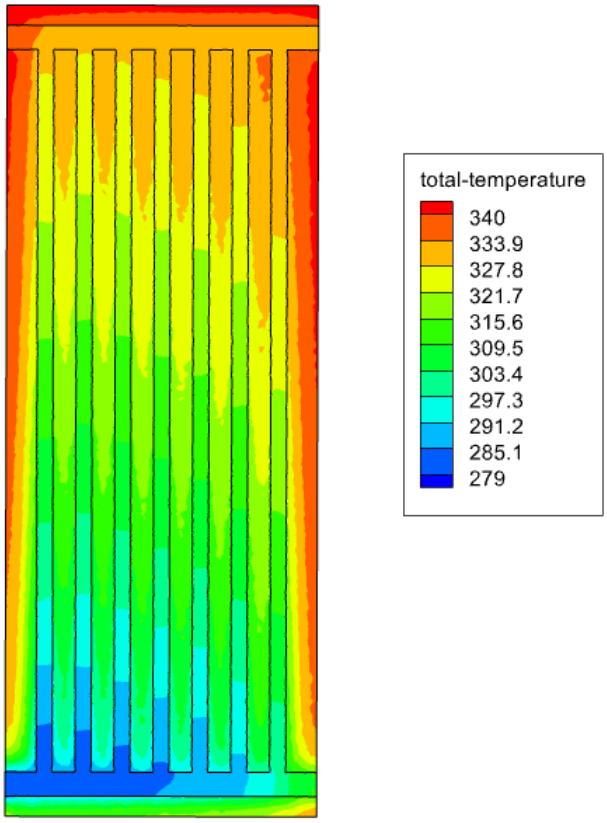


Figure 4.8: Evolution of the (X, Z)-temperature profiles of the water for a flow rate of 0.0001 kg/s at 10:00 am (Tamb = 278,95 K, Di = 922 W/m², DH = 49 W/m²)

Figure 4.8 shows the evolution of the water temperature profiles inside the seven tubes and the absorbing wall on an (X.Z) plane in the middle of the solar preheater, for a water flow rate of 0.0001 kg/s at 10:00 am, where the ambient temperature Tamb = 278.95 K, the direct normal irradiation Di = 922 W/m², and the diffuse horizontal irradiation DH = 49 W/m².

It can be seen that the air enters the collector with a temperature of 278.95 K, the

temperature of the air in the collector increases progressively in the x- and z-direction until it arrives at the outlet with a temperature of 60°C (333 K), so the air leaves the collector with a gain of almost 54 degrees at this time because the solar radiation has not yet reached its maximum, but it offers us a better efficiency than it did at 8:00 am.

**c/ 12 h 00 (Tamb = 285, 95, Di = 1025 W/m², DH = 60 W/m²)**

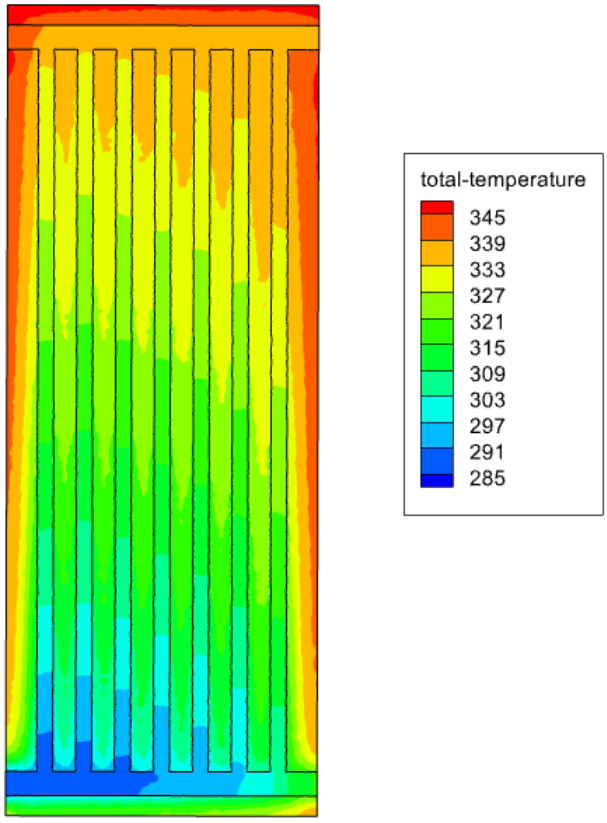


Figure 4.9: Evolution of the (X, Z)-temperature profiles of the water for a flow rate of 0.0001 kg/s at 12:00 (Tamb = 285, 95, Di = 1025 W/m², DH = 60 W/m²)

Figure 4.9 shows the evolution of the water temperature profiles inside the seven tubes and the absorbing wall on an (X.Z) plane in the middle of the solar preheater, for a water flow rate of 0.0001 kg/s at 12:00 a.m , where the ambient temperature Tamb = 285.95 K, the direct normal irradiation Di = 1025 W/m², and the diffuse horizontal irradiation DH = 60 W/m².

It can be seen that the water enters the collector with a temperature of 285.95 K, the temperature of the water in the collector increases progressively in the x- and z-direction until it arrives at the outlet with a temperature of 66°C (339 K), so the

water leaves the collector with a gain of almost 53 degrees at this period, so it offers us a better performance than at 10:00 am and 8:00 am, which is satisfying.

**d/ 13:30 (Tamb = 289, 95, Di = 1044 W/m², DH = 60 W/m²)**

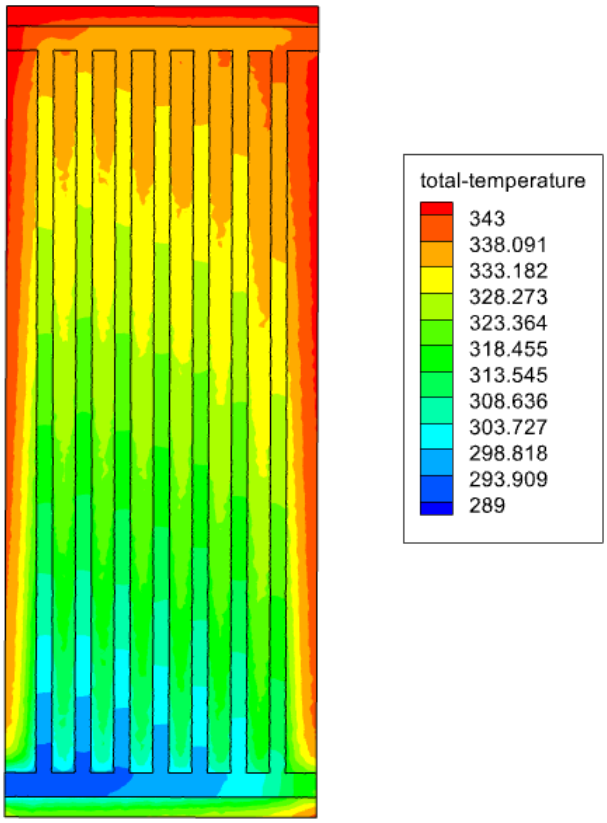


Figure 4.10: Evolution of the (X, Z)-temperature profiles of the water for a flow rate of 0.0001 kg/s at 13:30 (Tamb = 289, 95, Di = 1044 W/m², DH = 60 W/m²)

Figure 4.10 shows the evolution of the water temperature profiles inside the seven tubes and the absorbing wall on an (X.Z) plane in the middle of the solar preheater, for a water flow rate of 0.0001 kg/s at 13:00 hrs, where the ambient temperature Tamb = 289.95 K, the direct normal irradiation Di = 1044 W/m², and the diffuse horizontal irradiation DH = 60 W/m².

It can be seen that the water enters the collector with a temperature of 289.95 K, the temperature of the water in the collector increases slightly in the x- and z-direction until it reaches the outlet with a temperature of 69°C (342 K), so the water exits the collector with a gain of almost 52 degrees in this period, which is the maximum gain achieved so far this day.

**e/ 14:00 (Tamb = 291, 05, Di = 1037 W/m², DH = 60 W/m²)**

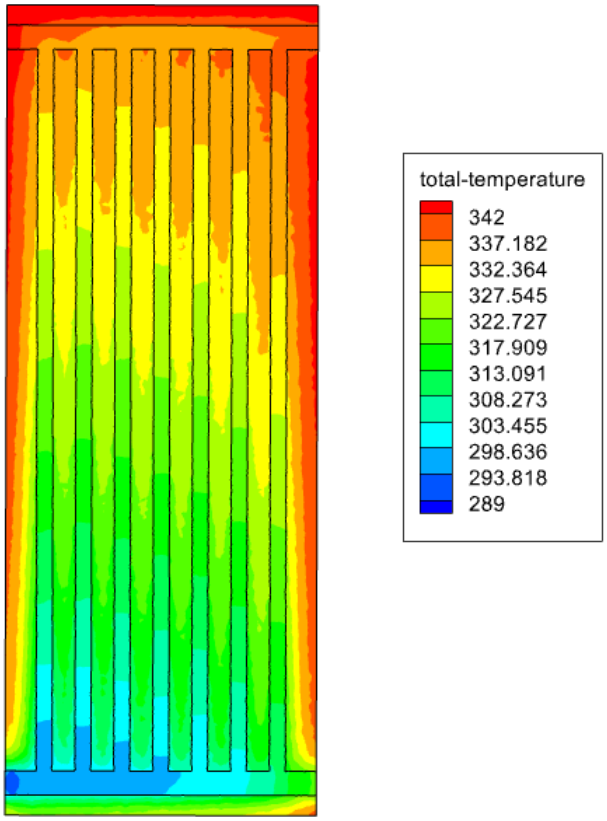


Figure 4.11: Evolution of the (X, Z)-temperature profiles of the water for a flow rate of 0.0001 kg/s at 14:00 (Tamb = 291, 05, Di = 1037 W/m², DH = 60 W/m²)

Figure 4.11 shows the evolution of the water temperature profiles inside the seven tubes and the absorbing wall on an ( X.Z) plane in the middle of the solar preheater, for a water flow rate of 0.0001 kg/s at 13:00, where the ambient temperature Tamb = 291.05 K, the direct normal irradiation Di = 1037 W/m², and the diffuse horizontal irradiation DH = 60 W/m².

It can be seen that the air enters the collector with a temperature of 291.05 K, the temperature of the air in the collector increases progressively in the x- and z-direction until it reaches the outlet with a temperature of 69°C (342 K), so the air leaves the collector with a gain of almost 51 degrees at this time. In which the ambient temperature is close to the maximum value of the day.

**f/ 16 h 15 (Tamb = 293,15 K , Di = 903 W/m², DH = 55 W/m²)**

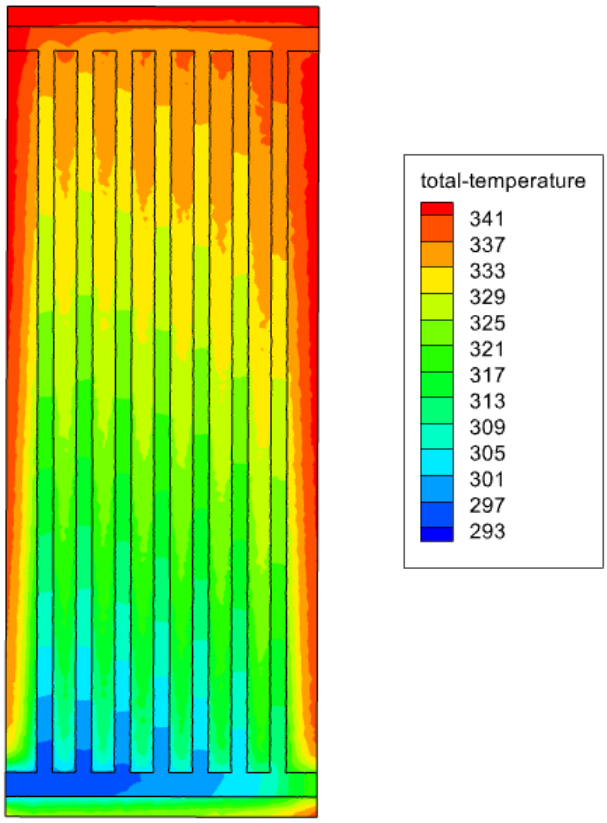


Figure 4.12: Evolution of the (X, Z)-temperature profiles of the water for a flow rate of 0.0001 kg/s at 16:15 (Tamb = 293,15 K , Di = 903 W/m², DH = 55 W/m²)

Figure 4.12 shows the evolution of the water temperature profiles inside the seven tubes and the absorbing wall on an (X.Z) plane in the middle of the solar preheater, for a water flow rate of 0.0001 kg/s at 16:15 h, where the ambient temperature Tamb = 293.15 K, the direct normal irradiation Di = 903 W/m², and the diffuse horizontal irradiation DH = 55 W/m².

It can be seen that the water enters the collector with a temperature of 293.15 K, the temperature of the water in the collector increases progressively in the x- and z-direction until it reaches the outlet with a temperature of 68°C (341 K), so the water leaves the collector with a gain of almost 48 degrees at this period in which the ambient temperature and the solar irradiation are at their maximum values of the day.

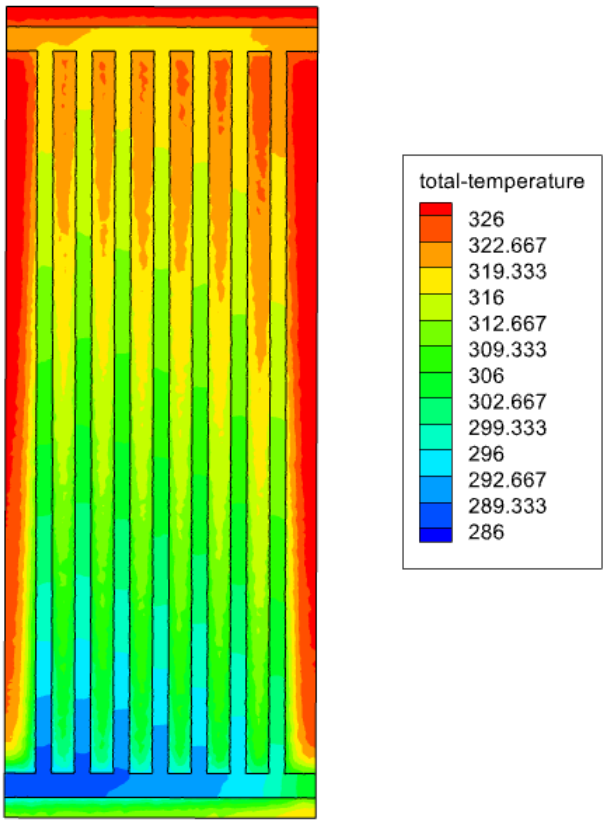


Figure 4.13: Evolution of the (X, Z)-temperature profiles of the water for a flow rate of 0.0001 kg/s at 20:00 (Tamb = 286,75 K, Di = 0 W/m², DH = 0 W/m²)

**g/ 20:00 (Tamb = 286,75 K, Di = 0 W/m², DH = 0 W/m²)**

Figure 4.13 shows the evolution of the water temperature profiles inside the seven tubes and the absorbing wall on an (X.Z) plane in the middle of the solar preheater, for a water flow rate of 0.0001 kg/s at 20:00, where the ambient temperature Tamb = 286.75 K, the direct normal irradiation Di = 0 W/m², and the diffuse horizontal irradiation DH = 0 W/m².

It can be seen that the water enters the collector with a temperature of 286.75 K, the temperature of the water in the collector increases slightly in the x- and z-direction until it reaches the outlet with a temperature of 50°C (322 K), so the water exits the collector with a gain of almost 36 degrees at this period in which the ambient temperature is low and the radiation is nil because it is night.

It can be seen that the maximum efficiency is reached at 13:30 with a gain of almost 52 degrees. In the following figures, we can see the temperature distribution through the different main regions of the collector (GLASS, TUBES, INLET, OUTLET)

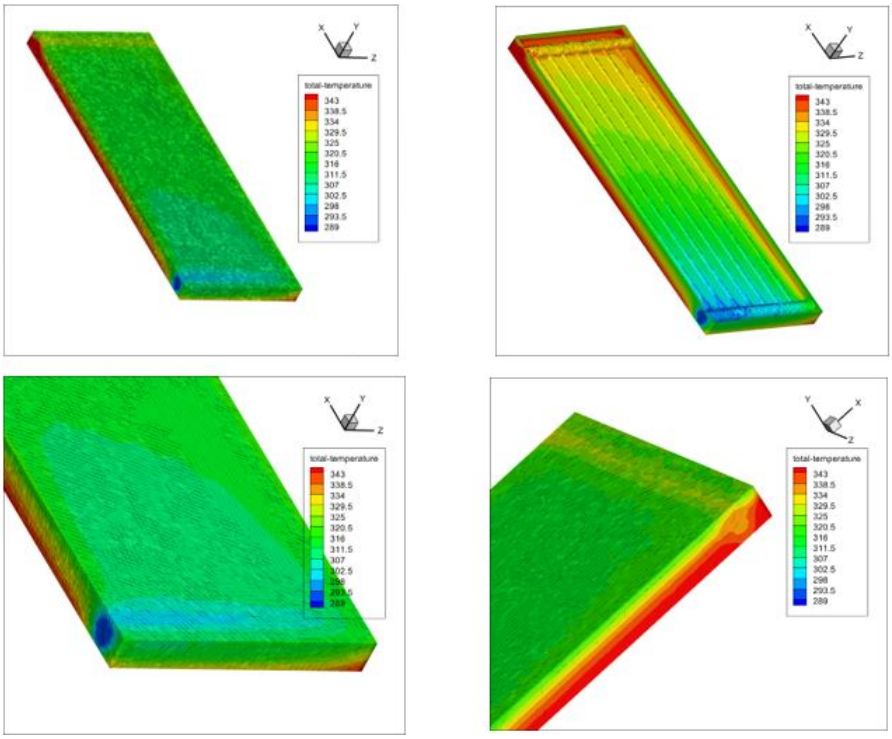


Figure 4.14: 3D distribution of the temperature evolution on the main regions of collector at 13:00 (GLASS, TUBES, INLET, OUTLET)

## 4.3 Conclusion

- In this chapter, we presented the results of a simulation of a solar water collector with the goal of studying the thermal and thermodynamic behavior of the water in the collector and determining numerically the ideal case with the highest possible efficiency.

- The data from the Adrar region measured experimentally by the URERMS for 5 January 2020 was used because if the 5th of January performance is acceptable as a minimum, we may expect a higher performance in the remaining months of the year.

- The problem was approached numerically, based on the finite volume method, using a CFD code (Ansys Fluent).

- At first, the tests were carried out using four mass flow rates (0.001 kg/s, 0.0008 kg/s, 0.0004 kg/s and 0.0001 kg/s) taken from the current literature and the external market as being the most frequently used flow rates.

- After the tests we noticed that 0.0001 kg/s is the best flow rate that with the desired operation and it gives us the best performance with a gain of almost 50 degrees which is very satisfying.

- Then,taking into account temperature and radiation changes throughout the day, we simulated the behaviour of the collector in different periods of the day with the recently chosen flow rate and we saw that the efficiency is between 30 and 49 degrees.

# General Conclusion

In this work, we have undertaken a 3D numerical simulation of the thermal fields of a flat plate solar water heater (preheater), in steady state. This study is based on the comparison between different flow rates in order to optimise the residence time of the water circulating in a parallel tube configuration, and to have a larger temperature difference at the collector outlet. Our numerical model is based on the general equations of conservation of mass (continuity), momentum and energy.
The results obtained from the proposed geometry, materials and dimensions highlight the influence of the flow rate on the water temperature, as the heat transfer between the absorbing wall and the tubes will be increasingly important when the water flows slowly. The lower the flow rate, the slower the residence time and the higher the outlet temperature. It can also be seen that there is an optimum flow rate for the system, even if the flow rate is further reduced the same results are obtained. We also notice that the distribution of the thermal field is not homogeneous in the whole system, because the flow rate is divided over the seven tubes connected in parallel. The flow rate in the first tubes near the water inlet is greater than in the last tubes. The lower the flow rate, the more energy it receives.
Finally, the study of the solar water heater with the serpentine tube shape is proposed as a perspective. This solution can correct the non-homogeneity of the thermal field in the whole system, as it will have only one flow circulating in all the tubes.

# Bibliography


[1] URL https://www.vecteezy.com/vector-art/1142243-diagram-showing-structure-of-the-sun.

[2] Yassine BADDOU. Solar thermal systems for domestic water heating applications in residential buildings. efficiency and economic viability analysis of monitored plants. Master's thesis, 2017.

[3] apparent motion of the sun. URL https://www.pveducation.org/pvcdrom/properties-of-sunlight/motion-of-the-sun.

[4] URL https://astronomy.swin.edu.au/cosmos/c/Celestial+Sphere.

[5] URL https://www.smithsonianmag.com/science-nature/plan-replace-geographic-coordinates-earth-unique-strings-three-words-180949946/.

[6] Ricardo Padilla. Simplified methodology for designing parabolic trough solar power plants. 01 2011.

[7] URL https://www.sciencedirect.com/topics/engineering/solar-altitude-angle.

[8] URL https://www.worlddata.info/africa/algeria/sunset.php.

[9] URL http://www.greenrhinoenergy.com/solar/radiation/characteristics.php.

[10] URL https://www.researchgate.net/figure/Solar-radiation-potential-in-Algeria-9_fig1_32753174.

[11] M. Savadkohy M.R. Assari, H.B. Tabrizi. Numerical and experimental study of inlet-outlet locations effect in horizontal storage tank of solar water heater. *Sustainable Energy Technologies and Assessments*, 2018.

[12] F. Qiu X. Zhang X. Zhao Z. Wang, W. Yang. Solar water heating : From theory, application, marketing and research. *Renewable and Sustainable Energy Reviews*, 2015.

[13] Hosni I. Abu-Mulaweh. Design and development of solar water heating system experimental apparatus. *Global Journal of Engineering Education*, 2012.

[14] A. Brahimi. Etude de performances d'un capteur solaire plan à eau. Master's thesis, 2016.

[15] URL `www.ladictionnairevisuel.com`.

[16] L. El maimouni N. Hassanain O. Tata Y. Belkassmi, K. Gueraoui. Numerical investigation and optimization of a flat plate solar collector operating with cu/cuo/al2o3–water nanofluids. *Sustainable Energy Technologies and Assessments*, 2020.

[17] Lee Layton. Solar water heating systems. 2012.

[18] S. Chaussedent. *Statique et dynamique des fluides*, 2011.

[19] Y. Çengel. *Fluid Mechanics: Fundamentals And Applications*. Tata McGraw Hill Education Private, 2010.

[20] Bernard J. *Energie solaire calculs et optimisation*. Ellipse Edition Marketing, 2004.

[21] Sen Z. *Solar energy fundamentals and modeling techniques*. Springer, 2008.

[22] Alain Ricaud. *Gisement solaire et transferts énergétiques*. Université de CERGYPONTOISE, 2008.

[23] B. Mourad. Contribution a l'étude, la simulation et l'analyse des pompes à chaleur assistées par l'énergie solaire. Master's thesis, 2008.

[24] Y. Jannot. *Thermique solaire*, 2011.

[25] K. Salima. Effet des paramètres opérationnels sur les performances d'un capteur solaire plan. Master's thesis, 2009.

[26] SANDALI Messaoud. Etude dynamique et thermique d'un capteur solaire à air à double passe avec milieu poreux. Master's thesis, 2013-2014.

[27] Modes of heat treatment. URL `https://learnmechanical.com/modes-of-heat-transfer-conduction-convection-and-radiation-pdf/`.

[28] URL `www.solairethermique.fr`.

[29] ABABSA Dalila. Optimisation du rendement d'un capteur solaire par minimisation des pertes convectives. Master's thesis, 2009/2010.

[30] R. ALILI A. IBERRAKEN. Modélisation mathématique et simulation de capteurs solaires. Master's thesis, 2012.

[31] H. Schlichting. *Boundary layer Theory, 7th ed*. Springer, 1979.

[32] O. Reynolds. *On the dynamical theory of incompressible viscous fluids and the determination of the criterion*. the Royal Society of London, 1894.

[33] I. Paraschivoiu. *Aérodynamique subsonique*. l'École Polytechnique de Montréal (Québec), Canada, 1998.

[34] S.V Patankar. *Numerical Heat Transfer and Fluid Flow*. CRC Press. New York, 1980.

[35] B. Djenhi. Contribution à l'étude du transfert de chaleur par convection mixte entre deux plaques parallèles soumises à un chauffage dissymétrique. Master's thesis, 2013.

[36] I.C. Popa. Modélisation numérique de trensfert thermique - méthode des volumes finis. 2002.